Aus der Klinik für Neuroradiologie
der Medizinischen Fakultät Charité – Universitätsmedizin Berlin

DISSERTATION

Investigation of Molecular Subtypes of WHO Grade II-IV Gliomas by Use of T2 Mapping Sequences in Magnetic Resonance Imaging

zur Erlangung des akademischen Grades
Doctor medicinae (Dr. med.)

vorgelegt der Medizinischen Fakultät
Charité – Universitätsmedizin Berlin

von

Maike Lizanne Kern

aus Berlin

Datum der Promotion: 04. März 2022

Für Papa †

Inhaltsverzeichnis

Abkürzungen

αKG	alpha-ketoglutarate
A2	WHO grade II diffuse astrocytoma
AA3	WHO grade III anaplastic astrocytoma
ADC	apparent diffusion coefficient
ANOVA	analysis of variance
ATRX	alpha-thalassemia X-linked mental retardation protein
AUC	area under the curve
BBB	blood-brain-barrier
CE	contrast enhancing
CI	confidence interval
CM	centimeters
CNS	central nervous system
CT	computer tomography
cROI	central region of interest
D2HG	D-2-hydroxyglutarate
^{18}F-FDOPA	6-[18F]-L-fluoro-L-3, 4-dihydroxyphenylalanine
FLAIR	fluid attenuated inversion recovery
FOV	field of view
GBM	glioblastoma multiforme
HGG	high grade glioma
HIF- 1α	hypoxia-inducible factor -1 alpha
i.e.	id est (in other words)
IDH	isocitrate dehydrogenase
IDH-mut	mutational IDH
IDH-wt	IDH-wildtype
Max	maximal T2 relaxation time
Min	minimal T2 relaxation time
MPRAGE	magnetization-prepared rapid gradient-echo
MS	milliseconds
MRI	magnet resonance imaging
PACS	picture archiving and communication system
PCR	polymerase chain reaction
PET	positron emission tomography
pROI	peripheral region of interest
RANO	Response Assessment in Neuro-Oncology

RIS	radiology information system
ROC	receiver operating characteristics
ROI	regions of interest
SI	T2 relaxation times/ signal intensity
T	Tesla
T2w	T2 weighted
TE	echo time
TR	repetition time
VEGF	vascular endothelial growth factor
vs.	versus
WHO	World Health Organization
WM	white matter
TP53	tumor suppressor protein 53

Vorwort

In den folgenden Kapiteln wird eine ausführliche Darstellung von Forschungsstand und Methodik, die wesentlichen Ergebnisse sowie die sich aus den Ergebnissen ergebenden wissenschaftlichen Fragestellungen der Publikationen der Promovendin [1-3] diskutiert. Inhalte der Publikationen werden dabei in einen umfassenderen, wissenschaftlichen Kontext gesetzt und ausgeführt.

Die Teilergebnisse wurden dabei bereits veröffentlicht in:

[1] Kern, M., Auer, T. A., Picht, T., Misch, M., & Wiener, E. (2020). T2 mapping of molecular subtypes of WHO grade II/III gliomas. *BMC Neurology*, *20*(1), 8. https://doi.org/10.1186/s12883-019-1590-1

[2] Kern, M., Auer, T. A., Fehrenbach, U., Tanyildizi, Y., Picht, T., Misch, M., & Wiener, E. (2020). Multivariable non-invasive association of isocitrate dehydrogenase mutational status in World Health Organization grade II and III gliomas with advanced magnetic resonance imaging T2 mapping techniques. *The Neuroradiology Journal*, *33*(2), 160–8. https://doi.org/10.1177/1971400919890099

[3] Auer, T. A., Kern, M., Fehrenbach, U., Tanyildizi, Y., Misch, M., & Wiener, E. (2021). T2 mapping of the peritumoral infiltration zone of glioblastoma and anaplastic astrocytoma. *The Neuroradiology Journal*, 0(0), 1–9. https://doi.org/10.1177/1971400921989325

Zusammenfassung

Einleitung: Im Jahr 2016 integrierte die World Health Organization (WHO) erstmalig den molekularen Subtyp von Gliomen in die Klassifikation für Tumoren des zentralen Nervensystems. Dieser hat einen großen Einfluss auf die Prognose und das Therapieansprechen der Patienten. Wie in zahlreichen Studien beschrieben, können Mutationen wie zum Beispiel die der Isozitrat-Dehydrogenase (IDH) in der Magnetresonanztomographie (MRT) zu bildmorphologischen Veränderungen führen. Ziel dieser Arbeit ist es, quantitative T2 mapping Sequenzen bezüglich des Mutationsstatus von Gliomen zu untersuchen.

Methoden: Es wurden 52 MRT-Untersuchungen von Patienten mit histopathologisch nachgewiesenem WHO-Grad II-IV Gliom retrospektiv ausgewertet. Unter Verwendung von quantitativen T2 mapping Sequenzen wurden genau definierte „regions of interests" (ROIs) analysiert, welche im Tumor und in der peritumoralen Zone beziehungsweise im umgebenden Ödem platziert wurden. Die Messungen wurden von zwei unabhängigen Untersuchern durchgeführt. Die T2 Relaxationszeiten wurden pixelweise gemessen und ausgewertet. Weitere Parameter wie Patientenalter, Tumorlokalisation, Kontrastmittelanreicherung, Nekrose, Tumor- und Ödemgröße wurden ebenfalls untersucht. Statistische Methoden, wie beispielsweise der Mann-Whitney-U-Test, Analysen der multivariaten „receiver-operation characteristics" (ROC) und ein speziell entwickeltes Fit-Modell mit einer Polynomfunktion zweiten Grades, wurden angewendet, um aussagekräftige Ergebnisse zu erzielen.

Ergebnisse: Insgesamt zeigten IDH-mutierte Gliome eine signifikant höhere Signalintensität in T2 mapping Sequenzen, was längere T2 Relaxationszeiten und breitere Streuung der T2 Werte bedeutet. Ein jüngeres Erkrankungsalter und eine fronto-parieto-temporale Tumorlokalisation zeigten sich ebenfalls mit der IDH Mutation assoziiert. ROC-Analysen der Parameter Alter, Lokalisation, T2 Relaxationszeit und T2 Wertebereich ergaben eine „area under the curve" (AUC) von 0,955, sowie eine hohe Testgenauigkeit und Sensitivität. Die T2 Werte und ihr Wertebereich ergaben die höchsten Korrelationskoeffizienten in den Einzelbewertungen. Das Fit-Modell zeigte einen signifikant höheren Modellparameter bei IDH-Wildtyp Gliomen. Mutationen des Tumorsuppressorproteins 53 (TP53) und des Alpha-Thalassämie assoziierten X-chromosomalen Gens (ATRX) waren stark mit der IDH-Mutation assoziiert. Es wurden sehr hohe Übereinstimmungen zwischen den Untersuchern erzielt.

Diskussion und Schlussfolgerung: Diese Arbeit zur quantitativen Untersuchung von Gliomen in T2 mapping Sequenzen ergab signifikante Unterschiede der Signalintensität hinsichtlich des Mutationsstatus. Bereits zuvor beschriebene IDH-assoziierte Parameter wie Alter und Tumorlokalisation zeigten auch in dieser Studie signifikante Ergebnisse. Darüber hinaus waren alle bisher beschriebenen mutationsassoziierten qualitativen oder quantitativen MR-Techniken dem T2 mapping gleichauf oder unterlegen, womit wir die zukünftige Bedeutung dieser Sequenz überzeugend aufzeigen können. Die einfache klinische Anwendung von T2 mapping ist hervorzuheben. Diese Forschungsarbeit liefert eine Grundlage für die Implementierung von T2 mapping Sequenzen im Bereich der Neuroradiologie.

Abstract

Introduction: The revised World Health Organization (WHO) classification for tumors of the central nervous system, presented in 2016, included the molecular subtype of gliomas for the first time as this has a major influence on patient prognosis and response to therapy. It has been observed in several studies that some mutations, such as isocitrate dehydrogenase (IDH), may be capable of causing imaging alterations on magnetic resonance imaging (MRI). The aim of this study was to investigate quantitative T2 mapping in relation to the mutational status of gliomas.

Methods: MRI examinations in 52 patients with WHO grade II-IV glioma as demonstrated by histopathology were included in a retrospective evaluation. Accurately defined region of interest (ROI) analyses of quantitative T2-mapping sequences were performed in the tumor, the peritumoral zone, as well as in any surrounding areas of edema. T2 relaxation times and their range were measured pixel-by-pixel. Further parameters were also investigated, such as the patient age, tumor localization, contrast enhancement, necrosis, tumor size and edema size. Statistical methods such as the Mann-Whitney-U test, multivariate receiver-operating characteristics (ROC) analyses and a specially-developed fit-model of a second-degree polynomial function, were applied to generate diagnostically conclusive results.

Results: Overall, IDH-mutated gliomas had a significantly higher signal intensity, meaning longer T2 relaxation times and higher T2 value ranges in T2 mapping sequences. Younger age and fronto-parieto-temporal localization was also associated with the IDH mutation. ROC analyses of the parameters age, localization, T2 relaxation time and range produced an area under the curve (AUC) of 0.955 with expressively high accuracy and sensitivity. T2 values and their ranges yielded the highest single score correlation coefficients. The fit-model revealed a significantly higher model parameter in IDH-wildtype gliomas as well as in glioblastomas. Mutations of tumor-suppressor protein 53 (TP53) and alpha-thalassemia X-linked mental retardation syndrome gene (ATRX) are strongly associated with the IDH mutation. High interobserver concordances were obtained.

Conclusion: First-time quantitative evaluation of T2 mapping sequences revealed significant differences in signal intensity with respect to the mutational status of glioma. Reinforcement of previously described IDH-associated parameters, such as age and tumor localization, could also be achieved. As clinical applicability is essential, and all further descriptions of mutation-associated qualitative or quantitative MRI techniques were invariably equal to or inferior to T2 mapping, we could convincingly demonstrate the future importance of this technique. This study provides a basis for the implementation of T2 mapping sequences in the field of neuroradiology.

Manteltext

1 Introduction

1.1 The 2016 World Health Organization Classifications and Gliomas

With a worldwide incidence of approximately 6 per 100,000 citizens per year, gliomas are the most frequent brain tumors seen in adults [4–12]. They are usually derived from glial cells and demonstrate a wide variety of different behaviors [12,13]. The prognostic patient survival time remains poor, especially in cases of high-grade glioma [11,14]. Since the inclusion of gliomas into the classifications created by the WHO for tumors of the central nervous system (CNS), this has always been based on a concept of histogenesis [8,11,14,15]. Additionally, the tumor's grade (on a scale from I to IV) is defined by the degree of anaplasia [11,14]. WHO grades III and IV describe malignant or high-grade gliomas (HGGs), are associated with a poor prognosis, and represent the majority of diffuse gliomas [8,11,14,16]. It is important to note that histopathological grading is always subject to significant interobserver variability [14]. The WHO CNS from 2016 added genotypic parameters to the histogenesis-based assessment for the first time, representing the largest modification since the initial classification dating back to 1979 [14,15,17,18]. The new classification subdivided different molecular genetic tumor markers to give a more precise division into subgroups with distinct molecular signatures [8,14,15,17]. At present, the literature indicates that these subgroups correlate with their histologic subtype, therapeutic response and the patient prognosis [8,15,17,19,20].

There are three major genetic alterations in the WHO classification from 2016: promotor methylation of O-methylguanine-DNA methyltransferase (MGMT), co-deletion of 1p/19q, and the mutation of genes coding for the enzyme isocitrate dehydrogenase (IDH) 1 or 2 [8,15,21]. According to the 2016 WHO classification, gliomas with 1p/19q co-deletion are most common in oligodendrogliomas, which can see benefits from application of combined radiotherapy and chemotherapy [14,15]. The occurrence of MGMT promotor methylation is predictive for a sensitive response to alkylating chemotherapeutics, especially in IDH-wildtype (IDH-wt) gliomas [14]. Moreover, mutations of the alpha-thalassemia X-linked mental retardation syndrome gene (termed 'ATRX loss') seem to be associated with mutations of IDH and an improved prognosis in cases of glioma [8,22]. In this study, the occurrence of mutations of tumor-suppressor protein 53 (TP53) was investigated on the basis of a known association with IDH mutation and ATRX loss [8,22].

The mutation of IDH 1 or 2 (IDH-mut) represents one of the key genetic alterations and seems to be of significant predictive value for the patient's prognosis [8,13,14,19,20,23,24]. IDH-wildtype (IDH-wt) is present in >90% of cases of glioblastoma (GBM) (WHO grade IV) but only in 10-20% of WHO grade II/III gliomas [4,6,8,9,15,19,23–26]. It is associated with a significantly poorer prognosis, while the IDH-mut is generally associated with a better prognosis [4,6,8,9,15,19,23–26]. This mutation usually occurs in codon R132, termed IDH1, or R172, termed IDH2 [27,28]. The IDH-mut enzyme, on the other hand, metabolizes

alpha-ketoglutarate (αKG) to D-2-hydroxyglutarate (D2HG), which increases the levels of D2HG, a known oncometabolite [6,8,9,13,14,29–31]. Furthermore, the IDH-mut inhibits the PI3K/Akt pathway, which generally has anti-apoptotic effects, and its inhibition may induce apoptosis at a higher rate [25]. Additionally, the IDH1 mutation may stabilize hypoxia-inducible factor-1 alpha (HIF-1α), which is important for angiogenesis and vascularization [6,29,32]. According to *Villanueva-Meyer et al. (2018)*, considering the parameter of age is also relevant as patients with IDH-wt gliomas are significantly older than patients with IDH-mut [28]. This indicates that the mutation seems to have a large impact on the tumor's specific biology and behavior. In general, several studies have reported that the molecular analyses of gliomas might be more important than their histological classification [8,14].

Another important aspect of gliomas, aside from their molecular profile, is the surrounding tissue: the peritumoral zone [33]. In radiology, the peritumoral zone is defined as the healthy brain area a few centimeters surrounding the tumor, exhibiting vasogenic edema while indicating the infiltration of tumor cells [34,35]. The exact definition of outer tumor margins as well as the differentiation of infiltration from pure edema remains challenging [33–35]. A dysfunctional blood-brain-barrier (BBB) might lead to increased vascular permeability, thus plasma fluid and proteins are able to invade into the peritumoral tissue, which is the main hypothesis for the genesis of vasogenic edema [35,36]. Further investigations showed that the brain tumor cells might produce specific cytokines, in particular vascular endothelial growth factor (VEGF), which would be able to increase perfusion and to cause vasodilatation [36]. Especially when standard imaging techniques are used, the distinction between "vasogenic" and "tumor-infiltrated" edema in particular is insufficient [33–35]. Edema and infiltration zone are major to value for various factors. Firstly, edema/infiltration zone produce a mass effect, just like the tumor itself, possibly leading to symptoms and neurological disorders. Secondly, as previously mentioned, the accurate demarcation of tumor margins and tumor infiltration is necessary as recurrence tends to appear within 2-3 centimeters (cm) [33,37]. Differentiation by means of a standardized technique that can be used in routine clinical practice is urgently needed. This is particularly the case as radiological imaging has long had a major impact on noninvasive diagnosis, monitoring and surgical planning for brain tumors. Subsequently, there has been a great effort to identify imaging phenotypes of molecular profiles. As mentioned above, the molecular profile has had a major influence since the revised WHO classification in 2016. Unfortunately, it can only be identified by biopsy or surgery, with both interventions having various risks for the patient. In this context, noninvasive diagnosis and differentiation is an important goal to achieve, especially with respect to the molecular subtype.

1.2 Magnetic Resonance Imaging and Imaging Correlates of Molecular Subtypes

MRI is the main technique used in the diagnosis of gliomas. It functions on the basis of the spin of protons along an axis to generate images: inside an MRI scanner, protons align parallel or anti-parallel to the axis of the scanner's magnetic field, termed longitudinal magnetization [38,39]. This produces a difference in

energy levels, which accelerates according to the scanners field strength [39]. A radiofrequency pulse shifts the longitudinal magnetization into the transversal plane, termed transversal magnetization [39]. Afterwards, the vector gently approaches the longitudinal alignment once again, which is termed longitudinal or spin-lattice relaxation [39]. The time taken to recovery of longitudinal alignment is called T1, and T1 relaxation time is dependent on the field strength [39]. The loss of transversal alignment is induced by the mutual interference of the different spins, which occurs due to an energy transfer between them, on the one hand, and inhomogeneities of the magnetic field on the other [39]. It is important to state that there is no energy dissipation of the spins to the surrounding protons, unlike longitudinal relaxation, but rather among themselves [39]. Due to the energy exchange of spin-spin interactions, the spins loose coherence, which is called transverse relaxation, T2, or dephasing [39,40]. For this process, only spin-spin interactions are important, which is why T2 is independent of the scanner's field strength [39,40]. Tissues or fluids that are able to hold the transversal magnetization longer, such as cerebrospinal fluid or water, have longer T2 relaxation times and appear bright or hyperintense on T2-weighted images [35,39]. Gliomas usually appear hyperintense and heterogeneous: their edema/infiltration zone, however, appears more homogenous in T2-weighted MR images [11,12,34,35,41]. Usually, T2 relaxation times depend on the original sequence T2 echo time, which is the time elapsed between the excitation pulse and the observation time of the MRI signal [39,41]. Mapping techniques in MRI allow for pixelwise quantification of relaxation times at different echo times, whereby these are detected and undergo an online reconstruction onto the T2 map [39]. With the aim of representing all echo times, the measurements in the T2 map give more detailed information on the tissue composition and are both reproducible and transferable [42].

Therapy response in HGG is currently assessed on the basis of criteria published in 2010 by the Working Group for Response Assessment in Neuro-Oncology (RANO) [7,43,44]. RANO criteria include an increase in the T2/fluid-attenuated inversion recovery (FLAIR) sequence independent of the assessment in T1-weighted sequences [43]. A significantly increased size in T2/FLAIR in non-enhancing lesions is now defined as T2 progression [7,43,44]. The T2 progression itself seems to be an event preceding T1 progression, emphasizing the importance of its inclusion [44]. Through integration into the RANO criteria, the importance of T2 weighted images became strongly accentuated, even if common assessment mainly relies on the T2 mass or volume, and not on the signal intensity. Even the RANO criteria are only based on two measures of length; T2 mapping might provide a new quantitative approach to image therapy response and progression. By using T2 mapping, it might be possible to show that the signal intensity is just as important as the tumor size in T2-weighted images. Additionally, it is worthwhile noting that the RANO criteria align with the WHO grading, and genotypic parameters have not yet been included.

Nevertheless, until just a few years ago few researchers had addressed the issue of differences in imaging presentations that were usable on a daily basis with regard to the molecular status of gliomas. In recent years, more investigations have been published: sample sizes are relatively small in the main, which further complicates the interpretation of results. A review by *Smits et al. (2017)* summarized that there are no significant associations with imaging features with respect to MGMT promotor methylation [8]. Gliomas

with 1p/19q co-deletion appear heterogenous and have calcifications, in addition to also having no clear imaging features [8]. The majority of investigations were regarding the IDH mutation as it produces the most expressive results [8]. *Qi et al. (2013)* examined WHO grade II/III gliomas and detected an association between IDH mutation and homogenous signal intensity/reduced contrast enhancement [4,8,20]. In a previous study, *Metellus et al. (2010)* reported that the absence of IDH mutation in low-grade gliomas reveals a subgroup including older patients, fronto-temporo-insular localization and infiltrative growth patterns [19]. They had already made the observation that there might be divergent results regarding some MRI features such as heterogeneity, contrast enhancement and sharp borders [19]. An early study concerning mapping and IDH was carried out by *Wang et al.* in 2015, even if their study did relate to anatomical tumor localization and not signal intensity [45]. Different observers delineated the tumors, which were overlaid by voxel-based lesion-symptom mapping [45]. In their study, IDH-mut WHO grade II and III gliomas were mostly located in the frontal lobe and surrounding the rostral extension of the lateral ventricles [45]. Even predating this, it had been reported that this might be the localization where the distinct precursor cells are located [4,8,19,20,45]. Some authors have suggested that gliomas might originate from these precursor cells [4,8,19,20,45].

Nevertheless, several methods other than MRI, such as positron emission tomography (PET)-computer tomography (CT) and MRI spectroscopy, have been investigated regarding their potential for detection of molecular subtypes. PET-CT is considered as a standard modality for visualizing tumor biology: it mainly relies on the uptake from the tracer, and also gives information about different tumor characteristics. *Verger et al. (2017)* and showed an increased ^{18}F-FDOPA uptake in PET-CT in IDH-mut gliomas [46]. On the other hand, several studies showed that MRI spectroscopy is able to identify IDH-mut tumors as it detects the increased levels of D2HG [6,8,27,47]. Both metabolic imaging techniques measure only specific molecules, which leads to the serious disadvantage that both require specific questioning. T2 mapping itself assesses completely different aspects of tumor biology as it represents tissue composition, with the resulting radiologic information varying widely [42].

In summary, there are some valid proven qualitative MRI characteristics that are associated with IDH-mut in gliomas. The parameters, age, localization, enhancement, necrosis, homogeneity and diameter seem to be most promising. In relation to qualitative techniques, there are significant requirements in terms of the evaluation of reliable quantitative techniques [42]. Mapping techniques are able to provide quantified information, while conventional MRI imaging only allows for qualitative image analysis [42]. Nevertheless, the field of this promising application in neuroradiology remains largely unexplored. There has been less evidence in the past for T2 mapping used in neuroradiology in general and as previously mentioned, there have been some studies regarding molecular subtypes such as IDH and MRI features, but most of these are based on macroscopic characteristics, which are not objectifiable to any significant degree. *Hattingen et al. (2013)* investigated the usefulness of T2 mapping for monitoring recurrent glioblastoma under treatment with bevacizumab (monoclonal antibody against VEGF), which was the first published clinical-neuroradiological study using T2 mapping [28]. Establishing this promising technique in

neuroradiology is an important goal to achieve as the technique itself is already applied as standard in myocardial imaging and in other organs [42].

1.3 Purpose of This Study

Existing classification algorithms mainly rely on the histological phenotype of gliomas, i.e. the WHO grade. However, since the implementation of the revised WHO classification in 2016, the genotype might be even as important or even more important for prognosis and therapy response than the WHO grade. As such, current studies are striving to find and establish techniques for noninvasive characterization in clinical practice. The current state of the literature is inconsistent, presenting partly divergent results. Several studies have demonstrated that it is mainly the IDH mutation that brings about imaging changes, which is why this is the main mutation that was examined in our study [8].

With the aim of analyzing changes in signal behavior in T2-weighted images in WHO grade II-IV gliomas resulting from their molecular subtype, our study mainly relies on three hypotheses and lines of questioning, which the three publications are based on:

1) There is a difference in signal behavior detected by T2 mapping, especially regarding the IDH-status in WHO grade II and III gliomas.
2) T2 signal intensity is the most expressive factor to identify IDH-mutated WHO grade II /III gliomas in T2-weighted images. What is the highest level of validity we can achieve by combining IDH-associated imaging parameters?
3) There are differences in the signal intensity of the peritumoral zone of WHO grade III and IV gliomas detectable by use of T2 mapping, also considering the mutational status.

Established imaging features which showed a likely correlation to the IDH-status could not fully meet up to expectations in clinical practice. The study from *Lee et al. (2015)* showed that advanced MR imaging is able to detect alterations on a genetic and cellular level [48]. T2 mapping allows for pixelwise quantification of T2 relaxation times at different echo times to potentially provide accurate information about the tissue and its composition. The sequence itself is easy to handle, providing transferable values; for this reason it is already fully-integrated into other subareas of radiology [42]. Accordingly, it could be rather straightforward to integrate it into standardized preoperative imaging of gliomas.

This study proposes a new approach investigating the ability of quantitative T2 mapping to detect imaging changes associated with mutational status in WHO grade II-IV gliomas. Furthermore, it compares T2 mapping parameters to established clinical and qualitative imaging characteristics with respect to the tumor and the peritumoral zone. The aim of this study is to analyze the known imaging characteristics of IDH-mut gliomas in MRI, and to evaluate these compared to T2 mapping with respect to their objective validity.

2 Methods

2.1 Study Population

The ethical board of our institution has approved this study (application number EA1/306/16). All participants were enrolled after informed consent was obtained verbally. The study was conducted according to the Declaration of Helsinki in its revised revision from 2002. Patients with a diagnosis of WHO grade II astrocytoma (A2), WHO grade III anaplastic astrocytoma (AA3) and WHO grade IV glioblastoma (GBM) with an MRI examination of the whole brain performed between April 2015 and March 2018 were included in the final study. The data were evaluated retrospectively from April 2017 to March 2019 by using the Centricity radiology information system (RIS)-I 5.0 (Version 5.0.11.6;2;4;6;8;10;11;14;15;19;20;23; 2015 General Electric Company) radiologic data bank and the complementary picture archiving and communication system (PACS). All patients obtained preoperative radiologic imaging at Charité Virchow or Charité Benjamin Franklin Hospital in Berlin, Germany. Patients suffering from gliomas with 1p/19q deletion, which are oligodendrogliomas according to the 2016 WHO classification were excluded as they exhibit divergent biological and clinical behaviors [4,8]. The data collection was performed in pseudonymized form with individual codes assigned.

Patients younger than 18 years, those suffering from multiple tumors, or those with a history of previous surgical treatment on the CNS with imaging alterations such as biopsy tracts from previous biopsy, artifacts and surgical cavities were excluded. Additionally, we had to exclude all subjects for whom the required sequences were not available. In the end, the study included a total of 52 patients; 22 with GBM; 21 with AA3; 9 with A2; 19 with IDH mutation; and 33 without IDH mutation. ATRX loss was mostly associated with mutation of IDH. No patients exhibited 1p/19q co-deletion.

2.2 Histopathological Assessment

Information about the tumor markers was extracted from the pathological reports of the Charité, which were available for all patients included. The mutational status of IDH1, ATRX and TP53 was determined during the pathologic/anatomic examination. The sample was embedded in paraffin and cut into slices. Subsequently, as part of immunohistochemical testing, the cells were dyed with antibodies against the respective mutation-specific marker. Dyeing of the cells was considered a positive result. If the result was inconclusive, amplification and sequencing of the representative parts of the genes followed for IDH1 (codon R132) and 2 (codon R172) by use of the polymerase chain reaction (PCR) and pyrosequencing analysis. On request, additional markers such as MGMT and 1p/19q co-deletion were determined.

2.3 Data Acquisition

MRI was performed preoperatively using either a 1.5 Tesla (T) (Avanto Magnetom; Siemens, Erlangen, Germany) or a 3T (Skyra; Siemens, Erlangen, Germany) scanner. MRI examination was conducted both with and without contrast media: Gadovist (Bayer AG, Leverkusen, Germany) or Dotarem (Guerbet GmbH,

Villepinte, France) were administered at a weight-adjusted dose. We obtained the following sequences: axial T1-weighted sequence [repetition time (TR) 550 milliseconds (ms); echo time (TE) 8.9ms; slice thickness 5 millimeter (mm); in-plane resolution 0.8984mm x 0.8984mm; acquisition matrix 256x216]; T2-fat-saturation (T2-fs) axial [TR 4000ms; TE 92ms; slice thickness 3mm; field of view (FOV) 186x230 rows; in-plane resolution 0.4492mm x 0.4492mm]; axial FLAIR sequence [TR 8000ms; TE 84ms; slice thickness 4mm; acquisition matrix 320x210; in-plane resolution 0.7188mm x 0.7188mm]; T1 magnetization-prepared rapid gradient echo (MPRAGE) transversal, sagittal and coronal, after contrast [TR 2200; TE 2.67ms; slice thickness 1 mm; inversion time 900ms; in-plane resolution 0.9766 x 0.9766 mm; acquisition matrix 256 x 246] and T2 mapping [TR 3100ms; TE 13.8-165.6ms with twelve TEs: 13.8 ms, 27.6 ms, 41.4 ms, 55.2 ms, 69 ms, 82.2 ms, 96.6 ms, 110.4 ms, 124.2 ms, 138 ms, 151.8 ms, 165.6 ms; total acquisition time 5 minutes 19 seconds]. T2 maps were reconstructed online by MapIt (Siemens, Erlangen, Germany). MapIt uses a voxel-wise, monoexponentially nonnegative least-squares fit analysis with a voxel size of 1.9 x 1.0 x 3 mm^3.

2.4 Image Processing and Analysis

Quantified data assessment was performed using the visage software tool by Visage Client (Visage Imaging/Pro Medicus Limited, Version 7.1.10), with all measured values collected here. Subsequently, ROI were manually drawn (M.K., E.W.) on the T2 mapping sequences for quantitative analysis by calculation of T2 relaxation times in this sequence. The ROI size was always 5 mm in diameter (area 19mm^2). Determination of the slice to be used was always decided based on the largest extent of tumoral and peritumoral T2w/FLAIR hyperintensity. All ROI's covered parts that were representative of the whole area's tissue; in other words, the ROI was meant to reflect the tumor's homogeneity or heterogeneity. The aim was not to include the most hypointense nor the most hyperintense part, but rather something in between. If vessels, necrosis, sulci or artifacts were present, the ROI was shifted by a few millimeters. Representative regions which were free of cysts, and necrotic cavities were consistently selected to create reliable measurements.

We always delineated the central ROI (cROI) additionally depending on the hypothesis of a peripheral ROI (pROI) or three ROI's in the edema/infiltration zone. The anatomic center of the tumor was marked with the cROI. All other ROIs were selected on the same slice as the cROI. Oriented toward the anatomical tumor margins, the pROI was located within the outer tumor border at the transition to the infiltration zone, or at an area of edema with 1/10 of the ROI. The tissue included in the pROI was directly adjacent to the edema/infiltration zone. To assess the peritumoral zone/edema, we delineated three ROI's (ROI 1-3) on a beam from the cROI to the outer border of the edema/infiltration zone. The mean, minimal (min) and maximal (max) T2 relaxation time was measured. Furthermore, the range was calculated: $T2\,range = max - min$.

To examine the validity of our measurements, an additional ROI was placed in the healthy white matter (WM) of the contralateral hemisphere at a level not including the lateral ventricles. We preferred using the contralaterally paired lobe, following the method of *Badve et al. (2017)* [49]**.** If there was not any normal-appearing WM present, we shifted the ROI to a different localization, most often in the frontoparietal region [49]**.** To demonstrate the reliability of our T2 measurements, we took the mean value for the WM which is supported by recent studies which reported ranges from 84 to 87 ms ± 3 ms in 1.5 T MRI [31]; and 74 to 80 ms ± 1 ms in 3.0 T [50]. Additionally, we compared the WM values of 1.5 T and 3 T MRI to rule out the source of error occurring through the mixture of field strengths.

Tissue heterogeneity was rated on a scale from 1 (low) to 3 (high); > 25% heterogeneity within the tumor was defined on a visual basis as a heterogeneous pattern. Additionally, enhancing tumor (yes/no) and necrosis (yes/no) were evaluated in T2 mapping, T2w/FLAIR, T1/contrast enhancing (CE) and T1 MPRAGE sequences. Hypointense tissue within the tumor volume without any signs of CE behavior was determined as necrosis. Finally, the tumor's mean maximal T1 perpendicular diameter and T2w/FLAIR diameter, i.e. edema/infiltration zone, was also assessed. A significantly increased T2w/FLAIR signal intensity of more than 25 % after administration of contrast material compared with the T1/CE-sequences was defined as edema (yes/no).

The tumor localization was assessed anatomically; statistical evaluation was carried out between frontoparietal or frontotemporal localization, and "other". In the second publication, regarding the results from *Villanueva-Meyer et al. (2018)*, the age was recorded as a binary measure with a cut off at > 45 years, which may be predictive for IDH-wt [28].

2.5 Interobserver Variability

An experienced neuroradiologist (> 10 years of experience) and a second evaluator (2 years of experience) marked out the central, peripheral and parenchymal ROI's in WHO grade II and III gliomas, following the same procedure as described in the previous section. They were blinded with respect to the mutational status and the WHO grade. Subsequently, the values for both measurements were compared by use of Cronbach's alpha statistical test for a significant interobserver concordance.

2.6 Statistics

Data analysis was performed using XLSTAT (Version 2011,0,01; Addinsoft SARL, New York, USA) and SPSS Software (Version 25; IBM; New York, USA). Results were determined as statistically significant when $p < 0.05$. Asymptomatic significance was selected for $n \geq 30$; where $n < 30$, we used the exact significance. To assess the group median values, Mann-Whitney-U was applied as a two-tailed test. A rank sum test/variance analysis was performed by applying the Kruskal-Wallis-Test. Outlier analysis was performed by means of the Z-score. Effect size of the group mean values was calculated by use of Cohen's d. Interpretation of effect size was conducted following the method of Cohen (1988): for $r = \left|\frac{z}{\sqrt{n}}\right|$,

$|r| < 0.1$ was determined as small effect; $0.1 \leq |r| < 0.3$ as medium; and $|r| \geq 0.5$ as a strong effect $[-1; 1]$. Spearman's Rho for non-normally distributed data sets was used to determine correlation coefficients. Analysis of the differences between the group means was performed by analysis of variance (ANOVA).

To investigate their distribution, the data were analyzed using the Kolmogorov-Smirnov-Test. Subsequently, multivariate analyses of receiver operating characteristics (ROC) were used to ascertain the quality of the chosen parameter, to compare single parameter distributions concerning WHO grade and IDH mutation status, and to identify suitable parameters. The significant or trending parameters were then used as part of multivariate ROC analyses, and the AUC was evaluated. Standardized coefficients [95% confidence intervals (CI)] were evaluated and single AUCs were generated to define the statistical influence for all score categories. Finally, cross validation was performed for ROC analyses.

To evaluate the regional T2 value distribution in the peritumoral zone in relation to the tumor and parenchyma signal intensity, mean T2 values were obtained from the cROI, the ROI 1-3 and the parenchymal ROI. These were modeled applying a second-degree polynomial function, whose coefficients were calculated by a minimization of the data's deviations square sum. The basic function in the fit model was: $y = ax^2 + bx + c$. The stretch factor a thus represents the T2 increase in the peritumoral zone/edema. Plots were generated showing the original data and the model data. A second-degree fit was chosen as it precisely matches the data's basic shape and a higher degree polynomial does not improve the results. The determined model parameter a describes the curve's opening angle, and is therefore the stretch factor. The higher the fit-model value, either positive or negative, the narrower the angle is. The more the value approaches zero, the more the curve approaches a horizontal. Overall, the stretch factor of the second-degree fit shows the increase of T2 values in the peritumoral zone/edema. It was calculated for every subject and presented in the model function.

A coefficient of determination (R^2) ranging between 0 and 1 was calculated to assess the validity of the model. The narrower R^2 is to 1, the better the model data fit with respect to the original data. The Mann-Whitney-U test was used to compare the determination coefficients and model parameters/stretch factors.

3 Results

General information in relation to our study subjects and the exact value distributions for the separate tumor entities are presented in the respective study.

3.1 T2 Mapping of Molecular Subtypes of WHO Grade II/III Gliomas

General information: Within both subgroups, the patients with IDH-mut WHO grade II and III astrocytoma were significantly younger than those with the IDH-wt (**p=0.0105**). Frontal and parietal localizations predominate in IDH-mut tumors **(p<0.0001)**. ANOVA demonstrates no statistically significant impact of age, gender and localization on the T2 values of gliomas. (p=0.573; p=0.8461; p=0.6145).

Quality of the study: There was no significant difference between the T2 values of WM obtained using 1.5 T (83.6 ± 3.1 [80-89 ms]) and 3 T (81.3 ± 2.4 [78-86 ms]) MRI (**p=0.053**). Overall there was no significant interobserver variability (**p=0.9509**).

MRI examination: Firstly, the results showed significantly longer T2 relaxation times in the cROI than in the pROI (**p=0.0021; p=0.0288; p=0.0362; p=0.0185; p=0.0014; p=0.0433**). This difference between the inner and outer ROI represents the outwardly decreasing signal intensity of WHO grade II and III astrocytomas (Table 2)[1]. Secondly, evidence was found for the higher signal intensity of IDH-mut astrocytomas compared to the IDH-wt, represented by the significantly longer T2 relaxation times (**p=0.0037; p=0.0094; p=0.0190; p=0.0056**). A large impact of IDH-mut on the T2 values was shown by the ANOVA (**p<0.001**). Interestingly, by contrast with respect to the WHO grade, the results in equal differentiation by use of T2 mapping were not significant (p=0.2276; p=0.5547). Moreover, the central part of A2 reaches the same intensity as the peripheral part of AA3 (p=0.9890). Significant differences were found not only for the central T2 relaxation times, but also for their ranges, thus the difference between their maximum and minimum values. In addition to the aforementioned results, IDH-mut astrocytomas had a significantly larger range than the IDH-wildtype (**p=0.0017; p=0.0042**). Cohen's d showed a large effect size and a strong impact of IDH-mut on central and peripheral T2 values (**d=1.766**; r=0.654; **d=1.506**; r=0.594). As ATRX loss is predominantly associated with IDH-mut, significantly longer T2 relaxation times were found in central ROI (**p=0.001**; r=0.622), peripheral ROI (**p=0.001**; r=0.646) and a larger T2 range (**p=0.006**; r=0.518). MGMT promotor methylation was correlated with higher signal intensity as well in cROI (**p=0.005**; r=0.529) and pROI (**p<0.001**; r=0.661). A strong effect size was determined for all calculations. No significant difference was identified regarding the T2 range and MGMT (p=0.0980), while the effect size was medium (r=0.328). There was a significant correlation, with intermediate effect sizes, between higher rates of mutated TP53 (≥ 5%) and central T2 relaxation time (**p=0.009**; r=0.474) and the central T2 range (**p=0.014**; r=0.451) respectively. Peripheral T2 times did not show a significant result as the effect size is lower (p=0.107; r=0.294). No significant correlation was detected between tumor size, edema size and the WHO grade (p=0.562; p=0.2990) or the IDH mutation status (p=0.616; p=0.5054) respectively. ANOVA showed a small influence of the WHO grade on the T2 values in this cohort (**p=0.0472**). Curiously, A2 and IDH-mut gliomas showed significantly more necrosis (**p<0.0001**; **p<0.0001**) than AA3 or even the IDH-wt, while A2 and IDH-wt gliomas showed more CE (**p<0.0001**; **p<0.0001**). The mean values for heterogeneity revealed no significant disparity regarding the IDH-status (p=0.7957) or the WHO grade (p=0.583).

Spearman's Rho correlation coefficient: Further analyses showed a coincidence of IDH and ATRX (**r=1; p<0.001**). Correlation coefficients for IDH and MGMT (**r=0.754; p<0.001**) and TP53 (**r=0.577; p=0.001**) also showed strong correlations. The analysis did not confirm any correlations between IDH and the WHO grade (r=0.059; p=0.755).

3.2 Multivariable Non-Invasive Association of Isocitrate Dehydrogenase Mutational Status in World Health Organization Grade II and III Gliomas with Advanced Magnetic Resonance Imaging T2 Mapping Techniques

General information: As shown in the first study, patients with IDH-mut gliomas were significantly younger in binary calculation (>45/<45 years old) (**p=0.031**) than those with IDH-wt. Frontotemporal localization predominates in IDH-mut gliomas (**p=0.014**).

Quality of the study: No significant correlation was found between T2 values of WM obtained using 1.5 T (82.9 ± 4.4 [69-89 ms]) and 3 T (80.6 ± 3.1 [74-86 ms]) MRI (**p= 0.448;** r=0.150). There was no significant interobserver variability (**p=0.9450;** r=0.009).

MRI examination: The mean central T2 relaxation times and ranges of IDH-mut and IDH-wt gliomas differed significantly each respectively having strong medium effect sizes (**p=0.004;** r=0.631**; p=0.008;** r=0.433). No other examined parameter (heterogeneity, CE behavior, maximal T2w/FLAIR diameter, necrosis, maximal T1 perpendicular diameter) was significant with respect to the IDH-mutational status (p>0.05).

As mentioned above, ATRX loss shows significant results for longer central T2 relaxation time (**p=0.001**; r=0.630) and a higher range (**p=0.036**; r=383) with intermediate to strong effect sizes. MGMT methylation was associated with higher central SI (**p=0.006**; r=0.495), without a correlation to the T2 range (p=0.171; r=0.258). Central T2 relaxation times and ranges showed significant differences regarding TP53 (**p=0.026**; r=3.87; **p=0.026**; r=0.387). However, the effect size was only medium.

Multivariate ROC analyses in relation to the IDH-status were carried out for the parameters: central T2 relaxation time and range, localization and age; the results show an AUC of **0.955** (**p<0.001;** sensitivity 94.7%, specificity 92.3%, accuracy 0.937; 95% CI 0.887-1.000). By far the strongest correlation for single score category standardized coefficients was found for the central T2 relaxation time (AUC **0.872**; 95% CI 0.750-0.995), with a cut-off value for the IDH mutation of 231ms (sensitivity 89.5%; specificity 76.9%). Central T2 range showed an AUC of **0.767** (95% CI 0.587–0.948), and cut off of 99ms (sensitivity 84.2%; specificity 69.2). Age calculated as a metric variable showed the second highest AUC in ROC analyses (AUC **0.809**; 95% CI 0.657–0.963); the cut off was set at 49.0 years (sensitivity 84.2%; specificity 69.2%). AUC calculated for localization (binary) was **0.717** (95% CI 0.545–0.881), exhibiting high sensitivity (94.7%) but low specificity (53.8%). The analyses did not identify any significant parameters regarding the WHO grade (p>0.05), hence no multivariate ROC analysis was performed.

Spearman's Rho correlation coefficient: The highest correlation was found for IDH and ATRX once again (**r=1; p<0.001**). IDH and MGMT showed a strong effect correlation (**r=0.705; p<0.001**), while IDH and TP53 revealed only a medium Rho value (**r=0.487; p=0.004**). Again, there was no correlation found between IDH and the WHO grade (r=0.063; p=0.726).

3.3 T2 Mapping of the Peritumoral Infiltration Zone of Glioblastoma and Anaplastic Astrocytoma

General information: In this study, patients suffering from GBM or IDH-wt gliomas were significantly older than with AA3 or IDH-mut (**p<0.001; p<0.001**). MGMT promotor methylation was found significantly more often in IDH-mut (**p=0.001**); no differences regarding the WHO grade could be confirmed. No significant correlations were found for sex or tumor localization.

Quality of the study: No significant correlation was found between T2 values of WM obtained at 1.5 T (84.4 ± 3.8 [79-91 ms]) and 3 T (82.0 ± 3.3 [77-88 ms]) MRI (**p= 0.448;** r=0.150).

MRI examination: IDH-mut gliomas had a significantly larger tumor diameter (**p=0.025**); interestingly, no difference was found regarding the WHO grade (p=0.811). Remarkably, there is a significantly longer central T2 relaxation time (**p<0.001**; r=0.556) and a larger range (**p=0.040**; r=0.303) in AA3 than in GBM. Central T2 relaxation times were significantly longer in IDH-mut (**p<0.001**; r=0.680); they also showed a higher central T2 range (**p=0.001**; r=0.471). The analysis with respect to ATRX loss (**p>0.001**; r=0.600; **p=0.014**; r=0.372) and MGMT methylation (**p=0.001**; r=0.522; **p=0.021**; r=0.361) showed similar results. Effect size was always medium to high. No significant correlation was found between T2 time or range and TP53 (p=0.843; r=0.290; p=0.522; r=0.094), associated with a small effect size. In this study, IDH-wt gliomas and GBM showed significantly more necrosis and CE (**p=0.006;** r=0.0433; **p<0.001;** r=0.547; **p<0.001;** r=0.797; **p<0.001;** r=0.765). The largest effect size was found for correlation with WHO grade. Importantly, IDH-wt and GBM had a larger diameter of edema/peritumoral zone (**p=0.011; p=0.012**) than the IDH-mut or AA3. Investigation of the peritumoral zone with the fit-model revealed a significantly higher model parameter in GBM (**p=0.0049**) and IDH-wt gliomas (**p=0.0430**). There was a significantly narrower curve stretch factor in these subgroups, as IDH-mut and AA3 show flatter curves. The coefficient of determination showed strong statistical proof for both investigations (p=0.9987; $\mathbf{R^2 > 0.93}$; p=0.4180; $\mathbf{R^2 > 0.94}$).

Spearman's Rho correlation coefficient: In this study, there was high correlation between IDH and ATRX (**r=0.951; p<0.001**) and MGMT (**r=0.576; p<0.001**). A medium correlation was found for IDH and TP53 (**r=0.303; p=0.041**). There was a significant highly negative correlation between IDH and the WHO grade (r=0.608; p<0.001) as the IDH mutation is more likely to occur in AA3 than in GBM.

4 Discussion

This study investigated T2 mapping sequences in MRI for describing possible imaging changes caused by the molecular subtypes of WHO grade II-IV gliomas. The IDH mutation seems to cause the most expressive imaging alterations in this study population.

Firstly, there is a significantly increased T2 relaxation time and range in IDH-mut gliomas. Secondly, comparison of T2 mapping values with established imaging parameters for IDH-mut gliomas by use of multivariate ROC analyses showed the highest coherence for the central T2 relaxation times. The highest validity indicating IDH mutation on MRI was achieved by combination of central T2 relaxation time and range, age and localization, whereby an AUC of 0.955 could be demonstrated. Investigations of the

peritumoral zone of WHO grade III and IV gliomas with a specifically developed fit-model showed a significantly higher model parameter in GBM and IDH-wt gliomas, emphasizing imaging changes that were even found outside the definable tumor borders. In conclusion, all hypotheses of the study were validated by the highly interesting results which emerged from the data.

Further clarification of these results is necessary. In particular, concrete validation continues to be challenging as there are no other publications concerning glioma imaging and T2 mapping to date. Nevertheless, we assume that the apparently higher T2 signal seems to be characteristic of IDH-mut gliomas. The impressive large effect size supports this idea. An explanation could be the accumulation of D2HG, leading to altered tumor metabolism [41,46,51]. Additionally, the relaxation times in the T2 sequence might increase due to edema, increased vascularization, angiogenesis, apoptosis, or higher water content in the extracellular space [39,41,48]. A longer T2 relaxation time effectively means that the spins are able to maintain their transverse magnetization longer [39]. This is based on a lower energy exchange between the spins which might be caused by specific compositions of tissue and molecules [39].

The results also showed a larger range of T2 values in IDH-mut WHO grade II and III gliomas. This finding is noteworthy as it might support the IDH-specific heterogeneity of gliomas as postulated by *Darlix et al. (2017)* [20]. In line with these investigations, a study by *Lee et al. (2015)* also confirmed the so-called microenvironmental heterogeneity of IDH-mut WHO grade III/IV gliomas by using histograms from the MRI sequences DWI, ADC, and perfusion-weighted imaging [48]. A possible explanation could be that a higher rate of apoptosis may occur through the inhibited PI3K/Akt signaling pathway, leading to necrosis that is invisible macroscopically and which is displayed at lower T2 values [25]. Presence of stabilized HIF-1α results in extensive angiogenesis and vascularization, which may also produce heterogeneity and higher T2 values in IDH-mutated gliomas [6,29,32]. *Hattingen et al. (2013)* supported this theory in their study which showed a significantly decreased T2 relaxation time under anti-angiogenetic therapy with bevacizumab at the stage of tumor recurrence [41].

Results for heterogeneity as assessed in macroscopic examination did not show any significant differences regarding the IDH-status. This differs from previous studies, such as a study by *Qi et al. (2014)* which reported a significantly more homogenous signal intensity in IDH-mut gliomas, but is consistent with a study by *Metellus et al. (2010)* which described no significant IDH dependent difference in heterogeneity [19,52]. In summary, heterogeneity on macroscopic examination might not always correlate with the mutational status. Nevertheless, the IDH mutation seems to create some microenvironmental heterogeneity [48].

All the publications referred to demonstrated a significant correlation of IDH-mut with younger patient age. This fact has already been shown in several studies, however, supporting the thrust of our findings [19,22,28,29,46]. The parameter of age is an important factor to take into account at the time of diagnosis. In IDH-mut WHO grade II and III astrocytomas, fronto-temporal and/or fronto-parietal localizations predominate significantly. This is consistent with the current state of the literature, and as a result the tumor localization also shows a high degree of validity [4,8,19,22,45].

Furthermore, the examinations showed a significant difference between the central and peripheral tumor regions as there was a significant decrease in T2 relaxation times in the outer tumor zones. As this is the first study reporting this result, it is difficult to compare. The lower values in the peripheral tumor zone could have been generated due to a higher quantity of parenchymal cells with shorter T2 relaxation times, which would lower the mean values. This supports the idea that gliomas always grow outwardly and in an infiltrative manner [19,35].

A remarkable feature is the unexpectedly high predictive accuracy and sensitivity for IDH presented by multivariate ROC analyses. *Carrillo et al. (2012)* investigated the potential of a combination of conventional MRI features, such as localization and tumor size, to predict the IDH-status in HGG [8,53]. Their results showed good accuracy and specificity but only low sensitivity [8,53].

Another promising approach for the identification of IDH-mut tumors is the usage of MR spectroscopy as it is an established technique for visualization of tumor biology [6,8,27,47]. Several authors, such as *Elkhaled et al. (2012)* and *Andronesi et al. (2012)* used MR spectroscopy to detect higher levels of D2HG in gliomas [8,27,47]. The majority of those studies demonstrated that the IDH-status and D2HG levels correlate strongly, suggesting that determination of the IDH-status might be possible with MR spectroscopy as the calculated sensitivity was always high [8,27,47]. Nevertheless, MR spectroscopy remains highly specific, which could be the reason why it is not yet the clinical standard [8]. As conventional MRI is the modality of choice in clinical diagnosis and treatment planning, it is important to integrate a method and reliable prediction algorithms into standard MR imaging.

Our results were striking in the sense that the combination of advanced T2 mapping relaxation times and ranges with the conventional features of age and localization achieved nearly the same levels of high accuracy and sensitivity as MR spectroscopy [8]. Single score category standardized coefficients showed the highest correlations by far for the T2 mapping parameters, potentially indicating that these are predominating factors. Furthermore, the presentation of cut-off values (T2 relaxation time 231ms, range 99ms, age 49 years) provides a simple way to apply this system clinically.

The comparison of T2 relaxation times of WHO grade II/III gliomas resulted in no reproducible statistical significance, despite our data showing that A2 have lower intensities than AA3. Only ANOVA revealed a small impact of the WHO grade on the T2 values. These results share a number of similarities with *Schäfer et al.'s (2013)* and *Patel et al.'s (2018)* findings [54,55]. *Schäfer et al. (2013)* investigated different morphological MRI characteristics of 108 patients with WHO grade II and III gliomas [54]. By use of ROC analyses, they also found no significant difference in T2 sequences between gliomas of both grades, but did find significant differences on the basis of CE, cortical involvement, smooth delineation of CE and the width of the infiltration zone [54]. *Patel et al. (2018)* did not find differences in the segmented volume of T2 hyperintensity in relation to the WHO grade [55]. These results are genuinely meaningful as they pursue the same goal, which is to approach reliable predictions through noninvasive diagnostics and WHO grade identification. They further demonstrate that this might not be possible through use of T2 sequences. It seems that there is no evidence for the reliable differentiation between WHO grade II and III gliomas based

on T2 signal characteristics, whereby the IDH-mutational status might be more important than the WHO grade.

Divergent results were found regarding CE and necrosis. In the subgroup of WHO grade II and III tumors, there was significantly more necrosis in IDH-mut and A2 gliomas, while IDH-wt and A2 showed more CE. The second publication presenting an extended population could not confirm these results. No statistical significance was found regarding these parameters and the WHO grade or IDH-status respectively. These contrasting results are in line with the findings by *Schäfer et al. (2013)* who had previously postulated that valid distinction between WHO grade II and III gliomas is challenging as both grades can have abnormal features on imaging, such as CE and necrosis [54]. This supports findings by *Lee et al. (2015)* who had concluded that the T2 SI is superior to other imaging modalities like contrast-based imaging, as more components resulting in tumors heterogeneity can be studied using the T2 sequence [48].

In line with results from *Qi et al. (2014)*, edema and tumor size did not show any significant results in the first two subgroup analyses of WHO grade II/III astrocytomas [4]. However, when analyzing WHO grade III/IV gliomas, an increased tumor size could be identified in IDH-mutated gliomas. This result indicates that the tumor size might not always point to malignancy in HGG, even if clinical complications are evidently more likely to occur with increasing tumor mass. On the other hand, HGG with worse prognosis, similar to GBM and IDH-wt AA3, showed a larger peritumoral zone/edema, more necrosis and more CE. When all HGGs were included, these parameters could be representative of aggressiveness as 22/22 GBMs showed CE and 21/22 had necrosis [8].

Examination of the peritumoral zone/edema of HGG using the fit-model and the model parameter derived on that basis revealed similar results as GBM and IDH-wt gliomas had a significantly higher model parameter. As such, they show distinctly narrower curve shapes resulting from a larger difference in SI between the tumor and the peritumoral zone/edema. GBM and IDH-wt gliomas have shorter intratumoral T2 relaxation times and show an increased SI, especially in the region 5-10mm outside the visually defined tumor border (Figure 1-5) [3]. On the other hand, AA3 and IDH-mut gliomas showed flatter and more sharply decreasing curves as they have higher intratumoral T2 values and ranges as well as more T2 drawdown in the peritumoral zone/edema (Figure 1-5) [3]. Nevertheless, it is important to mention that due to remarkably less cases of IDH-mut GBM being included, these findings need to be interpreted with caution. Regrettably, we are unable to clearly explain if the data distribution was caused by the WHO grade or the IDH-mutational status. Either way, the results show that there is a significant difference in T2 relaxation times measured by T2 mapping sequences which needs further investigation.

Additionally, from the reported results in relation to the IDH-status, some surprising results regarding ATRX, MGMT and TP53 were found. Unfortunately, this study is not able to derive information about possible imaging changes caused by 1p/19 co-deletion as any patients with this mutation were initially excluded. ATRX loss showed some statistical significance with respect to SI and T2 range in WHO grade II-IV gliomas. A rate of mutated TP53 equal to or greater than five percent was also associated with higher SI and T2 range in WHO grade II/III gliomas. By contrast, there was no significant results for AA3 and

GBM. On the basis of these few outcomes, closer examination using the correlation coefficient revealed consistently medium to high correlations of IDH, ATRX and TP53. This is in line with the current state of the literature, just as we stated in the introduction that the IDH mutation is associated with ATRX loss and mutation of TP53 [8,22]. Interestingly, MGMT promotor methylated gliomas showed higher SI and also presented a larger T2 range in some subpopulation. Contrary to expectations and in contrast with previous studies, there was a high correlation of IDH-mut and MGMT in this study [8]. At the time of writing, there were no similar results found in literature [8]. It is very likely that the study population was not representative enough concerning MGMT, erroneously leading to these results. In summary, we cannot rule out that the other mutations may have influenced the results of IDH. However, in light of the fact that several other relevant studies have stated that IDH is most likely to cause imaging alterations, it can be reasonably assumed that IDH had the major influence on the results presented [8].

Further investigation of correlation coefficients revealed other interesting results. There was no correlation between IDH and WHO grade in WHO grade II and III gliomas. Examination of HGG on the other hand showed a highly negative correlation, which means that in our population the IDH mutation was more likely to occur in AA3. This finding is in line with findings by *Smits et al. (2017)* and several other studies as the mutation is less frequent in GBMs [4,6,8,9,15,19,23–26]. Even though, it should be interpreted with caution as it could be influenced by a bias due to imbalanced data distribution, particularly in GBM [4,6,8,9,15,19,23–26].

One of the most striking results is the high technical quality of this study. The mean values for WM in 1.5 T and 3 T are effectively in line with the literature, indicating reliable quality of the results [31,50]. To date, histopathological examination have been known for its large interobserver and intraobserver mismatch [22]. In contrast, our method presents a consistently high interobserver concordance, which is a major benefit. Of course, histopathological examination continues to be the gold standard for detecting IDH-mutational status, even though our procedure and the technique of T2 mapping has many beneficial applications [22,54]. The small interobserver variabilities demonstrate the reliability of this noninvasive technique, the reproducibility of the results and its independence from various observers. Nevertheless, there were significant discrepancies regarding the intratumoral SIs, highlighting that ROI localization is of immense importance when using this technique. Furthermore, there is no significant difference between T2 mapping techniques for comparing measurements of brain parenchyma performed using 1.5 and 3.0 T MR scanners. This is entirely consistent with the literature, as from a purely technical perspective, a strong impact of the field strength on T2 values cannot occur due to the fact that T2 sequences measure spin-spin interaction which is unaffected by the field strength [39,40]. T1 sequences, on the contrary, are highly influenced by the field strength as they measure spin-lattice interactions. In daily routine practice, it cannot always be guaranteed that scanners of the same field strength are available. In line with findings by *Dekkers et al. (2018),* this might imply that the T2 mapping sequence, compared to T1 mapping, can be more easily implemented in research and is a more stable technique for applications in a clinical setting [42].

Further studies with respect to advanced MRI features in specific T2 mapping are required. Volume-based histogram analyses are required to gather more detailed information about tissue composition and signal behavior of molecular subtypes of gliomas. Therefore, regular implementation of T2 mapping sequences in preoperative imaging is fundamental to generate larger sample sizes to broaden studies using this technique which has proven highly promising. The combination of automated multiparametric and algorithm-based MRI evaluation, including ADC Maps and T2 mapping, might be a promising avenue to pursue in future. In conclusion, even if some promising modalities for advanced noninvasive IDH determination already exist, T2 mapping represents a clear advance with respect to current methods.

5 Limitations

We are aware that this study may have some more limitations beyond those previously mentioned. The first is that the retrospective design and the very fact that the various observers are aware of this design, which may lead to intrinsic limitations. The second is the inclusion of pre-treated patients. However, it should be noted that all patients with visible or measurable imaging alterations caused by the earlier treatment were excluded to minimize the bias. Other limitations were the small sample size, the ROI and non-volume-based evaluation, as well as the lack of histogram analysis to obtain more precise information about the tissue composition. As mentioned in the discussion section, the imbalanced data distribution for HGG is another possible source of errors as we are not able to clearly define whether some of the results are influenced by this factor. The inclusion of MRI's obtained using 1.5 T and 3 T implies another possible bias; our results are in line with a study by *West et al.'s (2013)*, for example, which points out that no significant influence is found on T2 values of the brain parenchyma due to MRI scanner field strength [39,40].

6 Conclusion

The new WHO classification reinforces the importance of molecular genetic markers such as IDH, as they are predictive for prognosis and, as various studies have shown, MR imaging [4,8,15,19,28,29]. To the best of our knowledge, this is the first study investigating WHO grade II-IV gliomas by use of quantitative T2 mapping to detect possible imaging changes associated with their mutational status. The results demonstrate a significant correlation between the mutational status of gliomas and T2 relaxation times. Large ranges for T2 relaxation times provide evidence that the previously described IDH-associated heterogeneity exists on a microenvironmental level. Analyzing established clinical and qualitative imaging characteristics, this study has been able to confirm the findings from previous studies that IDH-mutated gliomas are associated with fronto-parieto-temporal localizations and younger patient age. The highest validity for predicting the IDH-status in cases of glioma is achieved by combination of T2 relaxation time characteristics and conventional qualitative MRI features. Not only intratumoral and intertumoral variations were detected, but rather first-time investigations of the peritumoral zone/edema of HGGs showed significant differences revealing a potential area of investigation for further trials.

Until now, there has been no established and sufficient investigated technology for noninvasive diagnosis of the mutational status of gliomas. Nevertheless, further studies in relation to advanced quantitative MRI techniques and molecular subtypes of gliomas are necessary. T2 mapping seems to be promising as it provides a powerful tool for not only qualitative, but also quantitative image analysis.

This study provides the basis for introducing quantitative T2 mapping sequences into imaging for gliomas. Its clinical applicability is essential. Furthermore, all qualitative or quantitative MRI techniques which have been described in the past were statistically similar or inferior to this method. This study is able to fully support a fundamental recommendation for T2 mapping for future implementation in the field of neuroradiology.

Literaturverzeichnis

1. Kern M, Auer TA, Picht T, Misch M, Wiener E. T2 mapping of molecular subtypes of WHO grade II/III gliomas. BMC neurology. 2020;20:8.
2. Kern M, Auer TA, Fehrenbach U, Tanyildizi Y, Picht T, Misch M, Wiener E. Multivariable non-invasive association of isocitrate dehydrogenase mutational status in World Health Organization grade II and III gliomas with advanced magnetic resonance imaging T2 mapping techniques. Neuroradiol J. 2020;33(2):160–8.
3. Auer TA, Kern M, Fehrenbach U, Tanyildizi Y, Misch M, Wiener E. T2 mapping of the peritumoral infiltration zone of glioblastoma and anaplastic astrocytoma. Neuroradiol J. 2021;0(0):1–9.
4. Qi S, Yu L, Li H, Ou Y, Qiu X, Ding Y, Han H, Zhang X. Isocitrate dehydrogenase mutation is associated with tumor location and magnetic resonance imaging characteristics in astrocytic neoplasms. Oncol Lett [Internet]. 2014 [cited 2018 Apr 12];7(6):1895–902. Available from: https://www.ncbi.nlm.nih.gov/pmc/articles/PMC4049752/pdf/ol-07-06-1895.pdf
5. Yan H, Parsons DW, Jin G, McLendon R, Rasheed BA, Yuan W, Kos I, Batinic-Haberle I, Jones S, Riggins GJ, Friedman H, Friedman A, Reardon D, Herndon J, Kinzler KW, Velculescu VE, Vogelstein B, Bigner DD. *IDH1* and *IDH2* Mutations in Gliomas. N Engl J Med [Internet]. 2009 Feb 19 [cited 2017 Jun 5];360(8):765–73. Available from: http://www.nejm.org/doi/abs/10.1056/NEJMoa0808710
6. Zhang C, Moore LM, Li X, Yung WKA, Zhang W. IDH1/2 mutations target a key hallmark of cancer by deregulating cellular metabolism in glioma. Neuro Oncol. 2013;15(9):1114–26.
7. Wen PY, Macdonald DR, Reardon DA, Cloughesy TF, Sorensen AG, Galanis E, Degroot J, Wick W, Gilbert MR, Lassman AB, Tsien C, Mikkelsen T, Wong ET, Chamberlain MC, Stupp R, Lamborn KR, Vogelbaum MA, Van Den Bent MJ, Chang SM, Robert P. Updated Response Assessment Criteria for High-Grade Gliomas: Response Assessment in Neuro-Oncology Working Group. J Clin Oncol [Internet]. 2010 [cited 2018 Apr 29];28:1963–72. Available from: http://ascopubs.org/doi/pdfdirect/10.1200/JCO.2009.26.3541
8. Smits M, van den Bent MJ. Imaging Correlates of Adult Glioma Genotypes. Radiology [Internet]. 2017 Aug 19 [cited 2018 Mar 6];284(2):316–31. Available from: http://pubs.rsna.org/doi/10.1148/radiol.2017151930
9. Zhang B, Chang K, Ramkissoon S, Tanguturi S, Bi WL, Reardon DA, Ligon KL, Alexander BM, Wen PY, Huang RY. Multimodal MRI features predict isocitrate dehydrogenase genotype in high-grade gliomas. Neuro Oncol [Internet]. 2017 Jan [cited 2018 Mar 6];19(1):109–17. Available from: http://www.ncbi.nlm.nih.gov/pubmed/27353503
10. Hess KR, Broglio KR, Bondy ML. Adult glioma incidence trends in the United States, 1977-2000. Cancer [Internet]. 2004 [cited 2017 Jun 1];101(10):2293–9. Available from:

http://onlinelibrary.wiley.com/store/10.1002/cncr.20621/asset/20621_ftp.pdf;jsessionid=6F3705FA1812B89423CF00FB2BADDF22.f01t04?v=1&t=j3eh06oy&s=e6ec13bbdfa42c661ecbcf244a1885376aa25b00

11. Wen PY, Kesari S. Malignant Gliomas in Adults — NEJM. Malig gliomas adults [Internet]. 2008;359(5):492–507. Available from: http://www.ncbi.nlm.nih.gov/pubmed/18669428
12. Weller M, van den Bent M, Tonn JC, Stupp R, Preusser M, Cohen-Jonathan-Moyal E, Henriksson R, Rhun E Le, Balana C, Chinot O, Bendszus M, Reijneveld JC, Dhermain F, French P, Marosi C, Watts C, Oberg I, Pilkington G, Baumert BG, Taphoorn MJB, Hegi M, Westphal M, Reifenberger G, Soffietti R, Wick W. European Association for Neuro-Oncology (EANO) guideline on the diagnosis and treatment of adult astrocytic and oligodendroglial gliomas. Lancet Oncol [Internet]. 2017;18(6):e315–29. Available from: http://dx.doi.org/10.1016/S1470-2045(17)30194-8
13. Otani R, Uzuka T, Ueki K. Classification of adult diffuse gliomas by molecular markers—a short review with historical footnote. Jpn J Clin Oncol. 2017;47(1):2–6.
14. Reifenberger G, Wirsching HG, Knobbe-Thomsen CB, Weller M. Advances in the molecular genetics of gliomas-implications for classification and therapy [Internet]. Vol. 14, Nature Reviews Clinical Oncology. 2017 [cited 2018 Feb 22]. p. 434–52. Available from: https://doi.org/10.1038/nrclinonc.2016.204
15. Louis DN, Perry A, Reifenberger G, Von Deimling A, Figarella-Branger D, Cavenee WK, Ohgaki H, Wiestler OD, Kleihues P, Ellison DW. The 2016 World Health Organization Classification of Tumors of the Central Nervous System: a summary. Acta Neuropathol. 2016;131:803–20.
16. Louis DN, Ohgaki H, Wiestler OD, Cavenee WK, Burger PC, Jouvet A, Scheithauer BW, Kleihues P. The 2007 WHO Classification of Tumours of the Central Nervous System. Acta Neuropathol [Internet]. 2007 Jul 12 [cited 2017 May 18];114(2):97–109. Available from: http://www.ncbi.nlm.nih.gov/pubmed/17618441
17. Banan R, Hartmann C. The new WHO 2016 classification of brain tumors—what neurosurgeons need to know [Internet]. Vol. 159, Acta Neurochirurgica. 2017 [cited 2018 Feb 25]. p. 403–18. Available from: https://link.springer.com/content/pdf/10.1007%2Fs00701-016-3062-3.pdf
18. Zülch KJ. Principles of the new World Health Organization (WHO) classification of brain tumors [Internet]. Vol. 19, Neuroradiology. 1980. p. 59–66. Available from: http://www.ncbi.nlm.nih.gov/pubmed/6245388
19. Metellus P, Coulibaly B, Colin C, De Paula AM, Vasiljevic A, Taieb D, Barlier A, Boisselier B, Mokhtari K, Wang XW, Loundou A, Chapon F, Pineau S, Ouafik L, Chinot O, Figarella-Branger D. Absence of IDH mutation identifies a novel radiologic and molecular subtype of WHO grade II gliomas with dismal prognosis. Acta Neuropathol [Internet]. 2010 [cited 2018 Apr 26];120(6):719–29. Available from: https://link.springer.com/content/pdf/10.1007%2Fs00401-010-0777-8.pdf
20. Darlix A, Deverdun J, Menjot de Champfleur N, Castan F, Zouaoui S, Rigau V, Fabbro M,

Yordanova Y, Le Bars E, Bauchet L, Gozé C, Duffau H. IDH mutation and 1p19q codeletion distinguish two radiological patterns of diffuse low-grade gliomas. J Neurooncol [Internet]. 2017 [cited 2018 Apr 26];133(1):37–45. Available from: https://link.springer.com/content/pdf/10.1007%2Fs11060-017-2421-0.pdf

21. Jiang M, Dong X, Li J, Li J, Qi J. [IDH1 mutation and MGMT expression in astrocytoma and the relationship with prognosis after radiotherapy]. Zhonghua bing li xue za zhi = Chinese J Pathol [Internet]. 2014 Oct [cited 2017 Jun 1];43(10):668–72. Available from: http://www.ncbi.nlm.nih.gov/pubmed/25567592
22. Delfanti RL, Piccioni DE, Handwerker J, Bahrami N, Krishnan AP, Karunamuni R, Hattangadi-Gluth JA, Seibert TM, Srikant A, Jones KA, Snyder VS, Dale AM, White NS, McDonald CR, Farid N. Imaging correlates for the 2016 update on WHO classification of grade II/III gliomas: implications for IDH, 1p/19q and ATRX status. J Neurooncol. 2017;135(3):611.
23. Riemenschneider MJ, Jeuken JWM, Wesseling P, Reifenberger G. Molecular diagnostics of gliomas: State of the art. Acta Neuropathol. 2010;120(5):567–84.
24. Claus EB, Walsh KM, Wiencke J, Annette M, Wiemels JL, Schildkraut JM, Melissa L, Berger M, Jenkins R, Wrensch M, Carolina N. Survival and low grade glioma: the emergence of genetic information. Neurosurg Focus. 2016;38(1):1–19.
25. Birner P, Pusch S, Christov C, Mihaylova S, Toumangelova-Uzeir K, Natchev S, Schoppmann SF, Tchorbanov A, Streubel B, Tuettenberg J, Guentchev M. Mutant IDH1 inhibits PI3K/Akt signaling in human glioma. Cancer [Internet]. 2014 Aug 15 [cited 2017 Jun 5];120(16):2440–7. Available from: http://doi.wiley.com/10.1002/cncr.28732
26. Lasocki A, Tsui A, Tacey MA, Drummond KJ, Field KM, Gaillard F. MRI grading versus histology: Predicting survival of world health organization grade II-IV astrocytomas. Am J Neuroradiol. 2015;36(1):77–83.
27. Elkhaled A, Jalbert LE, Phillips JJ, Yoshihara HAI, Parvataneni R, Srinivasan R, Bourne G, Berger MS, Chang SM, Cha S, Nelson SJ. Magnetic resonance of 2-hydroxyglutarate in IDH1-mutated low-grade gliomas. Sci Transl Med [Internet]. 2012 Jan 11 [cited 2018 Apr 13];4(116):116ra5. Available from: http://www.ncbi.nlm.nih.gov/pubmed/22238333
28. Villanueva-Meyer JE, Wood MD, Choi B, Mabray MC, Butowski NA, Tihan T, Cha S. MRI Features and IDH Mutational Status of Grade II Diffuse Gliomas: Impact on Diagnosis and Prognosis. Am J Roentgenol [Internet]. 2018 [cited 2018 Dec 20];210(3):621–8. Available from: https://www.ncbi.nlm.nih.gov/pmc/articles/PMC5823758/pdf/nihms931161.pdf
29. Waitkus MS, Diplas BH, Yan H. Isocitrate dehydrogenase mutations in gliomas. Neuro Oncol. 2016;18(1):16–26.
30. Macaulay RJ. Impending Impact of Molecular Pathology on Classifying Adult diffuse Gliomas. Cancer Control [Internet]. 2015 [cited 2017 May 18];22(2):200–5. Available from: https://moffitt.org/File Library/Main Nav/Research and Clinical Trials/Cancer Control

Journal/v22n2/200.pdf

31. Zhou J, Golay X, Van Zijl PCM, Silvennoinen MJ, Kauppinen R, Pekar J, Kraut M. Inverse T 2 Contrast at 1.5 Tesla Between Gray Matter and White Matter in the Occipital Lobe of Normal Adult Human Brain. Magn Reson Med 46 [Internet]. 2001 [cited 2017 Jun 2];46(2):401–6. Available from: http://onlinelibrary.wiley.com/store/10.1002/mrm.1204/asset/1204_ftp.pdf?v=1&t=j3fqo6ic&s=7462188d4613c0916574822b6c900fdf100feb88
32. Jeuken JWM, von Deimling A, Wick W, Herold-Mende C, Hartmann C, Wesseling P, Felsberg J, Mawrin C, Mueller W, Christians A, Capper D, Wolter M, Weller M, Meyer J, Balss J, Unterberg A, Reifenberger G. Type and frequency of IDH1 and IDH2 mutations are related to astrocytic and oligodendroglial differentiation and age: a study of 1,010 diffuse gliomas. Acta Neuropathol [Internet]. 2009 [cited 2018 Feb 22];118(4):469–74. Available from: http://www.mc.vanderbilt.edu/documents/singerlab/files/fulltext.pdf
33. Hoefnagels FWA, De Witt Hamer P, Sanz-Arigita E, Idema S, Kuijer JPA, Pouwels PJW, Barkhof F, Vandertop WP. Differentiation of edema and glioma infiltration: Proposal of a DTI-based probability map. J Neurooncol. 2014;120(1):187–98.
34. Lemée JM, Clavreul A, Menei P. Intratumoral heterogeneity in glioblastoma: Don't forget the peritumoral brain zone. Neuro Oncol. 2015;17(10):1322–32.
35. Claes A, Idema AJ, Wesseling P. Diffuse glioma growth: A guerilla war. Acta Neuropathol. 2007;114(5):443–58.
36. Roth P, Regli L, Tonder M, Weller M. Tumor-associated edema in brain cancer patients: Pathogenesis and management. Expert Rev Anticancer Ther. 2013;13(11):1319–25.
37. Burger PC, Dubois PJ, Schold SC, Smith KR, Odom GL, Crafts DC, Giangaspero F. Computerized tomographic and pathologic studies of the untreated, quiescent, and recurrent glioblastoma multiforme. J Neurosurg. 1983;58(2):159–69.
38. Liang ZP, Haacke EM. Magnetic resonance imaging. Biomed Imaging V - Proc 5th IEEE EMBS Int Summer Sch Biomed Imaging, SSBI 2002. 2002;324(January):2002.
39. Weishaupt D, Froehlich JM, Nanz D, Koechli VD, Pruessmann KP, Marincek B. How does MRI work?: An Introduction to the Physics and Function of Magnetic Resonance Imaging [Internet]. Springer Berlin Heidelberg; 2008. 1–19 p. (Lecture notes in mathematics). Available from: https://books.google.de/books?id=wbizuPJjD04C
40. West J, Blystad I, Engström M, Warntjes JBM, Lundberg P. Application of Quantitative MRI for Brain Tissue Segmentation at 1 . 5 T and 3 . 0 T Field Strengths. PLoS One. 2013;8(9):1–12.
41. Hattingen E, Jurcoane A, Daneshvar K, Pilatus U, Mittelbronn M, Steinbach JP, Bahr O. Quantitative T2 mapping of recurrent glioblastoma under bevacizumab improves. Neuro Oncol. 2013;15(10):1395–404.
42. Dekkers IA, Lamb HJ. Clinical application and technical considerations of T1 and T2(∗) mapping

in cardiac, liver, and renal imaging. Br J Radiol. 2018;91(1092):1–13.

43. Pope WB, Hessel C. Response assessment in neuro-oncology criteria: Implementation challenges in multicenter neuro-oncology trials. American Journal of Neuroradiology [Internet]. 2011 [cited 2018 Apr 29];32(5):794–7. Available from: http://www.ajnr.org/content/ajnr/32/5/794.full.pdf
44. Radbruch A, Lutz K, Wiestler B, Bäumer P, Heiland S, Wick W, Bendszus M. Relevance of T2 signal changes in the assessment of progression of glioblastoma according to the Response Assessment in Neurooncology criteria. Neuro Oncol [Internet]. 2012 [cited 2018 May 2];14(2):222–9. Available from: https://www.ncbi.nlm.nih.gov/pmc/articles/PMC3266385/pdf/nor200.pdf
45. Wang Y, Zhang T, Li S, Fan X, Ma J, Wang L, Jiang T. Anatomical localization of isocitrate dehydrogenase 1 mutation: A voxel-based radiographic study of 146 low-grade gliomas. Eur J Neurol. 2015;22(2):348–54.
46. Verger A, Metellus P, Sala Q, Colin C, Bialecki E, Taieb D, Chinot O, Figarella-Branger D, Guedj E. IDH mutation is paradoxically associated with higher18F-FDOPA PET uptake in diffuse grade II and grade III gliomas. Eur J Nucl Med Mol Imaging [Internet]. 2017 [cited 2018 Jul 30];44(8):1306–11. Available from: https://link.springer.com/content/pdf/10.1007%2Fs00259-017-3668-6.pdf
47. Andronesi OC, Kim GS, Gerstner E, Batchelor T, Tzika AA, Fantin VR, Vander Heiden MG, Sorensen AG. Detection of 2-hydroxyglutarate in IDH-mutated glioma patients by in vivo spectral-editing and 2D correlation magnetic resonance spectroscopy. Sci Transl Med [Internet]. 2012 Jan 11 [cited 2018 Apr 13];4(116):116ra4. Available from: http://www.ncbi.nlm.nih.gov/pubmed/22238332
48. Lee S, Choi SH, Ryoo I, Yoon TJ, Kim TM, Lee S-H, Park C, Kim J, Sohn C, Park S, Kim IH. Evaluation of the microenvironmental heterogeneity in high-grade gliomas with IDH1 / 2 gene mutation using histogram analysis of diffusion-weighted imaging and dynamic-susceptibility contrast perfusion imaging. J. 2015;121:141–50.
49. Badve C, Yu A, Dastmalchian S, Rogers M, Ma D, Jiang Y, Margevicius S, Pahwa S, Lu Z, Schluchter M, Sunshine XJ, Griswold M, Sloan A, Gulani V. MR fingerprinting of adult brain tumors: Initial experience. In: American Journal of Neuroradiology [Internet]. 2017 [cited 2018 Mar 5]. p. 492–9. Available from: http://www.ajnr.org/content/ajnr/early/2016/12/29/ajnr.A5035.full.pdf
50. Wansapura JP, Holland SK, Dunn RS, Ball WS. NMR relaxation times in the human brain at 3.0 Tesla. J Magn Reson Imaging. 1999;9(4):531–8.
51. Sibel I, Guillaume G, Fabien R, Marie B, Sophie P, Mohammad B C, Karcher G, Pierre-Yves M, Luc T, Antoine V. A high 18 F-FDOPA uptake is associated with a slow growth rate in diffuse grade II-III gliomas. Br J Radiol [Internet]. 2017 [cited 2018 Jul 30];20170803. Available from: https://www.birpublications.org/doi/pdf/10.1259/bjr.20170803

52. Qi S, Yu L, Li H, Ou Y, Qiu X, Ding Y, Han H, Zhang X. Isocitrate dehydrogenase mutation is associated with tumor location and magnetic resonance imaging characteristics in astrocytic neoplasms. Oncol Lett [Internet]. 2014 Jun [cited 2017 May 22];7(6):1895–902. Available from: http://www.ncbi.nlm.nih.gov/pubmed/24932255

53. Carrillo JA, Lai A, Nghiemphu PL, Kim HJ, Phillips HS, Kharbanda S, Moftakhar P, Lalaezari S, Yong W, Ellingson BM, Cloughesy TF, Pope WB. Relationship between Tumor Enhancement, Edema, IDH1 Mutational Status, MGMT Promoter Methylation, and Survival in Glioblastoma. Am J Neuroradiol [Internet]. 2012 [cited 2017 Jun 5];33(7). Available from: http://www.ajnr.org/content/33/7/1349.short

54. Schäfer ML, Maurer MH, Synowitz M, Wüstefeld J, Marnitz T, Streitparth F, Wiener E. Low-grade (WHO II) and anaplastic (WHO III) gliomas: Differences in morphology and MRI signal intensities. Eur Radiol. 2013;23(10):2846–53.

55. Patel CB, Fazzari E, Chakhoyan A, Yao J, Raymond C, Nguyen H, Manoukian J, Nguyen N, Pope W, Cloughesy TF, Nghiemphu PL, Czernin J, Lai A, Ellingson BM. 18F-FDOPA PET and MRI characteristics correlate with degree of malignancy and predict survival in treatment-naïve gliomas: a cross-sectional study. J Neurooncol [Internet]. 2018;0(0):1–11. Available from: http://dx.doi.org/10.1007/s11060-018-2877-6

Eidesstattliche Versicherung

„Ich, Maike Lizanne Kern, versichere an Eides statt durch meine eigenhändige Unterschrift, dass ich die vorgelegte Dissertation mit dem Thema: „Investigation of Molecular Subtypes of WHO Grade II-IV Gliomas by Use of T2 Mapping Sequences in Magnetic Resonance Imaging" selbstständig und ohne nicht offengelegte Hilfe Dritter verfasst und keine anderen als die angegebenen Quellen und Hilfsmittel genutzt habe.
Alle Stellen, die wörtlich oder dem Sinne nach auf Publikationen oder Vorträgen anderer Autoren/innen beruhen, sind als solche in korrekter Zitierung kenntlich gemacht. Die Abschnitte zu Methodik (insbesondere praktische Arbeiten, Laborbestimmungen, statistische Aufarbeitung) und Resultaten (insbesondere Abbildungen, Graphiken und Tabellen) werden von mir verantwortet.

Ich versichere ferner, dass ich die in Zusammenarbeit mit anderen Personen generierten Daten, Datenauswertungen und Schlussfolgerungen korrekt gekennzeichnet und meinen eigenen Beitrag sowie die Beiträge anderer Personen korrekt kenntlich gemacht habe (siehe Anteilserklärung). Texte oder Textteile, die gemeinsam mit anderen erstellt oder verwendet wurden, habe ich korrekt kenntlich gemacht.

Meine Anteile an etwaigen Publikationen zu dieser Dissertation entsprechen denen, die in der untenstehenden gemeinsamen Erklärung mit dem/der Erstbetreuer/in, angegeben sind. Für sämtliche im Rahmen der Dissertation entstandenen Publikationen wurden die Richtlinien des ICMJE (International Committee of Medical Journal Editors; www.icmje.og) zur Autorenschaft eingehalten. Ich erkläre ferner, dass ich mich zur Einhaltung der Satzung der Charité – Universitätsmedizin Berlin zur Sicherung Guter Wissenschaftlicher Praxis verpflichte.

Weiterhin versichere ich, dass ich diese Dissertation weder in gleicher noch in ähnlicher Form bereits an einer anderen Fakultät eingereicht habe.

Die Bedeutung dieser eidesstattlichen Versicherung und die strafrechtlichen Folgen einer unwahren eidesstattlichen Versicherung (§§156, 161 des Strafgesetzbuches) sind mir bekannt und bewusst."

_____

Datum Unterschrift

Anteilserklärung an den erfolgten Publikationen

Maike Lizanne Kern hatte folgenden Anteil an den folgenden Publikationen:

Publikation 1: Kern, Maike; Auer, Timo Alexander; Picht, Thomas; Misch, Martin; Wiener, Edzard; **T2-Mapping of molecular subtypes of WHO grade II/III glioma**; *BMC Neurology*; 2020
Beitrag im Einzelnen:

- Entwicklung der Fragestellung
- Datenerhebung (Tab. 1, Fig. 1-4)
- Auswertung der histopathologischen Befunde (Tab. 1)
- Patientenakquise und Patientenausschluss; Formulierung der Ein-und Ausschlusskriterien (Fig. 1) (Tab. 1)
- Datenformatierung
- Entwicklung des Messungs-Algorithmus zur Reproduzierbarkeit (Fig. 1)
- ROI-Auswertung (Fig. 2-4)
- radiologische Auswertung
- selbstständige statistische Auswertung der Patientendaten
- Vorgaben zur statistischen Auswertung durch E.W. (Fig. 2-4) (Tab. 2)
- Interpretation der Ergebnisse (Fig. 3-4) (Tab. 2)
- Literaturrecherche zum aktuellen Forschungsstand
- Einordnung der Ergebnisse in die aktuelle Literatur
- Limitationen
- Zusammenfassung der Hauptergebnisse
- Eigenständige Formulierung des Inhalts der Veröffentlichung
- Antwort auf die Fragen der Reviewer, Revision und Wiedereinreichen
- Korrespondenz mit den Editoren bis zur Veröffentlichung

Publikation 2: Kern, Maike*; Auer, Timo Alexander*; Fehrenbach, Uli; Tanyildizi, Yasemin; Picht, Thomas; Misch, Martin; Wiener, Edzard; **Multivariable non-invasive association of isocitrate dehydrogenase mutational status in World Health Organization grade II and III gliomas with advanced magnetic resonance imaging T2 mapping techniques**; *The Neuroradiology Journal*; 2020
Beitrag im Einzelnen:

- Entwicklung der Fragestellung
- Datenerhebung (Tab. 1, Fig. 1-4)
- Auswertung der histopathologischen Befunde (Tab. 1)
- Patientenakquise und Patientenausschluss; Formulierung der Ein-und Ausschlusskriterien
- Datenformatierung

- Entwicklung des Messungs-Algorithmus zur Reproduzierbarkeit
- ROI-Auswertung (Fig. 1-2)
- radiologische Auswertung (Tab. 1, Fig. 1-4)
- Vorgaben zur statistischen Auswertung durch E.W. (Fig. 1-4)
- Interpretation der Ergebnisse (Fig. 1-2)
- Limitationen
- Unterstützung bei der Formulierung des Inhalts der Veröffentlichung mit T.A.A.
- Unterstützung bei Revision und Wiedereinreichen

Publikation 3: Auer, Timo Alexander; Kern, Maike; Fehrenbach, Uli; Tanyildizi, Yasemin; Misch, Martin; Wiener, Edzard; **T2 mapping of the peritumoral infiltration zone of glioblastoma and anaplastic astrocytoma**; *The Neuroradiology Journal*; 2021

Beitrag im Einzelnen:

- Mitarbeit bei der Entwicklung der Fragestellung
- Datenerhebung (einschließlich Differenzierung 1,5 und 3T MRT)
- Auswertung der histopathologischen Befunde (Tab 1)
- ROI- Auswertung
- radiologische Auswertung
- selbstständige statistische Auswertung der Patientendaten
- Unterstützung bei der statistischen Auswertung durch E.W. und T.A.A. (Fig. 2-5)
- Datenformatierung
- Formulierung von Ein- und Ausschlusskriterien
- Unterstützung bei der Formulierung des Inhalts der Veröffentlichung
- Erstellung von Tabelle 1 und 2, sowie Abbildung 1

_____

Unterschrift, Datum und Stempel des betreuenden Hochschullehrers

_____

Unterschrift der Doktorandin

Druckexemplare der Publikationen

Kern et al. BMC Neurology (2020) 20:8
https://doi.org/10.1186/s12883-019-1590-1

BMC Neurology

RESEARCH ARTICLE Open Access

T2 mapping of molecular subtypes of WHO grade II/III gliomas

Maike Kern[1*], Timo Alexander Auer[2], Thomas Picht[3], Martin Misch[3] and Edzard Wiener[1]

Abstract

Background: According to the new WHO classification from 2016, molecular profiles have shown to provide reliable information about prognosis and treatment response. The purpose of our study is to evaluate the diagnostic potential of non-invasive quantitative T2 mapping in the detection of IDH1/2 mutation status in grade II-III gliomas.

Methods: Retrospective evaluation of MR examinations in 30 patients with histopathological proven WHO-grade II ($n = 9$) and III ($n = 21$) astrocytomas (18 IDH-mutated, 12 IDH-wildtype). Consensus annotation by two observers by use of ROI's in quantitative T2-mapping sequences were performed in all patients. T2 relaxation times were measured pixelwise.

Results: A significant difference ($p = 0{,}0037$) between the central region of IDH-mutated tumors (356,83 ± 114,97 ms) and the IDH-wildtype (199,92 ± 53,13 ms) was found. Furthermore, relaxation times between the central region (322, 62 ± 127,41 ms) and the peripheral region (211,1 ± 74,16 ms) of WHO grade II and III astrocytomas differed significantly ($p = 0{,}0021$). The central regions relaxation time of WHO-grade II (227,44 ± 80,09 ms) and III gliomas (322,62 ± 127,41 ms) did not differ significantly ($p = 0{,}2276$). The difference between the smallest and the largest T2 value (so called "range") is significantly larger ($p = 0{,}0017$) in IDH-mutated tumors (230,89 ± 121,11 ms) than in the IDH-wildtype (96, 33 ± 101,46 ms). Interobserver variability showed no significant differences.

Conclusions: Quantitative evaluation of T2-mapping relaxation times shows significant differences regarding the IDH-status in WHO grade II and III gliomas adding important information regarding the new 2016 World Health Organization (WHO) Classification of tumors of the central nervous system. This to our knowledge is the first study regarding T2 mapping and the IDH1/2 status shows that the mutational status seems to be more important for the appearance on T2 images than the WHO grade.

Keywords: Gliomas, MRI, IDH, T2-mapping

Background

Malignant gliomas are the most frequent primary brain tumors in adults [1–6]. In 2016 the World Health Organization (WHO) Classification of Tumors of the Central Nervous System initially "integrated" [7] genotypic parameters such as molecular genetic tumor markers in its revised version from 2016 [5, 8, 9]. This new classification adds the genetic markers and gives a more precise division into molecular subgroups with distinct molecular signatures [5, 8, 10]. These groups may correlate with their histologic subtype and define different patient's prognosis and treatment response [5, 8–12].

One of the most important markers in gliomas is the isocitrate dehydrogenase (IDH) 1 and 2 [5, 9, 11–13]. IDH1 and IDH2 are coding for isocitrate dehydrogenase, which catalyzes the conversion of isocitrate to alpha-ketoglutarate (AKG), leading to an increased level of D2HG in IDH mutated tumors [3, 5, 6, 13–15]. Another effect of IDH-mutation (IDH-mut) is the inhibition of the PI3K/Akt pathway, which may induce a higher level of apoptosis [16]. IDH mutations in general are associated with a better prognosis by influencing cell proliferation, angiogenesis and vascularization [1, 3, 5, 6, 8, 9, 11, 14, 16–18].

* Correspondence: maike.kern@charite.de
[1]Department of Neuroradiology, Charité – Universitätsmedizin Berlin, corporate member of Freie Universität Berlin, Humboldt-Universität zu Berlin and Berlin Institute of Health, Berlin, Germany
Full list of author information is available at the end of the article

High-grade gliomas treatment response used to be evaluated with the Macdonald-Criteria from 1990 [4, 19, 20]. In 2010, the Response Assessment in Neuro-Oncology (RANO) working group published the updated RANO criteria, that replaced the Macdonald-Criteria [4, 19–21]. RANO criteria include the T2/FLAIR (fluid-attenuated inversion recovery) sequences in addition to the recent clinical and imaging features [4, 19, 20]. Until then, imaging features used just T1w and T1w contrast-enhanced sequences [4, 19, 20]. The RANO- criteria now include a significantly increased T2/FLAIR perpendicular size (called "T2-progress") as a criterion [4, 19, 20]. As a future aspect T2 mapping could affect the evaluation of tumor progression according to RANO criteria by adding quantitative voxelvise measurements. Nevertheless, both classification systems are constructed to correlate with the histological grade and not with a genetic profile.

The importance of T2 mapping sequences was already emphasized by Hattingen et al. (2013) [22]. Their study shows, that this technic could be suitable to control the tumor progression under anti-angiogenetic therapy [22]. According to their results, by use of T2 maps it seems achievable to detect tumor progression by an increase in T2 relaxation times in healthy appearing brain tissue before demarcated changes are visible in usual MRI sequences [22]. Further examinations about the possible applications of this promising technic, especially in neuroradiological usage, are urgently needed.

The future key role in MR brain imaging will be to create imaging biomarkers for defining correct molecular subtypes.

The purpose of this study is to evaluate the potential of quantitative T2-mapping in the detection of IDH1/2 mutation status in grade II-III gliomas. In the new WHO classification, molecular profiles are providing reliable information about prognosis and treatment response. To the best of our knowledge, it is the first study for initial results by use of T2 mapping to demonstrate, that the mutational status causes characteristic alterations in the T2 values of glioma.

Methods

Study population

The ethical board of our institution approved the present study (application number EA1/306/16). All participants were enrolled after their informed consent was obtained. The study was conducted according to the Declaration of Helsinki in its revised revision. Patients with the diagnosis of WHO grade II astrocytoma (A2) and WHO grade III anaplastic astrocytoma (AA3) were identified within the period from April 2015 to March 2018 (Fig. 1). A total of 22 patients with A2 and 42 patients with AA3 were enrolled. Patients younger than eighteen years of age, with a previous central nervous surgical treatment with imaging alterations such as artefacts, considerable surgical cavity or mass effect were excluded. In total 9 patients with A2 and 21 patients with AA3, including 18 with and 12 without IDH mutation, were included. Histopathological reports including molecular typing were available for all patients.

Data acquisition

MR imaging was performed preoperatively on 1.5 Tesla (Avanto Magnetom; Siemens, Erlangen, Germany) (n = 20) and 3 Tesla (Skyra; Siemens, Erlangen, Germany) (n = 10) scanners with and without contrast media. Dotarem (Guerbet GmbH) or Gadovist (Bayer Healthcare) were administered weight adapted. Following sequences were acquired: T1 magnetization-prepared rapid gradient echo (MPRAGE) transversal, sagittal and coronar post contrast (repetition time (TR) 2200, echo time (TE) 2,67, slice thickness 1 mm, inversion time 900, in-plane resolution 0,9766 × 0,9766 mm, acquisition matrix 256 × 246) and T2 mapping (TR 3100 TE 13,8–165,6 with twelve TEs: 13,8 ms, 27,6 ms, 41,4 ms, 55,2 ms, 69 ms, 82,2 ms, 96,6 ms, 110,4 ms, 124,2 ms, 138 ms, 151,8 ms, 165,6 ms). T2 maps were reconstructed online by using a voxelwise, monoexponential nonnegative least-squares fit analysis (MapIt; Siemens, Erlangen, Germany) with a voxel size of 1.9 × 1.0 × 3 mm^3.

Image analysis

For quantitative analysis, regions of interest (ROI) were manually drawn (M.K., E.W.) on the T2-maps using the visage software tool (Visage Imaging/Pro Medicus Limited, Version 7.1.10). To test the accuracy of the T2 measurements, an additional ROI was placed in the healthy white matter (WM) of the contralateral lobe on a level without the ventricles. In the manner of Badve et al., we preferred the contralateral equal lobe [23]. If there was not any normal appearing white matter to be found, we placed the ROI with a different localization, most often frontoparietal [23]. To proof the reliability of our T2 measurements, we took the median value for the WM which supports recent studies which reported ranges from 84 to 87 ms ± 3 ms in 1.5 T MRI [24] and 74 to 80 ms ± 1 ms in 3.0 T [25]. Additionally, we compared the WM values of 1,5 T and 3 T MRI to rule out the source of error occurring through the mixture of field strengths. Next, two different locations for the ROI's were selected, a central ROI (cROI) and a peripheral ROI (pROI) based on the following criteria (Fig. 1). The ROI size was always 5 mm in diameter. For the cROI, the slice with the largest tumor dimension was chosen, followed by delineating of the anatomic center of the tumor. In case of present vessels, necrosis or artefacts, the cROI was placed a few millimeters off center. The pROI was placed on the same slice as the cROI. The

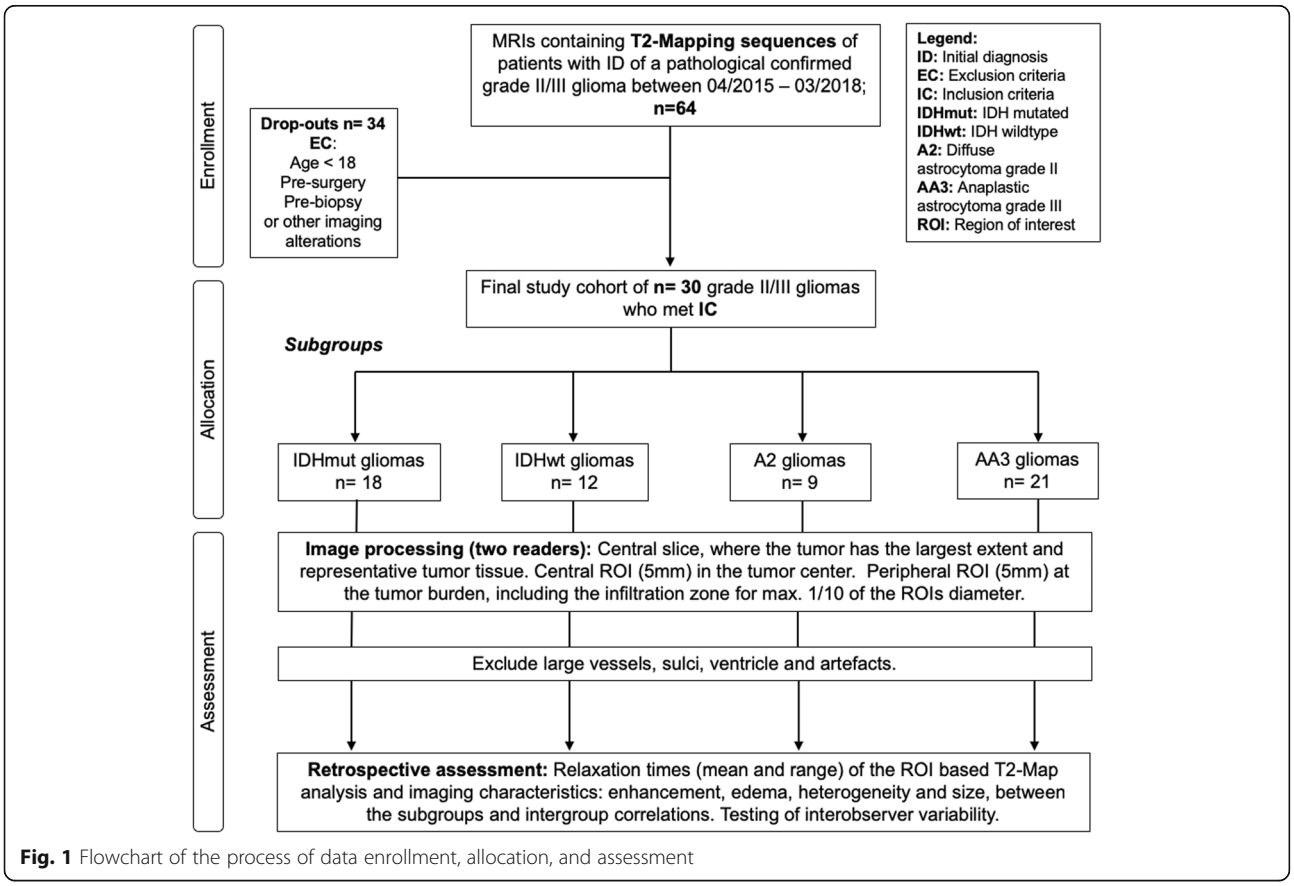

Fig. 1 Flowchart of the process of data enrollment, allocation, and assessment

pROI was located within the outer tumor border including the infiltration zone with 1/10 of the ROI, always bright on T2 maps and directly adjacent to healthy appearing brain tissue (Fig. 1 and Fig. 2). Vessels, artefacts and sulci were excluded as before (Fig. 1). All ROI's covered parts that were representative of the whole tumor's tissue. IDH mutation was defined by the use of immunohistochemistry. If the result was obscure, it was followed by a PCR and pyrosequencing analysis. Furthermore, enhancing tumor (yes/no), necrosis (yes/no), edema (yes/no), tumors heterogeneity (on a scale from low (1) to high (3)) and tumor size on the MPRAGE images were evaluated. We defined a signal heterogeneity of more than 25% (visually) in either T1w or T2w/FLAIR sequences as a macroscopic heterogenic pattern [1, 26, 27]. Both observers were constantly blinded to IDH status and the diagnosis during the measurements.

Statistical analysis

The statistical analysis was performed with XLSTAT (Version 2011,0,01; Addinsoft SARL, New York, New York). The Mann-Whitney-U Test as a two-tailed test was used to compare each groups median. Kruskal-Wallis-Test was used for variance analysis/ rank sum test. $P < 0,05$ was evaluated as statistical significance. Interobserver variability was calculated using Cronbach's alpha statistic with the values for parenchyma, central and peripheral ROI. Cohen's d was used to calculate the effect size of the significant parameters on the T2 values of gliomas. The analysis of variance (ANOVA) was used to analyze differences among the group means.

Results

Study subjects

General information of our study subjects for the separate tumor entities is summarized in Table 1. Overall there are more patients with IDH-mut ($n = 18$) than with IDH-wt ($n = 12$). Frontal and parietal ($n = 12$) localization prevail significantly in IDH-mut tumors ($p < 0,0001$). The patients with IDH-mut (41,32 ± 12,3 [28–74] years) were significantly younger than those with IDH-wt (55,69 ± 16,39 [34–81] years) ($p = 0,0105$).

MR examination

Figure 2 shows a T2 weighted image and the corresponding T2 map of a WHO grade III astrocytoma with IDH mutation. The median T2 values differed significantly between the central and peripheral ROI in gliomas of both grades ($p = 0,0021$), IDH-mut ($p = 0,0288$) and IDH wt ($p = 0,0362$) and in AA3 ($p = 0,0185$). In A2,

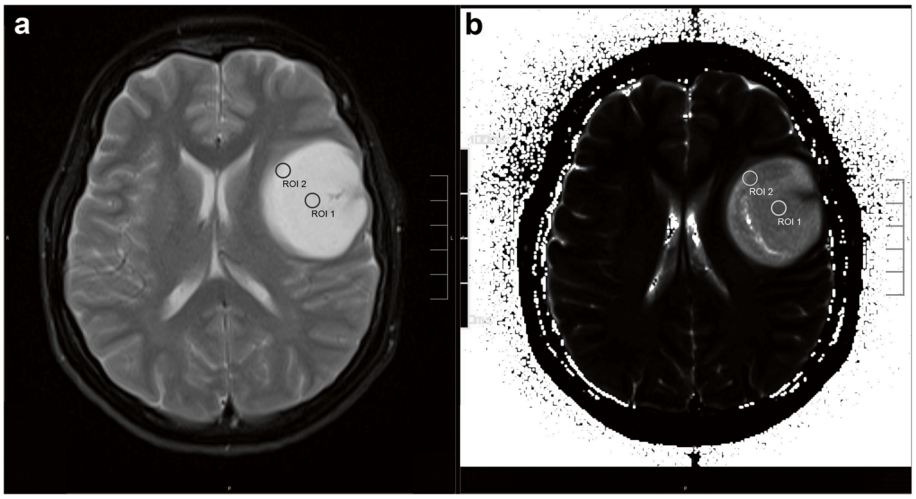

Fig. 2 MRI of a 32 years old female patient suffering from IDH-mut anaplastic astrocytoma WHO grade III. The T2 hyperintense tumor shows no enhancement or necrosis and only small edema can be assumed. The central ROI and peripheral ROI are delineated on the transversal T2 image (**a**) and on the corresponding T2 map (**b**)

there was no significant difference even if the figures show similar trends ($p = 0{,}4089$) (Table 2, Fig. 3 and Fig. 4). The T2 values were larger in the center ROI than in the peripheral ROI. This difference represents the SI decreasing from the center to the periphery, which occurs independently of the IDH-status (Table 2). Separated by the mutational status, the IDH-mut gliomas are central ($p = 0{,}0037$) and peripheral ($p = 0{,}0094$) more intense than the IDH-wt (Table 2, Fig. 3 and Fig. 4). IDH-mut gliomas are overall significantly more hyperintense than the wildtype (Table 2, Fig. 3 and Fig. 4). There was no significant difference between A2 and AA3, neither central ($p = 0{,}2276$) nor peripheral ($p = 0{,}5547$) (Fig. 3). Fig. 3 shows the previously mentioned trends in A2 (central vs. peripheral $p = 0{,}4089$, central mut vs. wt $p = 0{,}8831$; peripheral mut vs. wt $p = 1{,}0000$).

Table 1 General data of the study population

	IDH-mut ($n = 18$)	IDH-wt ($n = 12$)	p-value*
age, yr. (mean, range)	41,32 ± 12,3 [28–74]	55,69 ± 16,39 [34–81]	0,0105
A2	38,13 ± 11,53 [28–57]	64,22 ± 18,25 [41–81]	
AA3	42,55 ± 12,81 [29–74]	51,42 ± 14,73 [34–74]	
sex (no.)	$n = 18$	$n = 12$	< 0,0001
female	9 (50%)	1 (8,33%)	
male	9 (50%)	11 (91,67%)	
tumor grade	$n = 18$	$n = 12$	
A2	5 (27,78%)	4 (33,33%)	
AA3	13 (72,22%)	8 (66,67%)	
tumor localization	$n = 18$	$n = 12$	< 0,0001**
fronto-parietal	frontal (38,89%) parietal (16,67%) frontoparietal (11,1%)	frontal (16,67%) parietal (16,67%)	
other	fronto-parieto-temporal (16,67%) temporal (11,1%) parieto-temporal (5,56%)	thalamic (25%) temporal (16,67%) frontotemporal (8,33%) corpus callosum (8,33%) 5 single lesions (8,33%)	

*All p-values relate to the difference between IDH-mut and IDH-wt independently of the tumor grade. **This p-value concerns to fronto-parietal or not fronto-parietal localization in IDH-mut and IDH-wt tumors

Table 2 T2 values of ROIs from different location and tumor entities in dependence of the molecular subtype and the calculated *p*-values

	mean [median] T2 ± StD	mean [median] T2 ± StD	*p*-value
central vs. peripheral ROI			
both grades	294,07 [268,50] ± 122,2 ms	202,6 [186,50] ± 78,71 ms	**0,0021**
IDH-mut	356,83 [376,50] ± 114,97 ms	239,00 [257,00] ± 80,44 ms	0,0288
IDH-wt	199,92 [187,50] ± 53,13 ms	148,00 [138,00] ± 30,22 ms	0,0362
AA3	322,62 [298,00] ± 127,41 ms	211,10 [206,00] ± 74,16 ms	0,0185
A2	227,44 [204,00] ± 80,09 ms	182,78 [140,00] ± 89,87 ms	0,4089
IDH-mut vs. IDH-wt			
central ROI	356,82 [376,50] ± 114,97 ms	199,92 [187,50] ± 53,13 ms	**0,0037**
peripheral ROI	239,00 [257,00] ± 80,44 ms	148,00 [138,00] ± 30,22 ms	0,0094
AA3 central ROI	399,69 [425,00] ± 93,46 ms	197,38 [187,50] ± 49,47 ms	0,0022
AA3 peripheral ROI	251,85 [261,00] ± 61,93 ms	144,88 [132,00] ± 32,28 ms	0,0061
A2 central ROI	245,40 [249,00] ± 92,08 ms	205,00 [192,00] ± 67,74 ms	0,8831
A2 peripheral ROI	205,60 [140,00] ± 118,58 ms	154,25 [142,5,00] ± 28,95 ms	1,0000
range IDH-mut vs. IDH-wt			
central both grades	230,89 [249,50] ± 121,11 ms	96,33 [56,50] ± 101,46 ms	**0,0017**
central AA3	262,23 [273,00] ± 111,69 ms	69,63 [49,50] ± 43,39 ms	0,0042
central A2	149,40 [102,00] ± 116,80 ms	149,75 [79,50] ± 166,28 ms	0,9614

Bold data shows significant values

The range of the measurements is larger in IDH-mut than it is in IDH-wt ($p = 0{,}0017$; $p = 0{,}0042$) (Table 2, Fig. 3 and Fig. 4).

The median T2 value of white matter has been 82, 8 ± 3,13 [78–89] ms. There was no significant difference between the T2 values of WM obtained at 1,5 T (83, 6 ± 3,1 [80–89] ms) and 3 T (81,3 ± 2,4 [78–86] ms) MRI ($p = 0{,}053$).

We had good interobserver agreement by comparison of T2 values of parenchyma, central and peripheral ROI ($\alpha = 0{,}9509$).

There was a significant difference in the enhancement, IDH-wt gliomas ($n = 4$) had more CE than IDH-mut ($n = 4$) ($p < 0{,}0001$). However, there was significantly more necrosis in IDH-mut than in IDH-wt astrocytomas ($p < 0{,}0001$). There was no significant difference in macroscopic heterogeneity between A2 (1667 ± 0,866) and AA3 (1857 ± 0,793) ($p = 0{,}583$) nor between IDH-mut (1,78 ± 0,88) and IDH-wt (1,83 ± 0,72) ($p = 0{,}7957$) based on a nominal scale.

In this study the calculated Cohen's d of 1.506 and 1.766 represent a large effect size, indicating a strong impact of IDH status on T2 values of gliomas. ANOVA revealed no statistically significant impact of age ($p = 0.5730$), gender ($p = 0{,}8461$) and localization ($p = 0{,}6145$) on the T2 values of gliomas. The WHO grade revealed a small impact on T2 values in ANOVA variance analysis ($p = 0{,}472$).

Discussion

To our knowledge this is the first study, that quantitatively compared the diagnostic utility of T2 mapping sequences in distinguishing between WHO grade II and III astrocytomas in relation to the IDH status demonstrating a significant T2 increase in IDH-mut gliomas compared to the wild type. Furthermore, a significant difference between the central and peripheral tumor regions was found. Although, histopathological tissue examination remains the diagnostic gold standard, T2 mapping is a noninvasive examination and provides additional information about the macroscopic and microscopic composition [28, 29].

The new WHO classification from 2016 emphasizes the prognostic value of molecular subtypes. Current literature states that the IDH mutation is associated with a better prognosis and therapeutic response [5, 8, 14].

It is reported that patients with IDH-mut AA3 had a longer survival than with IDH-wt AA3 [14]. Several studies [11, 14, 29, 30] showed that the mutation is associated with younger age though ($p = 0{,}02$), which is in line with our results.

MRI is the modality of choice in the clinical diagnosis, treatment planning, and follow-up of brain tumors. Sufficient differentiation of grade II and III gliomas using conventional MRI remains challenging, due to similar imaging presentations as both grades are able to enhance and both grades may grow necrotic [28]. In agreement with the study of Qi et al. (2014) only for necrosis and CE could be found significant correlations, whereas edema and tumor size did not show significant results [1, 5].

The data show that A2 have lower intensities than AA3 but without significant results. Further studies who investigated the T2-volume didn't show convincing results [31]. Patel et al. (2018) did not find differences in the segmented volume of T2 hyperintensity in relation to the WHO grade [31]. Therefore, it seems that there is no evidence for the differentiation between WHO grade II and III gliomas based on T2 signal characteristics.

Earlier reports suggested highly promising clinical utility for MR spectroscopy and Positron Emission Tomography (PET)-CT [3, 5, 30, 32, 33]. Verger et al. (2017) for example showed an increased Tracer (F-FDOPA)

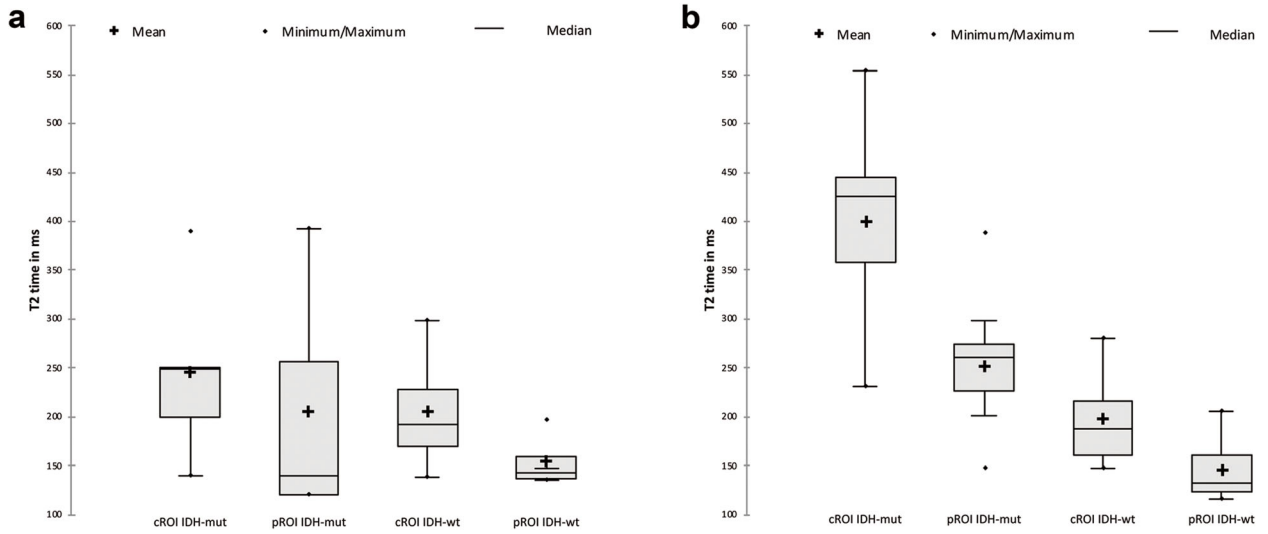

Fig. 3 Box plots of T2 values of IDH-mut and IDH-wt obtained from central ROIs and peripheral ROIs of a WHO grade II astrocytomas (**a**) and WHO grade III astrocytomas (**b**)

uptake in PET-CT in IDH-mut and WHO grade III glioma [30]. Even recent studies like Villanueva-Meyer et al. (2018) who found significant differences depending on the IDH status of WHO grade II glioma by use of ADC (apparent diffusion coefficient)-maps could not fully meet the expectations in clinical practice [9]. Nevertheless, no technique was valid enough to implement it into the clinical routine.

Our T2-map analyses show that IDH-mut AA3 have the highest SI, followed by IDH-mut A2, which are similar to IDH-wt AA3. IDH-wt A2 yield the lowest values. The median intensities of IDH-mut A2 are nearly equal to the ones of IDH-wt AA3. Furthermore, the comparison of the values of the cROI of A2 vs. AA3 ($p = 0{,}2276$) and IDH-mut vs. IDH-wt ($p = 0{,}0037$), demonstrates as well as the ANOVA analysis, that the mutational status seems to be more important for the SI than the WHO grade, which is surprising. The WHO grade describes different stages within the progression of the same condition, emphasizing the mutational status.

The IDH mutation might be accountable for several changes in tumors cell biology and metabolism. As

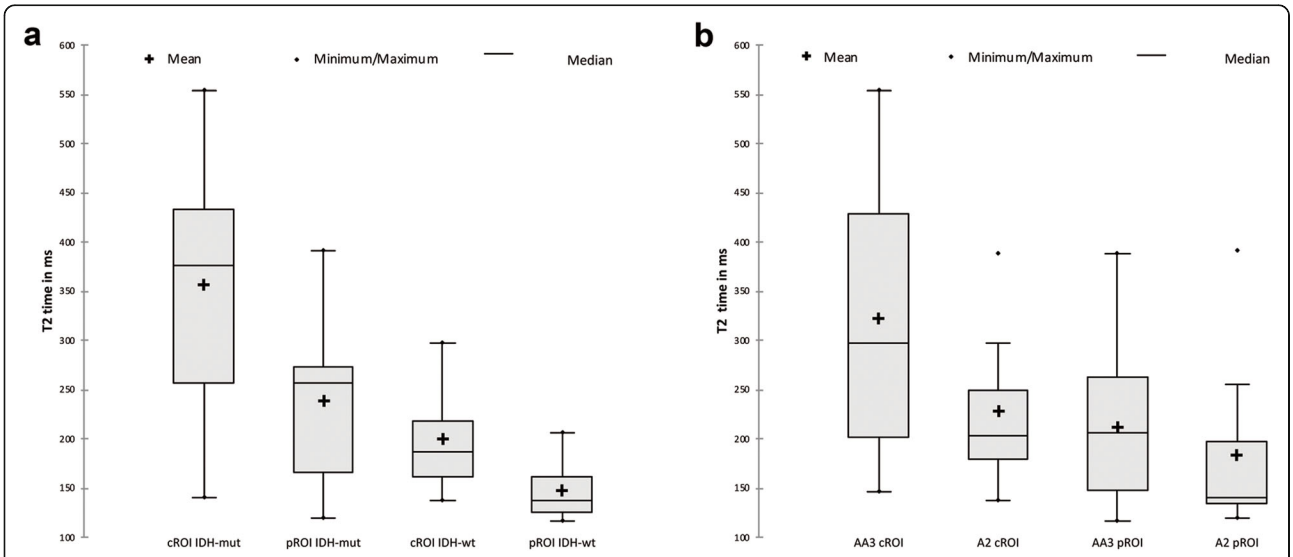

Fig. 4 Box plots of T2 values obtained from central ROIs and peripheral ROIs of IDH-mut and IDH-wt without the distinction between WHO grade II and III tumors (**a**) and analysis of T2 values only considering the WHO grade without the IDH status (**b**)

several previous studies mentioned, we presume that the evident T2 signal characteristic of IDH-mut tumors and tumor cells especially in the central region is caused by the accumulation of D2HG and the changed tumor metabolism [30, 34]. Increased vascularization, angiogenesis and apoptosis may cause edema, which is T2 hyperintense, too. Nevertheless, there are lower values in the peripheral tumor region. That might implicate, that there is a mixture of parenchyma with a lower SI and tumor cells with a higher SI leading to the hypothesis that gliomas always grow infiltrative from the inside out [11]. Parenchyma cells depress the overall values. We guess that the larger range of IDH-mut AA3 and IDH-mut tumors in general, could express a microscopic heterogeneity. This IDH-specific heterogeneity was also postulated by Darlix et al. (2017), caused by different factors [12]. First, throughout the inhibited PI3K/Akt pathway resulting in a higher rate of apoptosis, so there might be macroscopically invisible necrosis, which could be presented in lower T2 values [16]. Secondly, the stabilized HIF-1α increases vascularization and angiogenesis and may also result in heterogeneity [3, 14, 17]. Interestingly, the macroscopic heterogeneity did not vary in our cohort from IDH-mut to IDH-wt nor between A2 and AA3. Heterogeneity is used as another radiological criterion to differ between the WHO grades but might be marginal in differentiation between WHO grade II and III or IDH-mut and IDH-wt glioma. Although Wang et al. (2015) reported, the IDH-wt tumors are mostly located multilobar, frontal and temporal [11, 35]. In this study, the IDH-mut tumors are significantly more often located frontal and parietal region (Table 1), in line with the current literature [29, 35].

By use of two different locations for ROI analysis, we can show that it does not matter where the ROI-analysis inside the tumor area is performed. The RANO criteria firstly include the T2/FLAIR, showing that T2 weighted images are just as important as the T1 weighted post-contrast. It seems as T2 signal characteristics are at least as important as the tumor size.

Limitations of the study must be acknowledged. Our study sample included a minor portion of patients who were operated years ago with no considerable surgical cavity or mass effect visible in the included brain MRI. Further potential sources of bias in our study are selection bias, detection bias and lack of previous research studies on the topic. In addition, there is uneven sex distribution. Another limitation is the small sample size of patients, even if the effect size is already large. The remaining goldstandard, the histopathological classification, is known to have high inter- and intraobserver concordances [29]. The small interobserver variability in this study shows, that the technique of T2 mapping is reliable, reproducible and not observer-depending. The visual based and not volumetric evaluation is another possible bias. The comparison of the values of brains parenchyma between 3 T and 1,5 T scanners shows, that there is no significant difference among the technics regarding T2 mapping and that T2 mapping is a very robust technique for clinical routine. T2 values of brain parenchyma may not be affected so much by the field strength [36] . Due to the performance with two different scanners, it is possible that they had slightly different pulse sequences and settings, which might influence the results as well.

Like Villanueva-Meyer et al. (2018) and Qi et al. (2014) reported, newer imaging techniques, localization, growth behavior, margins, and CE are also predictive for the IDH-status [1, 5, 9, 11, 35]. Our results obtained out of mapping data might add important knowledge at this actual topic.

Conclusion

Quantitative evaluation of T2-mapping relaxation times shows significant differences regarding the IDH-status in WHO grade II and III gliomas as IDH-mut gliomas have a higher T2 SI, adding important information regarding the new 2016 World Health Organization (WHO) Classification of tumors of the central nervous system. Furthermore, T2 mapping seems to quantify the heterogeneity of grade III gliomas. This to our knowledge first study regarding T2 mapping and the IDH1/2 status shows that the mutational status seems to be more important for the appearance on T2 images than the WHO grade.

Abbreviations

A2: WHO grade II diffuse astrocytoma; AA3: WHO grade III anaplastic astrocytoma; CE: Contrast enhancement; cROI: Central region of interest; CT: Computer tomography; D2HG: D-2-hydroxyglutarate; FLAIR: Fluid-attenuated inversion recovery; HIF- 1A: Hypoxia-inducible factor – 1 alpha; IDH: Isocitrate dehydrogenase; IDH-mut: Mutational IDH; IDH-wt: IDH-wildtype; MPRAGE: Magnetization-prepared rapid gradient echo; MRI: Magnet resonance imaging; PCR: Polymerase chain reaction; pROI: Peripheral region of interest; RANO: Response Assessment in Neuro-Oncology; ROI: Region of interest; SI: Signal intensity; StD: Standard deviation; T: Tesla; TE: Echo time; TR : Repetition time; WHO: World Health Organization; WM: White matter; AKG: Alpha-ketoglutarate

Acknowledgements

I would like to offer my special thanks to Dr. B-C Kern for his advice and help during the planning and development of this research work.

Declarations

The manuscript has not been previously published, in whole or in parts, or submitted or presented elsewhere for review. All authors have approved the manuscript for submission.

Authors' contributions

All authors had major contribution to manuscript. MK contributed the creation of this manuscript and its idea, data acquisition and evaluation, implementation of ROI-analyses, the statistics and administrative concerns. TAA did major corrections and editing the manuscript, data acquisition, as well as providing support for the realization of the project. TP provided clinical and histological data, added neurosurgical aspects to the topic and

edited the manuscript. MM provided clinical and histological data and added neurosurgical aspects, too. EW was the supervisor of this study, performed ROI-analyses for interobserver variability, contributed data evaluation and statistics. All authors read and approved the final manuscript.

Funding
There was no funding or financial or material support.

Availability of data and materials
The data that support the findings of this study are available on request from the corresponding author MK.

Ethics approval and consent to participate
All procedures performed in studies involving human participants were in accordance with the ethical standards of the institutional and/or national research committee and with the 1964 Helsinki declaration and its later amendments or comparable ethical standards. Institutional review board approval of this retrospective study was obtained (Nr. EA1/306/16 of the Ethics Committee of the Faculty of Medicine of Charité – Universitätsmedizin Berlin). Informed consent was obtained verbally by all participants of this study as this is the standard for non-prospective studies at our institution. This was approved by our IRB (Nr. EA1/306/16).

Consent for publication
Not applicable.

Competing interests
The author Thomas Picht is an Editorial Board Member of BMC Neurology. The remaining authors declare that they have no competing interest.

Author details
[1]Department of Neuroradiology, Charité – Universitätsmedizin Berlin, corporate member of Freie Universität Berlin, Humboldt-Universität zu Berlin and Berlin Institute of Health, Berlin, Germany. [2]Department of Radiology, Charité – Universitätsmedizin Berlin, corporate member of Freie Universität Berlin, Humboldt-Universität zu Berlin and Berlin Institute of Health, Berlin, Germany. [3]Department of Neurosurgery, Charité – Universitätsmedizin Berlin, corporate member of Freie Universität Berlin, Humboldt-Universität zu Berlin and Berlin Institute of Health, Berlin, Germany.

Received: 15 March 2019 Accepted: 27 December 2019
Published online: 08 January 2020

References
1. Qi S, Yu L, Li H, Ou Y, Qiu X, Ding Y, et al. Isocitrate dehydrogenase mutation is associated with tumor location and magnetic resonance imaging characteristics in astrocytic neoplasms. Oncol Lett. 2014;7:1895–902. https://doi.org/10.3892/ol.2014.2013.
2. Yan H, Parsons DW, Jin G, McLendon R, Rasheed BA, Yuan W, et al. *IDH1* and *IDH2* mutations in Gliomas. N Engl J Med. 2009;360:765–73. https://doi.org/10.1056/NEJMoa0808710.
3. Zhang C, Moore LM, Li X, Yung WKA, Zhang W. IDH1/2 mutations target a key hallmark of cancer by deregulating cellular metabolism in glioma. Neuro-Oncology. 2013;15:1114–26.
4. Wen PY, Macdonald DR, Reardon DA, Cloughesy TF, Sorensen AG, Galanis E, et al. Updated response assessment criteria for high-grade Gliomas: response assessment in Neuro-oncology working group. J Clin Oncol. 2010; 28:1963–72. https://doi.org/10.1200/JCO.2009.26.3541.
5. Smits M, van den Bent MJ. Imaging correlates of adult Glioma genotypes. Radiology. 2017;284:316–31. https://doi.org/10.1148/radiol.2017151930.
6. Zhang B, Chang K, Ramkissoon S, Tanguturi S, Bi WL, Reardon DA, et al. Multimodal MRI features predict isocitrate dehydrogenase genotype in high-grade gliomas. Neuro-Oncology. 2017;19:109–17. https://doi.org/10.1093/neuonc/now121.
7. Louis DN, Perry A, Burger P, Ellison DW, Reifenberger G, von Deimling A, et al. International Society of Neuropathology-Haarlem Consensus Guidelines for nervous system tumor classification and grading. Brain Pathol. 2014;24:429–35.
8. Louis DN, Perry A, Reifenberger G, Von Deimling A, Figarella-Branger D, Cavenee WK, et al. The 2016 World Health Organization classification of tumors of the central nervous system: a summary. Acta Neuropathol. 2016; 131:803–20.
9. Villanueva-Meyer JE, Wood MD, Choi B, Mabray MC, Butowski NA, Tihan T, et al. MRI features and IDH mutational status of grade II diffuse Gliomas: impact on diagnosis and prognosis. Am J Roentgenol. 2018;210:621–8. https://doi.org/10.2214/ajr.17.18457.
10. Banan R, Hartmann C. The new WHO 2016 classification of brain tumors—what neurosurgeons need to know. Acta Neurochir. 2017;159:403–18. https://doi.org/10.1007/s00701-016-3062-3.
11. Metellus P, Coulibaly B, Colin C, De Paula AM, Vasiljevic A, Taieb D, et al. Absence of IDH mutation identifies a novel radiologic and molecular subtype of WHO grade II gliomas with dismal prognosis. Acta Neuropathol. 2010;120:719–29. https://doi.org/10.1007/s00401-010-0777-8.
12. Darlix A, Deverdun J, Menjot de Champfleur N, Castan F, Zouaoui S, Rigau V, et al. IDH mutation and 1p19q codeletion distinguish two radiological patterns of diffuse low-grade gliomas. J Neuro-Oncol. 2017;133:37–45. https://doi.org/10.1007/s11060-017-2421-0.
13. Otani R, Uzuka T, Ueki K. Classification of adult diffuse gliomas by molecular markers—a short review with historical footnote. Jpn J Clin Oncol. 2017;47: 2–6.
14. Waitkus MS, Diplas BH, Yan H. Isocitrate dehydrogenase mutations in gliomas. Neuro-Oncology. 2016;18:16–26.
15. Macaulay RJ. Impending impact of molecular pathology on classifying adult diffuse Gliomas. Cancer Control. 2015;22:200–5. https://doi.org/10.1177/107327481502200211.
16. Birner P, Pusch S, Christov C, Mihaylova S, Toumangelova-Uzeir K, Natchev S, et al. Mutant IDH1 inhibits PI3K/Akt signaling in human glioma. Cancer. 2014;120:2440–7. https://doi.org/10.1002/cncr.28732.
17. Jeuken JWM, von Deimling A, Wick W, Herold-Mende C, Hartmann C, Wesseling P, et al. Type and frequency of IDH1 and IDH2 mutations are related to astrocytic and oligodendroglial differentiation and age: a study of 1,010 diffuse gliomas. Acta Neuropathol. 2009;118:469–74. https://doi.org/10.1007/s00401-009-0561-9.
18. Lasocki A, Tsui A, Tacey MA, Drummond KJ, Field KM, Gaillard F. MRI grading versus histology: predicting survival of world health organization grade II-IV astrocytomas. Am J Neuroradiol. 2015;36:77–83.
19. Pope WB, Hessel C. Response assessment in neuro-oncology criteria: implementation challenges in multicenter neuro-oncology trials. Am J Neuroradiol. 2011;32:794–7. https://doi.org/10.3174/ajnr. A2582.
20. Radbruch A, Lutz K, Wiestler B, Bäumer P, Heiland S, Wick W, et al. Relevance of T2 signal changes in the assessment of progression of glioblastoma according to the response assessment in Neurooncology criteria. Neuro-Oncology. 2012;14:222–9. https://doi.org/10.1093/neuonc/nor200.
21. Röhrich M, Huang K, Schrimpf D, Albert NL, Hielscher T, von Deimling A, et al. Integrated analysis of dynamic FET PET/CT parameters, histology, and methylation profiling of 44 gliomas. Eur J Nucl Med Mol Imaging. 2018;45: 1573–84.
22. Hattingen E, Jurcoane A, Daneshvar K, Pilatus U, Mittelbronn M, Steinbach JP, et al. Quantitative T2 mapping of recurrent glioblastoma under bevacizumab improves. Neuro-Oncology. 2013;15:1395–404.
23. Badve C, Yu A, Dastmalchian S, Rogers M, Ma D, Jiang Y, et al. MR fingerprinting of adult brain tumors: initial experience. In: American Journal of Neuroradiology; 2017. p. 492–9. https://doi.org/10.3174/ajnr. A5035.
24. Zhou J, Golay X, Van Zijl PCM, Silvennoinen MJ, Kauppinen R, Pekar J, et al. Inverse T 2 Contrast at 1.5 Tesla Between Gray Matter and White Matter in the Occipital Lobe of Normal Adult Human Brain. Magn Reson Med. 2001; 46:401–6. https://doi.org/10.1002/mrm.1204.
25. Wansapura JP, Holland SK, Dunn RS, Ball WS. NMR relaxation times in the human brain at 3.0 tesla. J Magn Reson Imaging. 1999;9:531–8.
26. Forst DA, Nahed BV, Loeffler JS, Batchelor TT. Low-grade gliomas. Oncologist. 2014;19:403–13. https://doi.org/10.1634/theoncologist.2013-0345.
27. Weller M, van den Bent M, Hopkins K, Tonn JC, Stupp R, Falini A, et al. EANO guideline for the diagnosis and treatment of anaplastic gliomas and glioblastoma. Lancet Oncol. 2014;15:e395–403. https://doi.org/10.1016/S1470-2045(14)70011-7.
28. Schäfer ML, Maurer MH, Synowitz M, Wüstefeld J, Marnitz T, Streitparth F, et al. Low-grade (WHO II) and anaplastic (WHO III) gliomas: differences in morphology and MRI signal intensities. Eur Radiol. 2013;23:2846–53.
29. Delfanti RL, Piccioni DE, Handwerker J, Bahrami N, Krishnan AP, Karunamuni R, et al. Imaging correlates for the 2016 update on WHO classification of

grade II/III gliomas: implications for IDH, 1p/19q and ATRX status. J Neuro-Oncol. 2017;135:611.
30. Verger A, Metellus P, Sala Q, Colin C, Bialecki E, Taieb D, et al. IDH mutation is paradoxically associated with higher18F-FDOPA PET uptake in diffuse grade II and grade III gliomas. Eur J Nucl Med Mol Imaging. 2017;44:1306–11. https://doi.org/10.1007/s00259-017-3668-6.
31. Patel CB, Fazzari E, Chakhoyan A, Yao J, Raymond C, Nguyen H, et al. 18F-FDOPA PET and MRI characteristics correlate with degree of malignancy and predict survival in treatment-naïve gliomas: a cross-sectional study. J Neuro-Oncol. 2018;0:1–11. https://doi.org/10.1007/s11060-018-2877-6.
32. Andronesi OC, Kim GS, Gerstner E, Batchelor T, Tzika AA, Fantin VR, et al. Detection of 2-hydroxyglutarate in IDH-mutated glioma patients by in vivo spectral-editing and 2D correlation magnetic resonance spectroscopy. Sci Transl Med. 2012;4:116ra4. https://doi.org/10.1126/scitranslmed.3002693.
33. Elkhaled A, Jalbert LE, Phillips JJ, Yoshihara HAI, Parvataneni R, Srinivasan R, et al. Magnetic resonance of 2-hydroxyglutarate in IDH1-mutated low-grade gliomas. Sci Transl Med. 2012;4:116ra5. https://doi.org/10.1126/scitranslmed.3002796.
34. Sibel I, Guillaume G, Fabien R, Marie B, Sophie P, Mohammad BC, et al. A high 18 F-FDOPA uptake is associated with a slow growth rate in diffuse grade II-III gliomas. Br J Radiol. 2017;91:20170803. https://doi.org/10.1259/bjr.20170803.
35. Wang Y, Zhang T, Li S, Fan X, Ma J, Wang L, et al. Anatomical localization of isocitrate dehydrogenase 1 mutation: a voxel-based radiographic study of 146 low-grade gliomas. Eur J Neurol. 2015;22:348–54.
36. West J, Blystad I, Engström M, Warntjes JBM, Lundberg P. Application of Quantitative MRI for Brain Tissue Segmentation at 1 . 5 T and 3 . 0 T Field Strengths. PLoS One. 2013;8:1–12.

Publisher's Note

Original article

The Neuroradiology Journal
0(0) 1–9
! The Author(s) 2020
Article reuse guidelines:
sagepub.com/journals-permissions
DOI: 10.1177/1971400919890099
journals.sagepub.com/home/neu
SAGE

Multivariable non-invasive association of isocitrate dehydrogenase mutational status in World Health Organization grade II and III gliomas with advanced magnetic resonance imaging T2 mapping techniques

Maike Kern[1,*], Timo A Auer[2,*], Uli Fehrenbach[2], Tanyildizi Yasemin[3], Thomas Picht[4], Martin Misch[4] and Edzard Wiener[1]

Abstract

Aim: To investigate multivariable analyses for noninvasive association of the isocitrate dehydrogenase (IDH) mutational status in grade II and III gliomas including evaluation of T2 mapping-sequences.

Methods: Magnetic resonance imaging (MRI) examinations with histopathologically proven World Health Organization grade II and III gliomas were retrospectively enrolled. Multivariate receiver operating characteristics (ROC) analyses to associate IDH mutational status were performed containing quantitative T2 mapping analyses and qualitative characteristics (sex, age, localization, heterogeneity, oedema, necrosis and diameter). Relaxation times were calculated pixelwise by means of standardized ROI analyses. Interobserver variability also was tested.

Results: Out of 32 patients (mean age: 50.7 years; range: 32–83), nine had grade II gliomas and 24 grade III, while 59.5% showed a positive IDH mutated state (IDHm) and 40.5% were wildtype (IDHw). Multivariable ROC analyses were calculated for relaxation time and range, localization and age with a cumulative 0.955 area under the curve (AUC) ($p < 0.001$), while central T2-relaxation time had by far the highest single variable sensitivity (AUC: 0.873; range: 0.762; age: 0.809; localization: 0.713). Age (cut off: 49 years; $p = 0.031$) and localization ($p = 0.014$) were the only qualitative parameters found to be significant as IDHw gliomas were older and IDHm gliomas were preferentially located fronto-temporal.

Conclusions: This is the first study evaluating quantitative T2 mapping sequences for association of the IDH mutational status in grade II and III gliomas demonstrating an association between relaxation time and mutational status. Analyses of T2 mapping relaxation times may even be suitable for predicting the correct IDH mutational state. Prognostic accuracy increases significantly in predicting the correct mutational state when combing T2 relaxation time characteristics and the qualitative MRI features age and localization.

Keywords

Glioma, T2 mapping, Multiparametric imaging, IDH1/2-state (isocitrate-dehydrogenase), MRI (magnetic resonance imaging)

Introduction

Gliomas are the most common brain tumour in adults and are classified following the World Health Organization (WHO) classification.[1,2] These criteria, solely including the histologic morphology, remain the gold standard for treatment decision making and major prognostic parameters.[1–3] Numerous prospective randomized trials and studies have shown different therapy outcome for tumours within the same WHO graduation, indicating a need for an extended 'subhistological' classification, including different molecular marker profiles, as gliomas within the same WHO grade can show highly different molecular marker profiles.[4,5] As a consecutive reaction the revised WHO classification from 2016 firstly

[1]Department of Neuroradiology, Charite University Hospital Berlin, Germany
[2]Department of Radiology, Charite University Hospital Berlin, Germany
[3]Department of Neuroradiology, University Medicial Center Mainz, Germany
[4]Department of Neurosurgery, Charite University Hospital Berlin, Germany

*These authors contributed equally to this work.

Corresponding author:
Edzard Wiener, Department for Neuroradiology, Campus Berlin-Mitte, Charité – Universitätsmedizin Berlin, Augustenburger Platz 1, 13353 Berlin, Germany.
Email: edzard.wiener@charite.de

included genotypic parameters.[5–7] These molecular parameters provided more accurate diagnostic, prognostic and maybe even predictive information regarding therapy response and outcome.[6,7]

Low-grade gliomas represent an entity with a highly heterogeneous tumour biology, behaviour and prognosis.[8,9] Especially in grade II and III gliomas the isocitrate dehydrogenase (IDH) status seems to have a major predictive impact. The IDH wildtype (IDHw) (present in 10–20%) is associated with a significantly poorer prognosis, so that even histopathologically graded II gliomas can have a similar prognosis as high-grade glioblastomas (WHO °IV).[4,5,10,11] Magnetic resonance imaging (MRI) is the modality of choice to evaluate gliomas and besides accurate assessment of tumour extent, MRI features are known to correlate with the histopathological grade.[2,6,7,12] Though the future challenge lies in MRI-based tumour geno-/phenotyping and to implement these new, non-invasive possibilities of tumour characterization, into clinical routine.

Current literature states that the IDH state is associated with several imaging characteristics.[5,10,13–18] The molecular differences and biological behaviour of the tumour might be represented in imaging features as, for example, genotypes seem to correlate with the localization, contrast enhancement (CE)-behaviour and homo- or heterogeneity of the tumour.[5,10,13–17] There are several promising advanced MRI features such as spectroscopy, FLAIR volume measurement, dynamic susceptibility contrast perfusion imaging and analysis of apparent diffusion coefficient (ADC) maps; however, maps without distinct evidence in predicting the correct IDH state.[19–21] Nevertheless, so far the results of quantitative MRI assessed through ADC analyses seem to be most promising.[5,16–18,22]

Newer MRI mapping techniques allow a quantification of the relaxation at different echo times pixelwise, giving a more accurate information about the tissue and its composition.[23] The purpose of this study was to investigate quantitative evaluation of 'T2 mapping' relaxation times to predict and hereby assess a possible association with the IDH mutational state in low-grade gliomas non-invasively, and to compare these results with established qualitative MRI features.

Material and methods

Patients

All participants were enrolled retrospectively, and informed consent was waived. The institutional ethical board approved the present study (application number EA1/306/16). From April 2015 to March 2018, 33 patients with the diagnosis of a WHO grade II or III glioma were collected. Exclusion criteria were underage patients, imaging alterations caused by earlier surgery of the brain or insufficient image quality. Histopathological reports were available for all patients. IDH status was determined in 22 patients by immunohistochemistry, the remainder by Polymerase chain reaction. All patients had IDH1 mutations, 19 on codon R132H and one on codon R132L, so far, there were no IDH2 mutations. ATRX loss was present in 19 patients with IDH mutation (IDHm), in one it was not examined and no ATRX loss was demonstrated in all patients with IDHw. 1 p/19q-codeletion was not detectable in any patient.

Imaging

MRI with contrast media was performed preoperatively on 1.5 Tesla (Avanto Magnetom; Siemens, Erlangen, Germany) ($n = 22$) and 3 Tesla (Skyra; Siemens, Erlangen, Germany) ($n = 11$) MRI scanners. Since the T2 variation of brain tissue at 1.5 T and 3 T are not significantly different, imaging parameters were nearly identical. Gadolinium-DOTA (Dotarem, Guerbet, Villepinte, France) was used as a contrast agent. The evaluated sequences were: T1 magnetization-prepared rapid gradient-echo (MPRAGE) transversal (sagittal and coronar were reconstructed) and post-contrast (repetition time (TR) 2200, echo time (TE) 2.67, slice thickness 1 mm, inversion time 900, in-plane resolution 0.9766×0.9766 mm, acquisition matrix 256×246), T2/FLAIR-sequences (TE 88 and TR 9.000 ms and 3 mm slice thickness) and T2 mapping (TR 3100 TE 13.8–165.6 with 12 TEs: 13.8, 27.6, 41.4, 55.2, 69, 82.2, 96.6, 110.4, 124.2, 138, 151.8 and 165.6 ms). By use of MapIt (Siemens, Erlangen, Germany), T2 Maps were reconstructed online. The total acquisition time for the mapping sequence was 5 min 19 s.

Parameters

Radiological and clinical analyses parameters were as follows:

- sex;
- age;
- tumour localization, divided into two compartments 'fronto-temporal' and 'other';
- Contrast Enhancement (CE) = Increased signal intensity (SI) after a MRI contrast agent administration (more than 25%);
- macroscopic pattern, homogenous or heterogeneous (yes/no);
- necrosis;
- T2w/FLAIR oedema;
- maximal diameter in T1CEw and T2w/FLAIR images;
- region of interest (ROI)-based tissue T2-map analysis with evaluation of relaxation times and ranges in the centre of the tumour.

A heterogenous pattern was defined visually as a tissue heterogeneity in T1w sequences of more than

25% within the tumour volume/in one representable slice. Oedema was defined as peritumoral hyperintensity in T2w/FLAIR sequences. According to the Response Assessment Group in Neuro-oncology (RANO), positive CE was defined as an increased signal intensity of more than 25% after contrast-agent administration.[24] Necrosis was defined as hypointense tissue in T1-CE sequences within the tumour volume without any signs of CE behaviour. Images were post-processed with visage software tool (Visage Imaging/ Pro Medicus Limited, Version 7.1.10). T2 map ROI were drawn manually by an experiences neuroradiologist (> 10 years of experience) plus a second reader (two years of experience) with a standardized diameter of 5 mm. The ROIs covered representable tissue of the solid tumour, while areas of necrosis and vessels were excluded (M.K., E.W.).

Inter-reader variability was tested. The slice with the largest tumour dimension was chosen, the anatomic centre of the tumour was delineated. A second ROI was automatically copied and pasted in the healthy-appearing white matter of the contralateral lobe with help of the image processing program to assure reliability of the measurements.

Statistics

The statistical analysis was performed with XLSTAT (Version 2011,0,01; Addinsoft SARL, New York, USA) and SPSS Software (IBM; New York, USA). Kolmogorov–Smirnov test was performed to compare single parameter distributions between glioma grade and mutational state cohorts and to identify suitable parameters for multivariable analyses of receiver operating characteristics (ROC). Subsequently significant or trending parameters were fed into the multivariate ROC approach and area under the curve (AUC) was evaluated. Cross validation was applied for the ROC analyses. To define the statistical influence of every single score category, standardized coefficients (95% confidence intervals (CI)) were evaluated and single AUC were created. A p-value of less than 0.05 was defined as statistically significant. Inter-observer variability was calculated using Cronbach's alpha.

Results

Demographics and tumour characteristics

Out of 32 patients: 19 (59.5%) were classified as IDHm and 13 (40.5%) as IDHw; 28% (9/32) had grade II gliomas and 72% (23/32) grade III. Median age of the cohort was 50.7 years (range: 32–83); 36% (12/32) were female and 64% (20/32) male patients. In five patients (15.5%) pre-surgery and or pre-biopsy was performed without causing imaging alterations. Glioma localization was as followed: 65.5% (21/32) of all gliomas were located frontal and/or temporal, while 34.5% (11/32) were in other brain regions; 28% (9/32) showed a positive CE-behaviour while 72% (23/32) did not; 37.5% (12/32) of gliomas appearance was rated as heterogenous while 62.5% (20/33) were rated as homogenous. Necrosis was found in 9%. Oedema was described in 65.5% in the T2w/FLAIR sequences. Mean T1 perpendicular diameter was 40.1 ± 15.6 mm and T2w/FLAIR diameter was 50.1 ± 18.9 mm. Mean T2-Map relaxation time was 298.6 ± 121.9 ms in the central placed ROI-analyses and 82.3 ± 4.1 ms in the peripheral placed ROI analyses. The ROI placed in the contralateral brain tissue showed no significant variances. Inter-reader variability did not differ significantly. All results are listed in Table 1, and Figures 1 and 2 show two exemplary MRIs with IDHw and IDHm WHO grade III gliomas.

Multivariable and single-variable analyses between IDHm and IDHw mutational status cohorts

Kolmogorov–Smirnov test identified central T2-relaxation time ($p = 0.002$) and range ($p = 0.008$) as significant. For categorical variables only age ($p = 0.031$) and localization ($p = 0.014$) were found to be significantly associated with the IDH status. None of the other qualitative parameter were found to be significant ($p > 0.05$) (Table 1). Multivariate ROC analyses were performed for central relaxation time and range, localization and age with an 0.955 AUC and $p < 0.001$ (cut off: 0.601; sensitivity: 0.947; specificity: 0.923; positive predictive value (PPV): 0.947; negative predictive value (NPV): 0.923; accuracy: 0.937 and 95% CI 0.887–1.000) (Figure 3). Cross validation for the logistic regression model revealed a total accuracy of validation data of 0.710 ± 0.087 and mean AUC of the datasets created from cross-validation of 0.937 ± 0.057.

Single score category standardized coefficients (95% CI) showed the highest association for the central T2-relaxation time (Figure 4). AUC for central T2-relaxation times was 0.872 (cut off: 231.0; sensitivity: 0.895; specificity: 0.769; PPV: 0.850; NPV: 0.833; accuracy: 0.843 and 95% CI 0.750–0.995). AUC for T2 range was 0.767 (cut off: 99.0; sensitivity: 0.842; specificity: 0.692; PPV: 0.800; NPV: 0.750; accuracy: 0.781 and 95% CI 0.587–0.948). AUC for age as metric variable was 0.809 (cut off: 49.0; sensitivity: 0.842; specificity: 0.692; PPV: 0.800; NPV: 0.750; accuracy: 0.781 and 95% CI 0.657–0.963). AUC for localization was 0.717 (sensitivity: 0.947; specificity: 0.538; PPV: 0.750; NPV: 0.875; accuracy: 0.781 and 95% CI 0.545–0.881).

Multivariable and single-variable analyses between WHO grade II and III glioma cohorts

Kolmogorov–Smirnov test and/or chi-square test showed no significance for any single parameter association with glioma grading ($p > 0.05$). Subsequently multivariable ROC analyses were not performed.

Table 1. Patients characteristics.

	Overall ($n = 32$)	IDHm ($n = 19$)	IDHw ($n = 13$)	p-value
Age (years)	49.9 ± 2.6	43.9 ± 2.7	58.8 ± 4.3	0.031
Sex (m/f)	20/12	9/10	11/2	0.302
Localization				
Fronto-temporal	21	16	5	0.014
Other	11	3	8	
Heterogeneity				
heterogeneity	12	7	5	0.926
homogeneity	20	12	8	
CE behavior				
Positive	9	4	5	0.282
Negative	23	15	8	
Oedema				
Positive	21	14	7	0.246
Negative	11	5	6	
Necrosis				
Positive	3	2	1	0.751
Negative	29	17	12	
Diameter T1 (mm)	41.3 ± 2.8	42.4 ± 4.2	39.7 ± 3.2	0.565
Diameter T2 (mm)	50.6 ± 3.5	50.9 ± 4.5	50.3 ± 5.1	0.879
T2 map (ms)				
Mean relaxation	298.58 ± 21.3	363.2 ± 24.7	199.2 ± 14.2	0.004
Range	178.3 ± 21.6	226.1 ± 25.8	104.6 ± 28.2	0.008

CE: contrast enhancement; IDHm: isocitrate dehydrogenase mutation; IDHw: isocitrate dehydrogenase wildtype

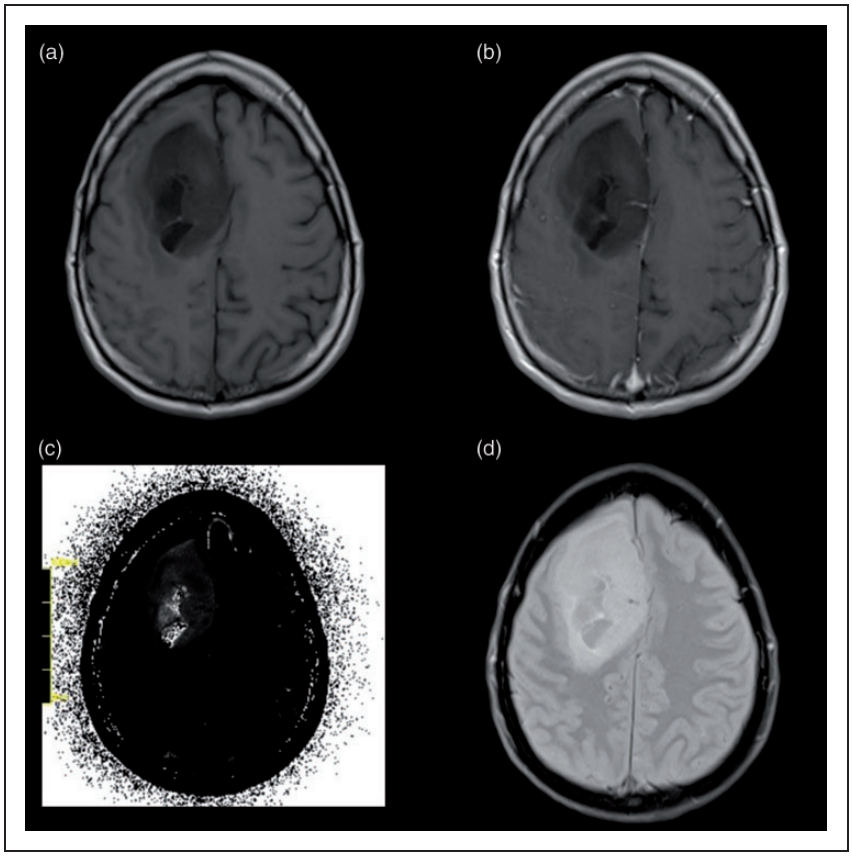

Figure 1. Patient, 49 years old, with a heterogenous IDHm grade III glioma located in the right frontal region (a) and without a significant positive CE in the T1CE sequences (b). (c) Shows the original raw T2 Map while (d) shows the corresponding FLAIR-sequence without a large oedema.

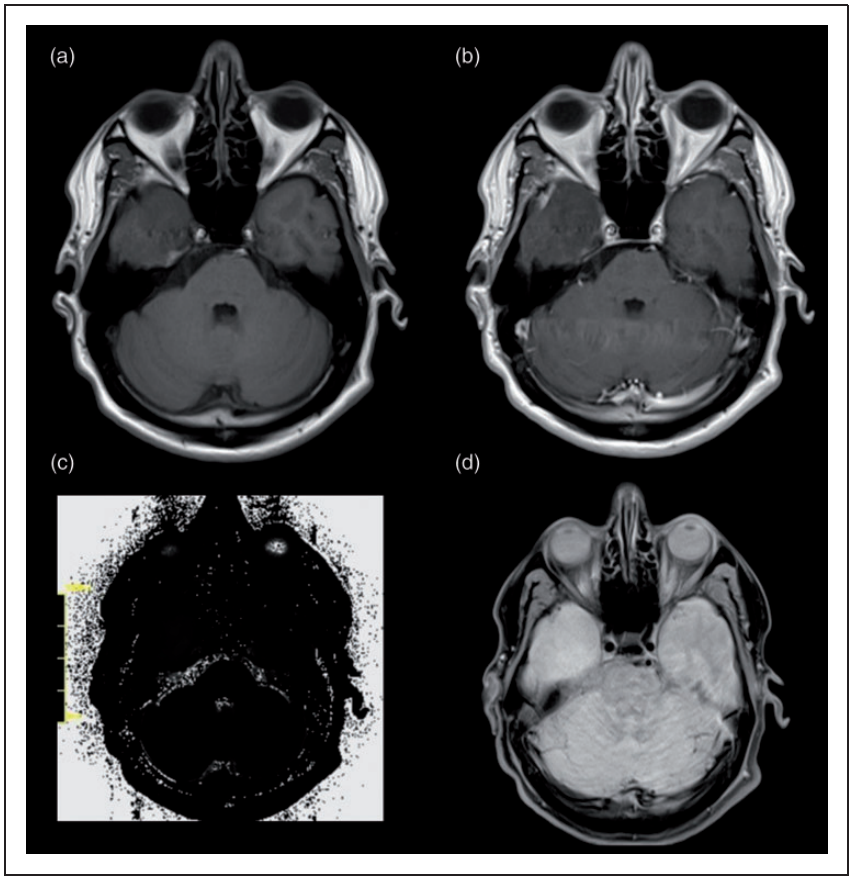

Figure 2. Patient, 38 years old, with a homogenous IDHw grade III glioma located in the lower temporal lobe (a) and without a significant pos. CE in the T1CE-sequence (b). (c) Shows the original raw T2 Map while (d) shows the corresponding FLAIR-sequence without a large oedema.

Discussion

As tumours within the same WHO grade but a different IDH mutational state may have totally divergent prognoses, the new WHO classification emphasizes the role of advanced MRI, predicting the correct mutational state.[5] This study implicates an association between T2 relaxation times and IDH mutational state in grade II and III gliomas. Furthermore, T2 mapping may even be a promising technique to predict the correct IDH mutational state noninvasively. In this study multivariable ROC analyses were calculated, showing a significant and strong association of shortened T2 relaxation times and smaller ranges in the central tumour region of IDHw gliomas. Alongside the quantitative measurements only age and localization were identified to be associated positively with IDH status, as IDHw tumours were found more often in older patients and mutated tumours were preferentially located in the fronto-temporal region. Besides age and tumour localization no qualitative characteristic was significantly associated with IDH status.[14,15]

In the current literature, only few a data are published regarding quantitative T2 mapping and glioma. A recently published study by Hattingen et al. is using T2 mapping for monitoring therapy outcome under bevacizumab treatment in patients with glioblastoma.[23] However, especially data regarding mapping sequences and gliomas' mutational states are missing.

Therefore, our quantitative measurements are difficult to compare. Nevertheless, with $p < 0.001$ and AUC = 0.955, a strong statistical proof is indicated for our results (Figure 3). After identifying central T2 relaxation time ($p < 0.004$) and the range ($p = 0.008$) as significant, we decided to add the two statistically most powerful qualitative parameters, who also had been previously described in literature as useful for determining the mutational status (Table 1).[14,15,17] Subdivided in each single parameter standardized coefficients showed that the quantitative 'mapping' measurements and patient's age had the major impact (Figures 3 and 4).

As mentioned, literature is limited on the significance of T2 relaxation time in gliomas and why times should differ between IDH statuses. Lee et. al. investigated the tissue with the help of diffusion weighted imaging (DWI) histogram analysis and dynamic susceptibility perfusion weighed imaging in high-grade gliomas, concluding that mutated subtypes are more heterogenic on a microenvironmental level.[22] This tissue heterogeneity may be represented by oedema, vascularization, angiogenesis or higher water content in the extracellular spaces, reflecting longer relaxation times and higher ranges in IDHm gliomas.

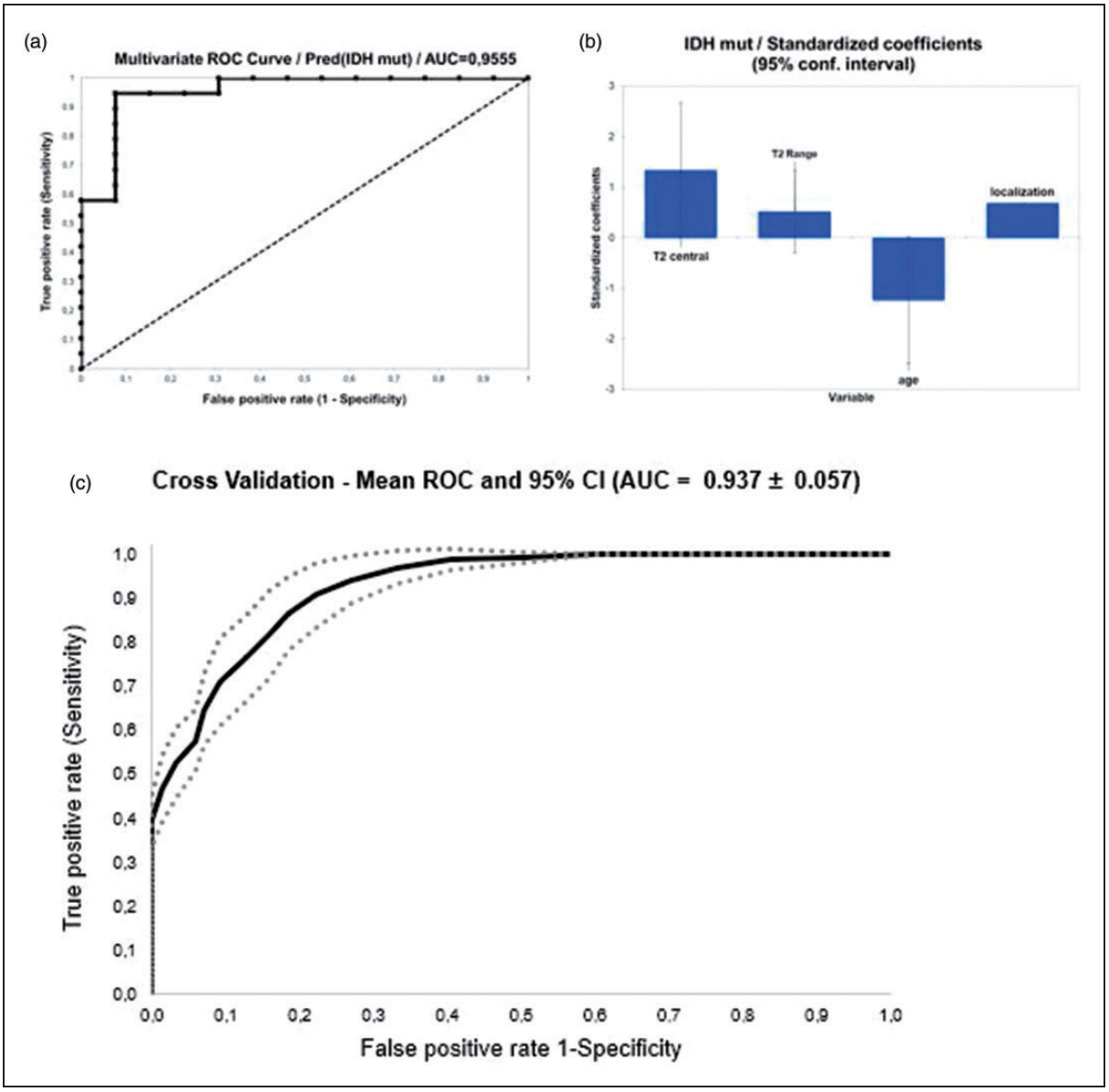

Figure 3. Multivariate receiver operating characteristics (ROC) analyses. (a) ROC curve analyses. The black panel represents the margin for the are under the curve (AUC). The black dashed panel represents the 0.5 AUC. (b) The power of the standardized coefficients upon the multivariate model for (from left to right): T2 relaxation time (central), T2 Range, age and tumour localization. (c) The cross validation for the logistic regression model (total accuracy). (IDHm: isocitrate dehydrogenase mutation).

This seem to be plausible as the wildtypes, associated with worse prognosis and known out of DWI/ADC analysis have a higher tumour tissue cellularity which decreases the extracellular spaces and the microenvironmental heterogeneity.[22,25–27] The overall longer T2 relaxation times in IDHm gliomas might be caused by the accumulation of D2HG, which is produced in large quantities by the altered function of IDH.[5,22,28,29]

In a recent study Bahrami et al. also introduced a quantitative approach by evaluating pixelwise tissue heterogeneity analysis and border distinctiveness (edge contrast) with the help of FLAIR sequences and radiomic features. The study highlights the potential of T2w/FLAIR tissue analysis in predicting the mutational status.[30] Nevertheless, the study by Bahrami et al. was limited as the majority (> 65%) of the collective underwent subtotal resections leading to distortion of the quantitative analyses.[30] In this study only the minority (15.5%) underwent pre-surgery and or prebiopsy. There are several more texture-based approaches and neuroimaging bases algorithms to predict the mutational state in gliomas, all of them with promising results but without implementing mapping sequences.[31,32]

Tumour localization is correlated with the IDH mutational state, as described elsewhere, for example Wang et al. report a preferable frontal and parietal localization in IDHm gliomas;[15] Qi et al. report an association between IDHm gliomas and a unilateral growth pattern, a homogenous signal intensity and no significant CE-behaviour.[14]

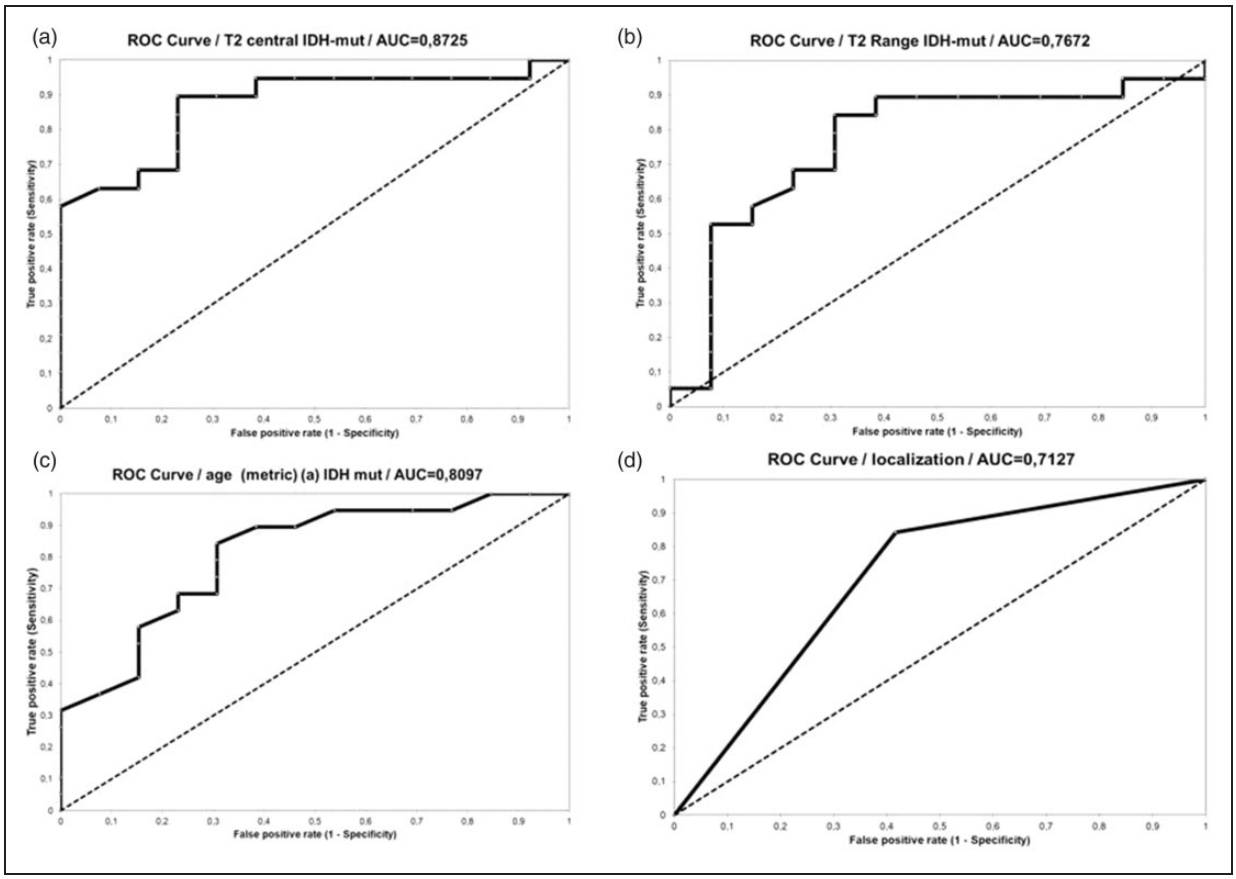

Figure 4. Single variate receiver operating characteristics (ROC) analyses. The black panel represents the margin for the area under the curve (AUC). The black dashed panel represents the 0.5 AUC. (a) T2 relaxation time (central); (b) T2 range; (c) age; (d) localization. (IDHm: isocitrate dehydrogenase mutation).

The underlying study assessed tumour localization for two compartments, either fronto-temporal or 'other', with a positively correlation for mutated gliomas located frontal and/or temporal, with a remarkable high sensitivity but a low specificity (Table 1 and Figure 4).

Villanueva-Meyer et al. noted that IDHw gliomas might be associated with an older age and defined 45 years as a cut off value throughout a regression analysis.[17] Our results are in line with Villanueva-Meyer et al. as our regression analysis also showed a positive correlation between higher age and glioma with IDHw, cut off age was 49 years. Within the multivariate ROC analyses age as a metric variable was significant ($p = 0.017$) and showed an AUC of 0.8097 (Table 1 and Figure 4). In accordance with the results of Villanueva-Meyer et al., we conclude that age is the most powerful qualitative patient characteristic for IDHw mutation, with a cut-off age between 45 and 50 years. Other studies implemented ADC analyses or MR spectroscopy for assessing mutation status.[5,16,17,22] Zang et al. achieved levels of accuracy up to 86% in predicting the IDH genotype of grade III and IV gliomas by using a machine-based algorithm, also containing MRI features such as ADC analyses and qualitative features such as size, shape and texture.[16] Further studies comparing or combining 'Mapping' sequences with ADC analyses maybe a promising step towards predicting the mutational status even more precise and valid. It is also interesting that no statistical co-evidence could be described for prediction of WHO grades by using any of our variable analyses.

The future of non-invasive genotype/phenotype imaging in gliomas and brain tumours in common will be fully automatic analyses of multiparametric algorithms like in other tumour entities.[12] It will be interesting to see what kind of role the analysis of mapping sequences will play.

Limitations

The retrospective and non-blind study design is a limiting factor. A further limitation of this study might be the relatively small patient cohort and a missing volume-based analysis, while this study used a regional based approach. However, the results of this study are promising and novel, indicating a correlation between relaxation time and IDH mutational state. Due to the small sample size though, the quality of the multivariate prediction model is limited. Therefore, larger patient numbers, examined with mapping techniques are required. Furthermore, even if only a minority of the examined cohort underwent pre-surgery and or pre-

biopsy, the collective was not treatment naïve, which may cause distortion. Another limitation is the use of two different scanners. Nevertheless, although two different types of scanner were used, T2 values of brain parenchyma may not be affected significantly by the field strength.[33]

Conclusion

To the best of our knowledge this is the first study evaluating quantitative T2 mapping sequences for prediction/ association of the IDH mutational state in grade II and III gliomas, demonstrating an association between relaxation time and mutational state. T2 mapping may even be suitable for predicting the correct IDH mutational state, as wildtypes had significantly shorter relaxation times in this cohort than mutated gliomas. Furthermore, age and tumour localization were reproducible qualitative MRI features. Wildtype mutation was associated with older patients and mutated types were preferentially found in the frontotemporal region. Prognostic accuracy for the correct mutational state is increasing significantly when combing T2 relaxation time characteristics and qualitative MRI features. Further investigations on MR mapping techniques for genotype and phenotype correlation are required, as this technique seems to be promising.

Funding

The authors received no financial support for the research, authorship, and/or publication of this article.

Conflicting of interests

The authors declared no potential conflicts of interest with respect to the research, authorship, and/or publication of this article.

ORCID iD

Timo A Auer https://orcid.org/0000-0002-5763-689X

References

1. Wen PY and Kesari S. Malignant gliomas in adults. *New Eng J Med* 2008; 359: 492–507.
2. Louis DN, Ohgaki H, Wiestler OD, et al. The 2007 WHO classification of tumours of the central nervous system. *Acta Neuropathol* 2007; 114: 97–109.
3. Weller M, van den Bent M, Hopkins K, et al. EANO guideline for the diagnosis and treatment of anaplastic gliomas and glioblastoma. *Lancet Oncol* 2014; 15: e395–403.
4. Riemenschneider MJ, Jeuken JW, Wesseling P, et al. Molecular diagnostics of gliomas: state of the art. *Acta Neuropathol* 2010; 120: 567–584.
5. Smits M and van den Bent MJ. Imaging correlates of adult glioma genotypes. *Radiology* 2017; 284: 316–331.
6. Banan R and Hartmann C. The new WHO 2016 classification of brain tumors-what neurosurgeons need to know. *Acta Neurochir* 2017; 159: 403–418.
7. Louis DN, Perry A, Reifenberger G, et al. The 2016 World Health Organization classification of tumors of the central nervous system: a summary. *Acta Neuropathol* 2016; 131: 803–820.
8. Yeh SA, Ho JT, Lui CC, et al. Treatment outcomes and prognostic factors in patients with supratentorial low-grade gliomas. *Brit J Radiol* 2005; 78: 230–235.
9. Sanai N, Chang S and Berger MS. Low-grade gliomas in adults. *J Neurosurg* 2011; 115: 948–965.
10. Metellus P, Coulibaly B, Colin C, et al. Absence of IDH mutation identifies a novel radiologic and molecular subtype of WHO grade II gliomas with dismal prognosis. *Acta Neuropathol* 2010; 120: 719–729.
11. Claus EB, Walsh KM, Wiencke JK, et al. Survival and low-grade glioma: the emergence of genetic information. *Neurosurg Focus* 2015; 38: E6.
12. Suh CH, Kim HS, Jung SC, et al. Imaging prediction of isocitrate dehydrogenase (IDH) mutation in patients with glioma: a systemic review and meta-analysis. *Eur Radiol* 2019; 29: 745–758.
13. Darlix A, Deverdun J, Menjot de Champfleur N, et al. IDH mutation and 1p19q codeletion distinguish two radiological patterns of diffuse low-grade gliomas. *J Neuro-Oncol* 2017; 133: 37–45.
14. Qi S, Yu L, Li H, et al. Isocitrate dehydrogenase mutation is associated with tumor location and magnetic resonance imaging characteristics in astrocytic neoplasms. *Oncol Lett* 2014; 7: 1895–1902.
15. Wang Y, Zhang T, Li S, et al. Anatomical localization of isocitrate dehydrogenase 1 mutation: a voxel-based radiographic study of 146 low-grade gliomas. *Eur Journal Neurol* 2015; 22: 348–354.
16. Zhang B, Chang K, Ramkissoon S, et al. Multimodal MRI features predict isocitrate dehydrogenase genotype in high-grade gliomas. *Neuro-oncol* 2017; 19: 109–117.
17. Villanueva-Meyer JE, Wood MD, Choi BS, et al. MRI Features and IDH mutational status of grade ii diffuse gliomas: impact on diagnosis and prognosis. *AJR* 2018; 210: 621–628.
18. Sonoda Y, Shibahara I, Kawaguchi T, et al. Association between molecular alterations and tumor location and MRI characteristics in anaplastic gliomas. *Brain Tumor Pathol* 2015; 32: 99–104.
19. Sahin N, Melhem ER, Wang S, et al. Advanced MR imaging techniques in the evaluation of nonenhancing gliomas: perfusion-weighted imaging compared with proton magnetic resonance spectroscopy and tumor grade. *Neuroradiol J* 2013; 26: 531–541.
20. Demerath T, Simon-Gabriel CP, Kellner E, et al. Mesoscopic imaging of glioblastomas: are diffusion, perfusion and spectroscopic measures influenced by the radiogenetic phenotype? *Neuroradiol J* 2017; 30: 36–47.
21. Ranjith G, Parvathy R, Vikas V, et al. Machine learning methods for the classification of gliomas: initial results using features extracted from MR spectroscopy. *Neuroradiol J* 2015; 28: 106–111.
22. Lee S, Choi SH, Ryoo I, et al. Evaluation of the microenvironmental heterogeneity in high-grade gliomas with IDH1/2 gene mutation using histogram analysis of diffusion-weighted imaging and dynamic-susceptibility contrast perfusion imaging. *J Neuro-Oncol* 2015; 121: 141–150.
23. Hattingen E, Jurcoane A, Daneshvar K, et al. Quantitative T2 mapping of recurrent glioblastoma under bevacizumab improves monitoring for non-enhancing tumor progression and predicts overall survival. *Neuro-Oncol* 2013; 15: 1395–1404.

24. Wen PY, Macdonald DR, Reardon DA, et al. Updated response assessment criteria for high-grade gliomas: response assessment in neuro-oncology working group. *J Clin Oncol* 2010; 28: 1963–1972.
25. Kono K, Inoue Y, Nakayama K, et al. The role of diffusion-weighted imaging in patients with brain tumors. *AJNR* 2001; 22: 1081–1088.
26. Di Costanzo A, Scarabino T, Trojsi F, et al. Proton MR spectroscopy of cerebral gliomas at 3 T: spatial heterogeneity, and tumour grade and extent. *Eur Radiol* 2008; 18: 1727–1735.
27. Kang Y, Choi SH, Kim YJ, et al. Gliomas: Histogram analysis of apparent diffusion coefficient maps with standard- or high-b-value diffusion-weighted MR imaging-correlation with tumor grade. *Radiology* 2011; 261: 882–890.
28. Verger A, Metellus P, Sala Q, et al. IDH mutation is paradoxically associated with higher (18)F-FDOPA PET uptake in diffuse grade II and grade III gliomas. *Eur J Nucl Med Mol Imaging* 2017; 44: 1306–1311.
29. Isal S, Gauchotte G, Rech F, et al. A high (18)F-FDOPA uptake is associated with a slow growth rate in diffuse Grade II–III gliomas. *Brit J Radiol* 2018; 91: 20170803.
30. Bahrami N, Hartman SJ, Chang YH, et al. Molecular classification of patients with grade II/III glioma using quantitative MRI characteristics. *J Neuro-Oncol* 2018; 139: 633–642.
31. Park YW, Han K, Ahn SS, et al. Prediction of IDH1-Mutation and 1p/19q-Codeletion Status Using Preoperative MR Imaging Phenotypes in Lower Grade Gliomas. *AJNR* 2018; 39: 37–42.
32. Batchala PP, Muttikkal TJE, Donahue JH, et al. Neuroimaging-based classification algorithm for predicting 1p/19q-codeletion status in IDH-mutant lower grade gliomas. *AJNR* 2019; 40: 426–432.
33. West J, Blystad I, Engstrom M, et al. Application of quantitative MRI for brain tissue segmentation at 1.5 T and 3.0 T field strengths. *PLoS One* 2013; 8: e74795.

Original Article

NRJ

The Neuroradiology Journal
0(0) 1–9


Article reuse guidelines:
sagepub.com/journals-permissions
DOI: 10.1177/1971400921989325
journals.sagepub.com/home/neu
SAGE

T2 mapping of the peritumoral infiltration zone of glioblastoma and anaplastic astrocytoma

Timo Alexander Auer[1], Maike Kern[2], Uli Fehrenbach[2], Yasemin Tanyldizi[3], Martin Misch[4] and Edzard Wiener[2]

Abstract

Purpose: To characterise peritumoral zones in glioblastoma and anaplastic astrocytoma evaluating T2 values using T2 mapping sequences.

Materials and methods: In this study, 41 patients with histopathologically confirmed World Health Organization high grade gliomas and preoperative magnetic resonance imaging examinations were retrospectively identified and enrolled. High grade gliomas were differentiated: (a) by grade, glioblastoma versus anaplastic astrocytoma; and (b) by isocitrate dehydrogenase mutational state, mutated versus wildtype. T2 map relaxation times were assessed from the tumour centre to peritumoral zones by means of a region of interest and calculated pixelwise by using a fit model.

Results: Significant differences between T2 values evaluated from the tumour centre to the peritumoral zone were found between glioblastoma and anaplastic astrocytoma, showing a higher decrease in signal intensity (T2 value) from tumour centre to periphery for glioblastoma ($P = 0.0049$ – fit-model: glioblastoma −25.02± 19.89 (−54–10); anaplastic astrocytoma −5.57±22.94 (−51–47)). Similar results were found when the cohort was subdivided by their isocitrate dehydrogenase profile, showing an increased drawdown from tumour centre to periphery for wildtype in comparison to mutated isocitrate dehydrogenase ($P = 0.0430$ – fit model: isocitrate dehydrogenase wildtype −10.35±16.20 (−51) – 0; isocitrate dehydrogenase mutated 12.14±21.24 (−15–47)). A strong statistical proof for both subgroup analyses ($P = 0.9987$ – glioblastoma R^2 0.93± 0.08; anaplastic astrocytoma R^2 0.94±0.15) was found.

Conclusion: Peritumoral T2 mapping relaxation time tissue behaviour of glioblastoma differs from anaplastic astrocytoma. Significant differences in T2 values, using T2 mapping relaxation time, were found between glioblastoma and anaplastic astrocytoma, capturing the tumour centre to the peritumoral zone. A similar curve progression from tumour centre to peritumoral zone was found for isocitrate dehydrogenase wildtype high grade gliomas in comparison to isocitrate dehydrogenase mutated high grade gliomas. This finding is in accordance with the biologically more aggressive behaviour of isocitrate dehydrogenase wildtype in comparison to isocitrate dehydrogenase mutated high grade gliomas. These results emphasize the potential of mapping techniques to reflect the tissue composition of high grade gliomas.

Keywords

Glioblastoma, glioma, MRI (magnetic resonance imaging), multiparametric imaging, T2 mapping

Introduction

Glioblastomas (GBMs) and anaplastic astrocytomas (AA3s) represent the majority of high grade gliomas (HGGs) and are the most common malignant adult brain tumours. For treatment, prediction and prognostic decision HGGs have to be classified. The gold standard therefore is the World Health Organization (WHO) classification. Within this classification, HGGs are categorised according to the histological morphology and since the last update in 2016 to genotypic parameters as they also have an impact on predicting the outcome. AA3s are categorised as WHO grade III and GBMs as WHO grade IV tumours.[1,2] Especially in HGGs, isocitrate dehydrogenase (IDH) seems to have the most crucial impact on prognosis. Furthermore, IDH mutation helps to distinguish between primary and secondary GBMs, as the mutation is rarely seen in de novo GBMs.[2]

[1]Department of Radiology, Charité University Hospital, Berlin, Germany
[2]Departement for Neuroradiology, Charite – University Hospital Berlin, Berlin, Germany
[3]Department of Neuroradiology, University Medical Center of the Johannes Gutenberg-University Mainz, Mainz, Germany
[4]Department of Neurosurgery, Charité University Hospital, Berlin, Germany

Corresponding author:
Edzard Wiener, Departement for Neuroradiology, Charite – University Hospital Berlin, Augustenburger Platz 1, Berlin 13353, Germany.
Email: edzard.wiener@charite.de

Within GBMs, another well-known molecular parameter with a reported predictive value is the methylation of the methylguanine methyltransferase (MGMT) promotor gene. Patients with a methylated MGMT promotor benefit from adjuvant chemotherapy.[2,3] As a reaction to these findings, the WHO classification included the genotypic parameters in the revised version from 2016.[4,5]

The management of such highly aggressive tumours as GBMs is difficult. The development of reliable and easy to realise response criteria is challenging. To date, the gold standard for response assessment is the response assessment in neuro-oncology (RANO) criteria.[6] However, the detection of any relapse situation after resection remains difficult. The reason for this might be that the majority of recurring HGGs is within 2–3 cm of the resection margin. This aspect reflects the importance of the peritumoral zone, which is the active spot of tumour growth and response.[7] With this the preoperative visualisation of the infiltrative peritumoral zone is crucial for planning the resection margin and subsequently directly affecting the frequency of margin recurrences.[8] The major problem with this zone is that the peritumoral zone may represent fluid-filled compartments due to the disruption of the blood–brain barrier (BBB) and/or accumulation of active tumour cells.[9] According to Lemee et al. the peritumoral zone is radiologically defined as the healthy, magnetic resonance non-enhancing brain area a few centimetres around the tumour. It is usually T2-hyperintense, representing vasogenic oedema, which may indicate an infiltration of tumour cells.[10] To date it is not possible to distinguish between peritumoral oedema or infiltration of tumour cells by using the 'established' magnetic resonance imaging (MRI) features. No 'newer' MRI technique (diffusion weighted imaging (DWI) and apparent diffusion coefficient (ADC), susceptibility weighted imaging (SWI), dynamic contrast enhancement (DCE), spectroscopy, etc.) enables a differentiation sufficiently. Furthermore, this zone is of great interest, regarding the different aggressive behaviour in tumours within the same WHO grade. It has been described elsewhere that isocitrate dehydrogenase wild-type (IDHw) AA3 HGGs show a more aggressive behaviour than isocitrate dehydrogenase mutated (IDHm) AA3 HGGs.[2] This might originate from more active tumour cells and with this theoretically directly influencing the resection margin. If IDHw are treated similarly to IDHm AA3 in accordance with their WHO grade, early recurrence might increase.

Advanced MRI mapping techniques quantify the relaxation time at different echo times pixelwise and are able to give more accurate information about tissue structure and composition. Usually the magnetic resonance image contrast is determined by the specific T2 relaxation times. Oedema, tumour infiltration and an increased blood flow or water diffusion processes are known to influence the image contrast in T2-weighted images. A quantitative approach measuring the T2 relaxation times as absolute numbers in milliseconds (ms) and coding them colour or gray-scaled, also known as T2 maps, seems to be the most reliable, objective and reproducible imaging technique to visualise the image contrast in T2-weighted/fluid-attended inversion recovery (FLAIR) images.[11–14] This might have the potential to distinguish between tumour cells and vasogenic oedema in the peritumoral zone. Recent studies report an association between T2 mapping relaxation times and the molecular background in gliomas.[15]

The purpose of this study was to characterise and gain more insights into the peritumoral zones of GBMs and AA3s according to their IDH profiles. Therefore, T2 values have been evaluated, at different echo times using T2 mapping sequences.

Materials and methods

Patients

A total of 41 patients with either singular GBM or AA3 were enrolled from April 2015 to December 2016. Patients younger than 18 years or with prior surgery were excluded. Patients were divided into a GBM ($n = 22$) and a AA3 ($n = 19$) cohort. Histopathological reports were available for all patients and IDH status was determined by immunohistochemistry. The study protocol (ethical application number EA1/306/16) conforms to the ethical guidelines of the 1975 Declaration of Helsinki. Some of the patients included in the present analysis participated in a previous study.[15]

Imaging

MRI was performed on a 1.5T (Avanto Magnetom; Siemens, Erlangen, Germany) or on a 3T scanner (Skyra; Siemens, Erlangen, Germany). MRI of the brain consisted of an axial T1-weighted sequence, repetition time (TR) 550 ms, echo time (TE) 8.9 ms, slice thickness 5 mm; in-plane resolution 0.8984 mm × 0.8984 mm, acquisition matrix 256 × 216), T2 fat saturation (T2-fs) axial (TR 4000 ms, TE 92 ms, slice thickness 3 mm, field of view (FOV) 186 × 230 rows, in-plane resolution 0.4492 mm × 0.4492 mm), axial FLAIR sequence (TR 8000 ms, TE 84 ms, slice thickness 4 mm, acquisition matrix 320 × 210; in-plane resolution 0.7188 mm × 0.7188 mm), T2 mapping (TR 3100 ms, TE 13.8–165.6 ms with 12 TEs: 13.8 ms, 27.6 ms, 41.4 ms, 55.2 ms, 69 ms, 82.2 ms, 96.6 ms, 110.4 ms, 124.2 ms, 138 ms, 151.8 ms, 165.6 ms) and magnetisation-prepared rapid gradient echo (MPRAGE) sequence post contrast (TR 2200 ms, TE 2.67 ms, slice thickness 1 mm, inversion time 900 ms, in-plane resolution 0.9766 × 0.9766 mm, acquisition matrix 256 × 246). T2 maps were reconstructed by using a voxel-wise, monoexponential non-negative least-squares fit analysis (MapIt; Siemens, Erlangen, Germany) with a voxel size of 1.9 × 1.0 × 3 mm^3.

Image processing and analysis

Images were postprocessed with the visage software tool (Visage Imaging/Pro Medicus Ltd., version 7.1.10). T2 map ROIs were drawn manually by an experienced neuroradiologist (>10 years of experience) plus a second reader (2 years of experience) with a standardised diameter of 5 mm in one representable slice. The ROIs were placed radiating out from the centre of the tumour in one line out into the peritumoral zone/oedema with a maximum of three ROIs around the tumour. The ROIs covered representable tissue of a peritumoral zone, while areas of necrosis and vessels were excluded (MK, EW). The slice with the largest diameter of peritumoral T2-weighted/FLAIR hyperintensity was chosen, the anatomical centre of the tumour was delineated. Another ROI was placed in the healthy-appearing white matter of the contralateral lobe using an image processing program to ensure reliability of the measurements (Figure 1).

Statistical analysis

The data were analysed by using XLSTAT, version 2011.3.01 (Addinsoft SARL, New York, NY, USA). The Mann–Whitney U-test was used as a two-tailed test to compare each group's median. P values of less than 0.05 were regarded as statistically significant. The spatial T2 value distribution across the tumour radius at four different locations from the tumour centre to the outer infiltration zone adjacent to healthy brain tissue was analysed based on the ROI evaluation. Mean T2 values obtained from these ROIs were modelled using a second-degree polynomial function. The coefficients of the polynomial were calculated by minimising the sum of the squares of the deviations of the data from the model. Both the original data and the model data were presented in the plots. The second-degree fit accurately follows the basic shape of the data. Higher-degree polynomial fitting does not improve the results of the model. A higher fit model value (positive or negative) describes the curve's opening angle. To validate the model the coefficient of determination (R^2) with an intercept range between 0 and 1 was calculated. The stretching factor of the second-degree fit is a measure of the increase of T2 across the tumour and was evaluated in every subject and presented in the model function. The coefficients of determination and stretching factors for both groups were compared using the Mann–Whitney U-test.

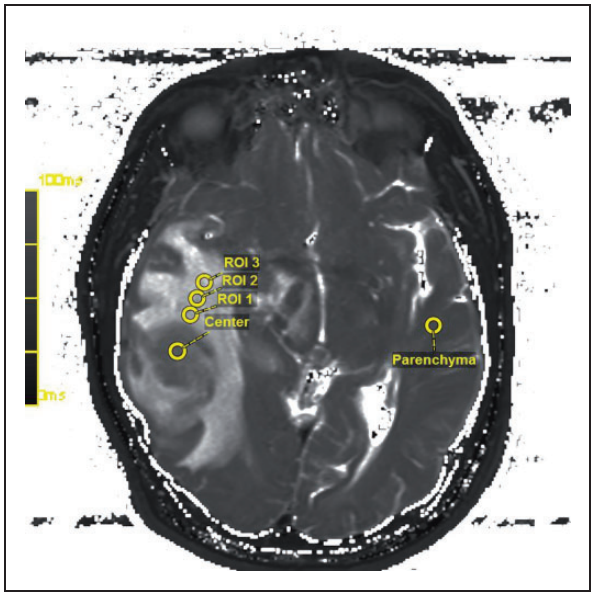

Figure 1. Region of interest (ROI) placement in the raw T2 map in accordance with the fluid-attended inversion recovery (FLAIR) sequences. The slice with the largest diameter of peritumoral T2-weighted/FLAIR hyperintensity was chosen, the anatomical centre of the tumour was delineated. Another ROI was placed in the healthy- appearing white matter of the contralateral lobe using an image processing program to ensure reliability of the measurements. The spatial T2 value distribution across the tumour radius was measured at four different locations from the tumour centre to the outer infiltration zone by the placement of three further ROIs.

Results

T2 mapping analyses

GBM versus AA3. Our calculated model parameter out of the T2 relaxation times showed a significantly different curve progression from tumour centre to periphery in GBM when compared to AA3 ($P = 0.0049$ – fit model (curves skewness): GBM –25.02±19.89 ((–54)–10); AA3 –5.57±22.94 ((–51)–47)). The R^2 fit model showed a strong statistical proof for both subgroup analyses ($P = 0.9987$ – GBM R^2 0.93±0.08; AA3 R^2 0.94±0.15) (Table 1, Figures 2, 3 and 4).

IDHw versus IDHm HGG. When divided by IDH mutational status the T2 relaxation times also showed significantly different curve progression behaviour in IDHw gliomas as compared to IDHm gliomas ($P = 0.0430$ – fit model: IDHw –10.35±16.20 ((–51)–0); IDHm 12.14±21.24 ((–15)–47)). The fit model showed a fair statistical proof for both subgroup analyses divided by mutational state ($P = 0.4180$ – IDHw R^2 0.94±0.17; AA3 R^2 0.96±0.13) (Table 1, Figures 3–5).

Patient characteristics

Overall, there is a strong difference in age concerning the IDH status ($P<0.001$) and the WHO grade ($P<0.001$). Patients with AA3 (43.11±11.22 years) are younger than patients with GBM (62.14±14.71 years), while IDHw is associated with an older age than IDHm. There were 17 female and 24 male subjects included. MGMT promotor methylation prevails significantly in IDHm gliomas ($P<0.001$). Regarding the WHO grade, no significant differences have been reported ($P = 0.052$). The tumour localisation does not correlate significantly with the WHO grade ($P = 0.510$) or the IDH status ($P = 0.061$). There was

Table 1. Patient characteristics.

	AA3 (n=19)	GBM (n=22)	P value
Age (mean, range)	43.11±11.22 (29–63)	62.14±14.71 (34–83)	<0.001*/<0.001
IDH mutated	38.55±8.71 (29–54)	39±0 (39)	
IDH wildtype	49.38±11.72 (34–63)	63.24±14.11 (34–83)	
Sex (no.)			0.184*/0.537
Female	9 (47.37%)	8 (36.36%)	
Male	10 (52.63%)	14 (63.64%)	
IDH			<0.001
Mutated	11 (57.89%)	1 (4.55%)	
Wildtype	8 (42.22%)	21 (95.45%)	
MGMT			0.001*/0.052
Mutated	13 (68.42%)	9 (40.91%)	
Wildtype	4 (21.05%)	12 (54.55%)	
Not determined	2 (10.53%)	1 (4.55%)	
Localisation			0.061†*/0.510†
	Frontal (26.32%)	Temporal (27.27%)	
	Parietal (15.79%)	Frontal (18.18%)	
	Fronto-parieto-temporal (15.79%)	Frontoparietal (18.18%)	
	Temporal (10.53%)	Bifrontal (9.09%)	
	Fronto-temporal (10.53%)	Parietal (9.09%)	
	Frontoparietal (5.26%)	Parieto-occipital (9.09%)	
	Parieto-temporal (5.26%)	Fronto-temporal (4.55%)	
	Multilobar (5.26%)	Periventricular (4.55%)	
	Thalamic (5.26%)		
T1w/T1w CE diameter (mm)	43.58±20.11 (17–81)	40.91±17.16 (18–86)	0.025*/0.811
IDH mutated	54.82±18.50 ([32–81)	26±0 (26)	
IDH wildtype	28.13±8.91 (17–43)	41.62±17.25 (18–86)	
T2w/FLAIR diameter (mm)	15.84±6.14 (8–29)	20.55±6.04 (10–36)	0.011*/0.012
IDH mutated	15.09±6.77 (8–29)	14±0 (14)	
IDH wildtype	16.88±5.44 (8–27)	20.86±6.00 (10–36)	

AA3: anaplastic astrocytoma; CE: contrast enhanced; FLAIR: fluid-attenuated inversion recovery; GBM: glioblastoma; IDH: isocitrate dehydrogenase; MGMT: methylguanine methyltransferase; T2w: T2-weighted.
*This P value relates to the difference between the isocitrate dehydrogenase mutated and the isocitrate dehydrogenase wildtype tumours independently of the tumour grade.
†This P value relates to fronto-parietal or not fronto-parietal localisation.

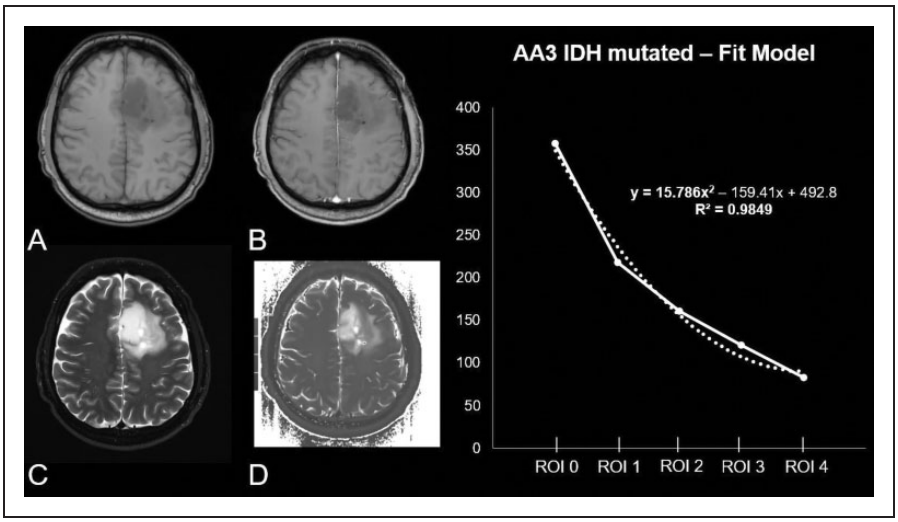

Figure 2. Patient, 49 years old, with a non-contrast enhanced (CE) T1-weighted heterogeneous-appearing anaplastic astrocytoma in the left frontal lobe (a) without a significant positive CE in the T1 CE sequence (b). (c) Unilateral surrounding oedema in the fluid-attended inversion recovery sequence. (d) The original raw T2 map. The diagram shows the curve progression from tumour centre to periphery calculated by means of a fit model. As reflected by $15.786x^2$ the curve's opening angle is positive.

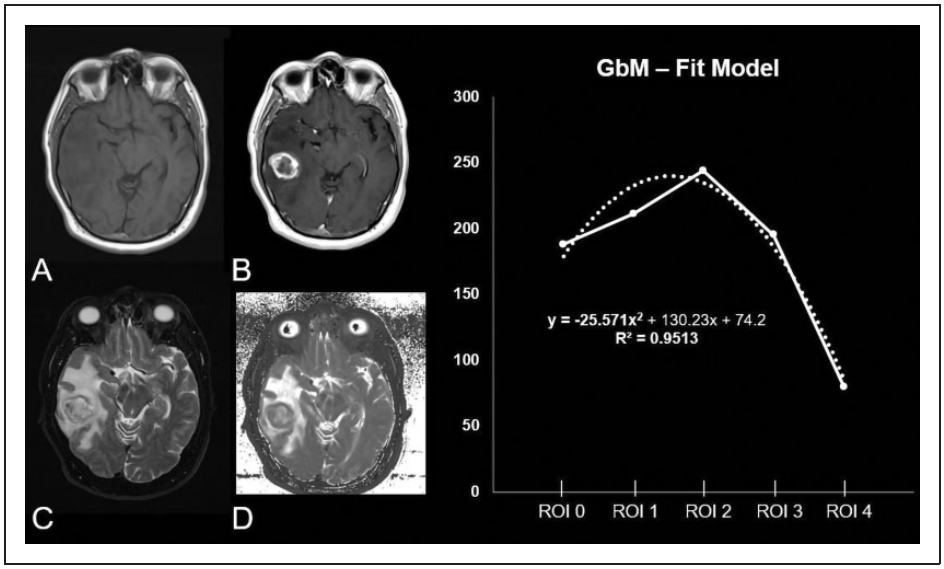

Figure 3. Patient, 63 years old, with a non-contrast enhanced (CE) T1-weighted heterogeneous glioblastoma in the right temporal lobe (a) and a significant positive CE in the T1 CE sequence (b). (c) A large perifocal oedema in the fluid-attended inversion recovery sequence. (d) The original raw T2 map. The diagram shows the curve progression from tumour centre to periphery calculated by means of a fit model. While the *y*-axis describes the median T2 values originating out of the T2 map; the *x*-axis shows the different regions of interest (ROIs) which were placed as follows: 1 – ROI 0: inside the tumour centre; 2 – ROI 1: 0–5 mm of the peritumoral oedema/zone; 3 – ROI 2: 5–10 mm of the peritumoral oedema/zone; 4 – ROI 3: 10–15 mm of the peritumoral oedema/zone and 5 – ROI within healthy brain parenchyma on the contralateral side. As reflected by $-25.571x^2$ the curve's opening angle is negative.

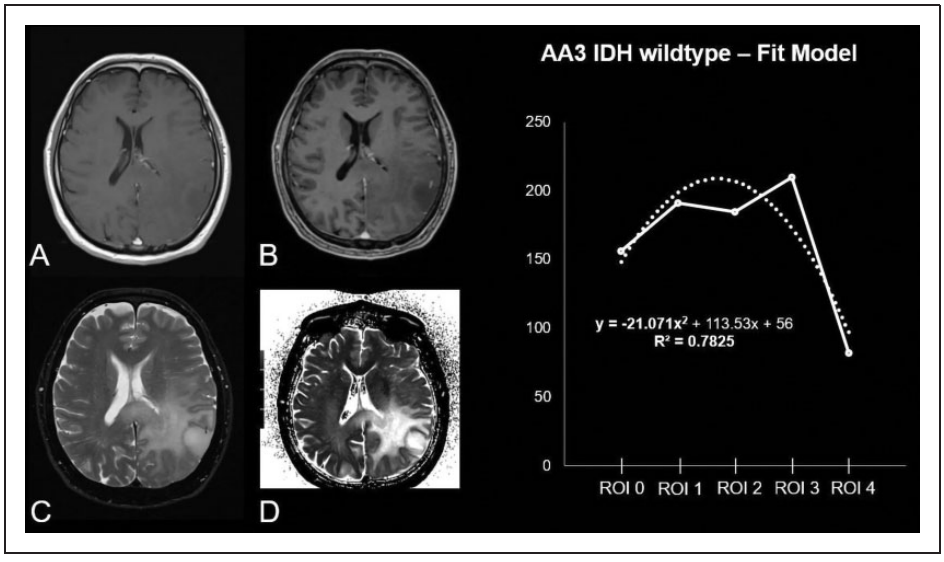

Figure 4. Patient, 63 years old, with a non-contrast enhanced (CE) T1-weighted homogeneous-appearing anaplastic astrocytoma isocitrate dehydrogenase wildtype in the left parietal lobe (a) with marginal CE in the T1 CE sequence (b). (c) Surrounding oedema in the fluid-attended inversion recovery sequence. (d) The original raw T2 map. The diagram shows the curve progression from tumour centre to periphery calculated by means of a fit model. As reflected by $-21.071x^2$ the curve's opening angle is negative.

no significant difference between the maximal axial tumour diameter in the T1/T1 contrast enhanced sequences from AA3 (43.58±20.11 (range 17–81) mm) and GBM (40.91±17.16 (range 18–86) mm); $P = 0.811$). Nevertheless, GBMs (20.55±6.04 (range 10–36) mm) had a larger diameter in the T2/FLAIR sequences, potentially reflecting the oedema/infiltration zone than AA3 (15.84±6.14 (range 8–29) mm; $P = 0.012$). Assorting by the IDH status revealed that IDHm gliomas had a significantly larger tumour diameter ($P = 0.025$) but a significantly smaller oedema/infiltration zone ($P = 0.011$) than IDHw gliomas. All other patient characteristics, distributions and values are provided in Table 2.

Discussion

This study evaluates quantitative T2 mapping sequences for characterising the peritumoral zone of HGG.

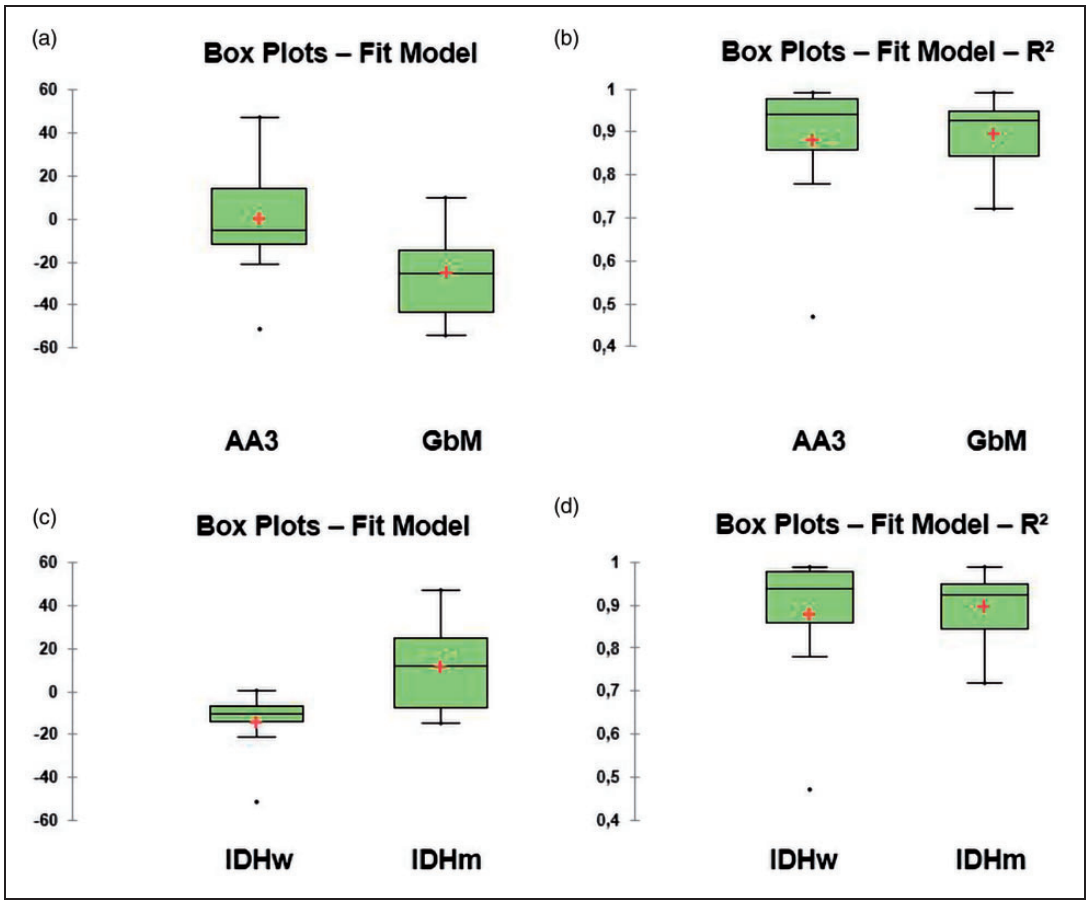

Figure 5. (a) Significant difference between the curve progression for the medians, when the cohort is divided into anaplastic astrocytoma and (b) illustrated with R2 a strong statistical validity for the analyses, when the cohort is subdivided by World Health Organization grade; (c) Significant difference in between curve progression for the medians, when the cohort is divided by isocitrate dehydrogenase (IDH) mutational state; (d) illustrated with R2 a strong statistical validity for the analyses, when the cohort is subdivided into IDH mutated and IDH wildtype high grade glioma.

Peritumoral T2 mapping relaxation times of GBMs differ from AA3s. GBM median relaxation times showed a significantly different curve progression from tumour centre to periphery compared to AA3. Furthermore, when subdivided by their IDH profile, T2 relaxation times also differed between IDHw HGG and IDHm HGG. Surprisingly, AA3 IDHw showed a similar curve progression from tumour centre to periphery like GBM (Figures 2 and 5). The quantitative evaluation by the use of mapping sequences may be an approach to distinguish between peritumoral oedema and the peritumoral infiltration zone and with this giving the possibility to prognosticate tumour growth behaviour.

To date characterisation of the peritumoral zone of HGG, especially GBM, remains challenging. Of course, the RANO criteria reacted in 2010 by adding T2-weighted sequences into their assessment scheme to diagnose T2 progress.[6] Peritumoral zones remain a spot of interest for radiologists, neurosurgeons and radiotherapy oncologists as the differentiation between pure oedema and the peritumoral infiltration zone is crucial. Non-enhancing oedema might contain tumour cells; however, this will not be visible on MRI and with this especially for neurosurgeons, a definitive resection margin remains challenging.[16]

The experience and evidence in the literature for HGG regarding mapping techniques is low, although during the past decade mapping techniques are becoming more and more popular within clinical routine (e.g. cardiac and musculoskeletal MRI) as it gives the opportunity to measure the tissue and its signal behaviour quantitatively.[17–22] Nevertheless, already in 2012 Ellingson et al. used T2 mapping sequences to quantify oedema reduction in recurrent GBM treated with bevacizumab, suggesting that post-treatment T2 values correlate with the progression-free survival. This is giving evidence to the fact that T2 mapping sequences may be suitable to characterise peritumoral oedema further.[23] A recent study published by Kern et al. (2020) showed that the relaxation times acquired by T2 mapping sequences were able to distinguish between IDHw and IDHm WHO grade II and III gliomas, with wildtypes showing lower T2 relaxation times.[15] In another recently published study also by Kern et al. (2020), the group investigated the tumour centre and the tumour periphery showing that values

Table 2. Results.

	AA3	GBM	*P* value
Fit	−5.57±22.94 ((−51)−47)	−25.02±19.89 ((−54)−10)	0.0049
ROI 0 (ms)	290.37±133.65 (121−497)	197.57±74.38 (109−419)	
Tumour centre			
ROI 1 (ms)	206.79±69.99 (104−357)	213.57±57.97 (123−306)	
Peritumoral zone 1			
ROI 2 (ms)	179.74±47.63 (110−297)	229.38±73.23 (112−334)	
Peritumoral zone 2			
ROI 3 (ms)	189.00± 66.55 (119−290)	228.07±62.18 (116−352)	
Peritumoral zone 3			
ROI 4 (ms)	82.72±3.50 (77−90)	84.81±3.84 (79−91)	
Contralateral: normal brain tissue			
R^2	0.94±0.15 (0.47−0.99)	0.93± 0.08 (0.72−0.99)	0.9987
	IDH wildtype	IDH mutated	
Fit	−10.35±16.20 ((−51)−0)	12.14±21.24 ((−15)−47)	0.0430
ROI 0 (ms)	189.11±73.39 (109−419)	364.25±102.33 (155−497)	
Tumour centre			
ROI 1 (ms)	204.75±63.63 (109−306)	223.42±62.94 (146−357)	
Peritumoral zone 1			
ROI 2 (ms)	216.75±74.34 (110−334)	180.25±33.40 (141−246)	
Peritumoral zone 2			
ROI 3 (ms)	217.90±66.24 (116−352)	194.33±79.61 (121−279)	
Peritumoral zone 3			
ROI 4 (ms)	84.36±3.75 (79−91)	82.99±3.73 (77−89)	
Contralateral: normal brain tissue			
R^2	0.94±0.17 (0.47−0.99)	0.96±0.13 (0.56−0.99)	0.4180

AA3: anaplastic astrocytoma; GBM: glioblastoma; ROI: region of interest.

decreased in the periphery.[15] The authors assumed that T2 values may reflect the peripheral tumour cellular activity as this is the spot of growth and infiltration.[15] The underlying study showed for GBM in comparison to AA3 an increased signal drawdown from tumour centre to periphery. According to the conclusion of Kern et al., the results of that study might indicate an increased tumour cellularity and with this an increased aggressiveness and increased occurrence of recurrence, after resection of GBMs compared to AA3s.

The WHO classification was revised in 2016 and now includes molecular marker profiles. The reason for this is that especially IDHw grade II and III gliomas can act like GBMs and have a similar dismal prognosis.[2,5] In this study HGGs were not only subdivided into GBM and AA3, but the cohort was further subdivided regarding the mutilation state. Peritumoral zones were investigated and in line and according to the abovementioned biologically more aggressive HGG wildtypes showed an increased drawdown from tumour centre to periphery, similar to GBMs. This may also emphasise the potential of T2 mapping sequences, for differentiating between HGG molecular subtypes and might give the possibility for assessing the risk of developing an early recurrence. To the best of our knowledge, no MRI method is established to define the peritumoral infiltration zone. The underlying data are emphasising further investigations regarding T2 mapping to define and gain more insight into the peritumoral zone. With this, the extent of tumour resection might be defined more precisely, directly influencing tumour burden and patient prognosis.[10,24,25]

An interesting study by Blystad et al. (2017) analysed the peritumoral oedema of malignant gliomas quantitatively also using T1 and T2 mapping sequences. The authors found a gradient of relaxation values in the peritumoral oedema closest to contrast-enhancing parts of the tumour and an increase of the gradients in the oedemas after contrast agent injection.[26] Future prospective aims will be to refine the prognostication of mapping relaxation values to establish values to characterise further the peritumoral zone and to differentiate between oedema and infiltration.

Limitations

The retrospective and non-blind study design has introduced some detection bias. Another limitation might be the relatively small patient cohort and a missing volume-based analysis, while this study used a regionally based approach. However, the results of this study are promising and novel. Furthermore, although the sample number is small the statistically calculated validity levels are sufficient. A further limitation is the use of two different scanners. Nevertheless, although two different types of scanner were used, T2 values of brain parenchyma are not affected significantly by the field strength.[27]

Conclusion

This is one of the first studies investigating T2 mapping sequences to characterise the tumour centre and peritumoral zone within HGGs. The results show that the peritumoral relaxation behaviour differs from GBMs to those of AA3s. Interestingly, when subdivided by their molecular IDH profile, the more aggressive IDHw show a similar relaxation behaviour as GBMs. These results emphasise the potential of T2 mapping techniques to reflect the tissue composition of HGGs. With this a differentiation between active tumour cells and vasogenic oedema in the peritumoral zone might be possible. The results of this study add information to the ongoing discussion on how to facilitate more accurate resection margins potentially decreasing early recurrence.

Conflict of interest

The author(s) declared no potential conflicts of interest with respect to the research, authorship, and/or publication of this article.

Funding

The authors received no financial support for the research, authorship, and/or publication of this article.

ORCID iDs

Timo Alexander Auer https://orcid.org/0000-0002-5763-689X
Uli Fehrenbach https://orcid.org/0000-0003-3622-3268

References

1. Wen PY and Kesari S. Malignant gliomas in adults. *N Engl J Med* 2008; 359: 492–507.
2. Smits M and van den Bent MJ. Imaging correlates of adult glioma genotypes. *Radiology* 2017; 284: 316–331.
3. Hegi ME, Diserens AC, Gorlia T, et al. MGMT gene silencing and benefit from temozolomide in glioblastoma. *N Engl J Med* 2005; 352: 997–1003.
4. Louis DN, Ohgaki H, Wiestler OD, et al. The 2007 WHO classification of tumours of the central nervous system. *Acta Neuropathol* 2007; 114: 97–109.
5. Louis DN, Perry A, Reifenberger G, et al. The 2016 World Health Organization classification of tumors of the central nervous system: a summary. *Acta Neuropathol* 2016; 131: 803–820.
6. Wen PY, Macdonald DR, Reardon DA, et al. Updated response assessment criteria for high-grade gliomas: response assessment in neuro-oncology working group. *J Clin Oncol: official journal of the American Society of Clinical Oncology* 2010; 28: 1963–1972.
7. Burger PC, Dubois PJ, Schold SC Jr, et al. Computerized tomographic and pathologic studies of the untreated, quiescent, and recurrent glioblastoma multiforme. *J Neurosurg* 1983; 58: 159–169.
8. Molinaro AM, Hervey-Jumper S, Morshed RA, et al. Association of maximal extent of resection of contrast-enhanced and non-contrast-enhanced tumor with survival within molecular subgroups of patients with newly diagnosed glioblastoma. *JAMA Oncol* 2020; 6(4): 495–503.
9. Roth P, Regli L, Tonder M, et al. Tumor-associated edema in brain cancer patients: pathogenesis and management. *Exp Rev Anticancer Ther* 2013; 13: 1319–1325.
10. Lemee JM, Clavreul A and Menei P. Intratumoral heterogeneity in glioblastoma: don't forget the peritumoral brain zone. *Neuro Oncol* 2015; 17: 1322–1332.
11. Hattingen E, Jurcoane A, Nelles M, et al. Quantitative MR imaging of brain tissue and brain pathologies. *Clin Neuroradiol* 2015; 25 (Suppl. 2): 219–224.
12. Hattingen E, Jurcoane A, Daneshvar K, et al. Quantitative T2 mapping of recurrent glioblastoma under bevacizumab improves monitoring for non-enhancing tumor progression and predicts overall survival. *Neuro Oncol* 2013; 15: 1395–1404.
13. Oh J, Cha S, Aiken AH, et al. Quantitative apparent diffusion coefficients and T2 relaxation times in characterizing contrast enhancing brain tumors and regions of peritumoral edema. *J Magnet Reson Imag: JMRI*. 2005; 21: 701–708.
14. Hoehn-Berlage M, Tolxdorff T, Bockhorst K, et al. In vivo NMR T2 relaxation of experimental brain tumors in the cat: a multiparameter tissue characterization. *Magnet Reson Imag* 1992; 10: 935–947.
15. Kern M, Auer TA, Picht T, et al. T2 mapping of molecular subtypes of WHO grade II/III gliomas. *BMC Neurol* 2020; 20: 8.
16. Grabowski MM, Recinos PF, Nowacki AS, et al. Residual tumor volume versus extent of resection: predictors of survival after surgery for glioblastoma. *J Neurosurg* 2014; 121: 1115–1123.
17. Hada S, Ishijima M, Kaneko H, et al. Association of medial meniscal extrusion with medial tibial osteophyte distance detected by T2 mapping MRI in patients with early-stage knee osteoarthritis. *Arthritis Res Ther* 2017; 19: 201.
18. Huber AT, Lamy J, Bravetti M, et al. Comparison of MR T1 and T2 mapping parameters to characterize myocardial and skeletal muscle involvement in systemic idiopathic inflammatory myopathy (IIM). *Eur Radiol* 2019; 29: 5139–5147.
19. Kim PK, Hong YJ, Im DJ, et al. Myocardial T1 and T2 mapping: techniques and clinical applications. *Korean J Radiol* 2017; 18: 113–131.
20. Mavrogeni S, Apostolou D, Argyriou P, et al. T1 and T2 mapping in cardiology: "mapping the obscure object of desire". *Cardiology* 2017; 138: 207–217.
21. Muscogiuri G, Suranyi P, Schoepf UJ, et al. Cardiac magnetic resonance T1-mapping of the myocardium: technical background and clinical relevance. *J Thorac Imaging* 2018; 33: 71–80.
22. Roux M, Hilbert T, Hussami M, et al. MRI T2 mapping of the knee providing synthetic morphologic images: comparison to conventional turbo spin-echo MRI. *Radiology* 2019; 293: 620–630.
23. Ellingson BM, Cloughesy TF, Lai A, et al. Quantification of edema reduction using differential quantitative T2 (DQT2) relaxometry mapping in recurrent glioblastoma treated with bevacizumab. *J Neurooncol* 2012; 106: 111–119.

24. Chaichana KL, Jusue-Torres I, Navarro-Ramirez R, et al. Establishing percent resection and residual volume thresholds affecting survival and recurrence for patients with newly diagnosed intracranial glioblastoma. *Neuro Oncol* 2014; 16: 113–122.
25. Lemee JM, Clavreul A, Aubry M, et al. Characterizing the peritumoral brain zone in glioblastoma: a multidisciplinary analysis. *J Neurooncol* 2015; 122: 53–61.
26. Blystad I, Warntjes JBM, Smedby O, et al. Quantitative MRI for analysis of peritumoral edema in malignant gliomas. *PLoS One* 2017; 12: e0177135.
27. West J, Blystad I, Engstrom M, et al. Application of quantitative MRI for brain tissue segmentation at 1.5 T and 3.0 T field strengths. *PLoS One* 2013; 8: e74795.

Lebenslauf

Mein Lebenslauf wird aus datenschutzrechtlichen Gründen in der elektronischen Version meiner Arbeit nicht veröffentlicht.

Publikationsliste

Kern, M., Auer, T. A., Picht, T., Misch, M., & Wiener, E. (2020). T2 mapping of molecular subtypes of WHO grade II/III gliomas. *BMC Neurology*, *20*(1), 8. https://doi.org/10.1186/s12883-019-1590-1

Impact factor 2019/2020 2.35

Kern, M., Auer, T. A., Fehrenbach, U., Tanyildizi, Y., Picht, T., Misch, M., & Wiener, E. (2020). Multivariable non-invasive association of isocitrate dehydrogenase mutational status in World Health Organization grade II and III gliomas with advanced magnetic resonance imaging T2 mapping techniques. *The Neuroradiology Journal*, *33*(2), 160–168. https://doi.org/10.1177/1971400919890099

Impact factor 2019/2020 1.14

Auer, T. A., Kern, M., Fehrenbach, U., Tanyldizi, Y., Misch, M., & Wiener, E. (2021). T2 mapping of the peritumoral infiltration zone of glioblastoma and anaplastic astrocytoma. *The Neuroradiology Journal*, 0(0), 1–9. https://doi.org/10.1177/1971400921989325

Impact factor 2019/2020 1.14

Danksagung

An dieser Stelle möchte ich allen Menschen danken, die mich bei der Anfertigung meiner Dissertation unterstützt haben.

Mein besonderer Dank gilt dabei meinem Doktorvater PD Dr. med. Dipl. Phys. Edzard Wiener, für die stets herzliche und kollegiale Betreuung und für die enorme Unterstützung bei der gesamten Arbeit.

Außerdem möchte ich mich bei Dr. med. Timo A. Auer bedanken, der mich auf meinem Weg mit Rat und Anregungen begleitet hat.

Nicht zuletzt einen großen Dank an meine Familie und Freunde, die mich jeden Tag mit ihrem Mut, ihrer Liebe und Stärke bewegen.